Geodynamics and Space Geodesy

The "Geo" sciences in the Laboratory of Terrestrial Physics consist of the Geodynamics Branch and the Space Geodesy Branch. Together these groups study a wide range of subjects in the broad disciplines of geophysics, geology, geodesy and geodynamics for both the Earth and solid planetary bodies, especially Mars. Present-day measurements using both surface and satellite data, models derived from these, and other observational and theoretical information are used to help improve our understanding of the evolution of the core, mantle and crust, and their interactions with the fluid envelopes at and above the surface. Major areas of work are described in more detail below, and examples of major accomplishments in the last year are provided in the following section.

Geodynamics includes studies of the surface and interior of the Earth and planets: their current state, including dynamics, and the processes which operate to produce the observed state and motions. Specific areas of research and study include the following:

(1) Core fluid motions and how it relates to changes in the Earth's magnetic field;

(2) Motions of the Earth's crust and the relationship with earthquake hazard, especially in areas of active subduction;

(3) Vertical rebound of paleolakes and the constraints it provides on lower crustal and upper mantle properties;

(4) Long term orbital-rotational evolution and its relationship to long term climate change;

(5) Magnetic properties of the Earth's crust and the nature of the sources of magnetic anomalies not just on the Earth but on Mars as well;

(6) Topographic characterization of the surface of the Earth and Mars, in the former case to understand landforms associated with active faulting, in the latter case to understand volcanic and tectonic structures and the origin of the fundamental crustal topographic dichotomy, and how large scale impacts affect early crustal evolution.

Space geodesy involves positional studies of the Earth's surface and its orientation in space, the Earth's gravity field, and the use of their time evolution to understand fundamental Earth processes. The latter include mantle convection, plate motion, and fluid mass transports both on the surface (e.g., ocean and atmospheric circulation, land hydrology, icesheets) and in the core. Active areas of work incorporate the following:

(1) Determination of the precise orbits for Earth satellites and planetary spacecraft and determination of the Earth's fundamental reference frame;

(2) Gravity field model development for Earth and other planets, both the static and time-varying components;

(3) Oceanic and solid body tidal processes and the resultant deformation of the Earth;

(4) The effects of redistribution of geophysical fluids (air, water, ice) on the Earth and their manifestation in, for example, the time-variable gravity field and Earth rotation parameters;

(5) Analysis and modeling of space-geodetic Very-Long-Baseline Interferomettry measurements and applications to Earth's rotation studies: and

(6) Development of space techniques that enable precise measurement of the above- mentioned geodetic observables.

Brief descriptions of each of the major areas of work and the Geodynamics or Space Geodesy personnel involved in them are provided below. Below each summary, individual significant highlights of the past year are provided, along with contact information for the relevant author. Publications, major presentations, and other information are shown in subsequent sections.

Geomagnetism

This cross-Branch area includes development of comprehensive models of the Earth's total magnetic field, involving simultaneous estimation and parameterization of the core, crust and external (magnetospheric and ionospheric) components. The latest version of this model has been accepted for publication and is being used to help study new satellite magnetic field data (see below). Main (core) field models are produced from satellite observations, including recent data from the Oersted and CHAMP missions. These descriptions include secular variations, and are used as constraints on models of the core dynamo. The lithospheric field is studied separately to infer properties of the Earth's crust. As described below, such studies have provided new insight about the edge of the North American craton. Recently effort has been devoted to studying the crustal magnetic anomalies of Mars discovered by the Mars Global Surveyor spacecraft, using techniques originally developed for analysis of terrestrial Magsat data. Spectral studies of both Earth and Mars magnetic fields have been done, and are reported below (see Planetary Geology and Geophysics). Scientific expertise is also applied to calibration of in-flight magnetometers on current missions, and towards development of possible new terrestrial and martian magnetic gradient missions, using both satellite and balloon platforms.

On the theoretical front, a geodynamo model is continually refined to understand, model, and help predict many geomagnetic, geodetic, and seismological phenomena that are caused by or related to the geodynamo actions in the fluid core. Called MOSST (MOdular, Scalable, Self-consistent, Three-dimensional), this numerical model has generated definitive insight on the nature of the core-mantle couplings and other geodynamic effects (see also the Global Geophysical Fluids and Their Mass Transports section below).

Comprehensive Models of the Earth's Magnetic Field

A single measurement of the Earth's magnetic field actually measures a combination of fields originating from different sources. Most of these sources are distinct concentrations of electrical currents which flow either inside the Earth or within several tens of Earth radii of its surface. The major sources contributing to the total magnetic field measured at the Earth's surface up through satellite altitude are the core, crust, ionosphere, magnetosphere, currents coupling the ionosphere and magnetosphere, and currents induced in the outer layers of the Earth's surface due to time-varying external (ionospheric or magnetospheric) fields. It is important to describe the extent and behavior of these current systems as well as to understand the processes by which they are established. Through the years, scientists have produced from available surface and satellite data increasingly sophisticated mathematical models of the spatial and temporal organization of these individual fields. The most accurate representation to date comes from a series of models developed at GSFC by a team of international investigators. Because these models include the effects of all the previously described sources, they are called "comprehensive models" or CMs. A paper describing a recent version of the GSFC comprehensive model was recently accepted for publication and the model itself is available for (electronic) distribution to interested investigators.

The key to the CM approach is understanding that the various magnetic fields in the near-Earth environment change or fluctuate on scales that overlap. This is true both in space and time. For instance, portions of the field from the Earth's core can change on scales of a decade, while on the same time frame fields in the crust induced by the magnetosphere will fluctuate as the magnetosphere

fluctuates with the 11 year sunspot cycle. Thus, it is very difficult to separate one field from another by simply arguing that a particular field changes at a given rate in space or time. The CMs are developed by taking into account these "correlations" and overlaps. The goal is to produce an optimal model which fits all the data and any other physical information that might be included.

The most advanced CM to date is CM3d. It is derived from data collected by the NASA POGO and Magsat satellites and the recent Danish Oersted satellite, and also includes data from a global distribution of permanent ground-based magnetic observatories. The model includes about 20,000 parameters and spans the years 1960-2000, and represents the magnetically quiet field in the near-Earth environment (i.e., within about 2,000 km of Earth's surface). An illustration of its power in resolving individual components of the total field is seen in Figure 1 for a particular pass of Magsat data at dusk.

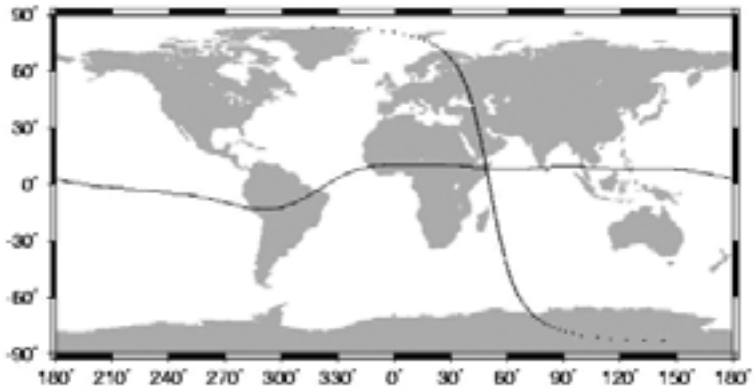

Figure 1.

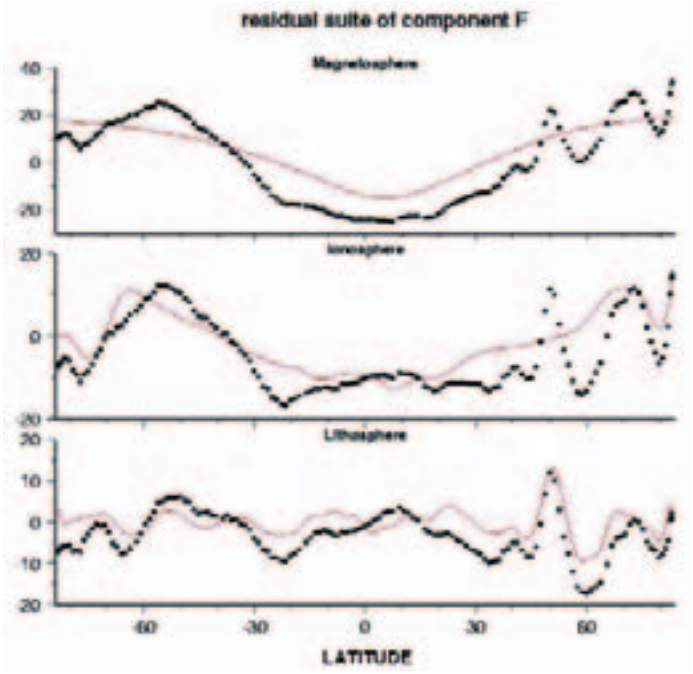

Figure 2.

The top panel of Figure 2 shows the residuals (black boxes) with respect to the long wavelength main (core) and crustal fields. The predicted magnetospheric field is shown as the red line.

The next panel of Figure 2 shows residuals with respect to main and magnetospheric fields, with the predicted ionospheric field in red. The bottom panel shows residuals with respect to main, magnetospheric and ionospheric fields, with the predicted medium to short wavelength crustal field in red. Clearly the model does a good job accounting for the different components of the near-Earth field measured along this pass. Note the large excursion in the crustal field at 40N latitude in the bottom panel. This is the well-known Kursk magnetic anomaly, which is the strongest of the terrestrial lithospheric anomalies and which has been studied by Taylor et al.

Modeling of crustal anomalies has become a "Holy Grail" for much of the magnetics community. Proper separation of the crustal signal from that of the ionosphere is difficult because of poor surface data coverage and overlapping spatial scales. Most methods employed to date use along-track filters to remove ionospheric signal from satellite passes. However, this can remove and usually does remove crustal signal along the pass in the north-south directions (most magnetic field satellites are in near-polar orbits). The CM avoids this ad hoc approach and preserves more of the crustal field structure by parameterization of the ionospheric contribution. The crustal anomaly maps derived from the CM show many N-S anomalies associated with known large-scale structure. Examples can be seen in Figure 3, which is a global map of the radial component of the crustal (lithospheric) field at 400 km altitude. This model resolves several north-south trending features far better than previous models, including the Andean subduction zone and mountains and the mid-ocean spreading ridge in the south Atlantic.

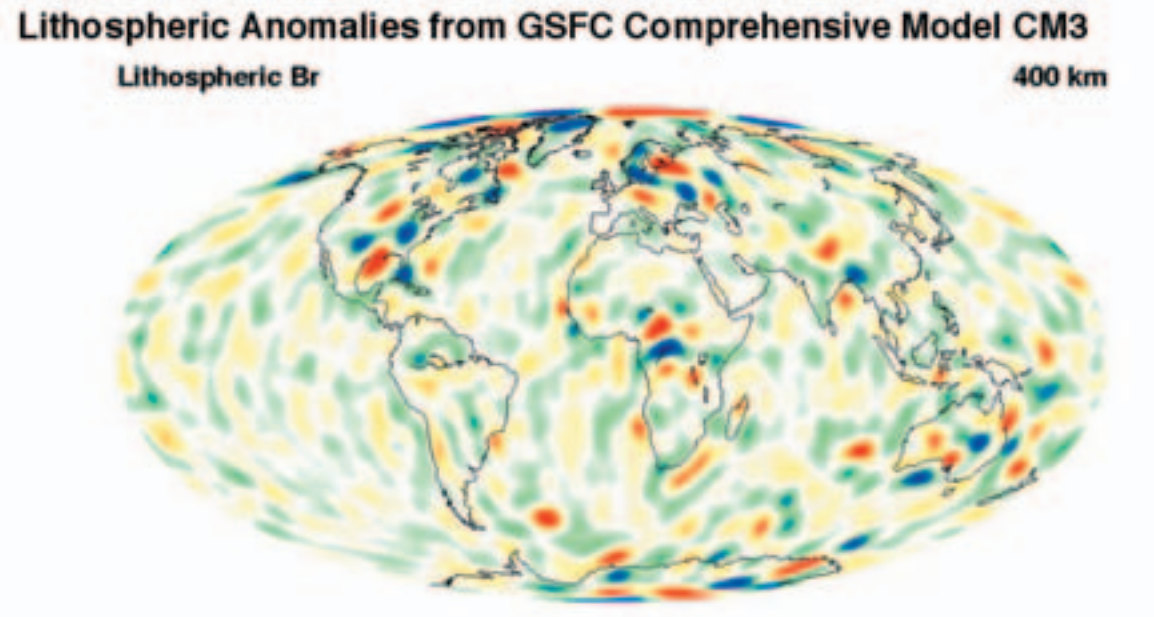

Figure 3.

Contact: Terence J. Sabaka, Geodynamics Branch, sabaka@geomag.gsfc.nasa.gov

New Satellite Magnetometer Observations Help Answer Some Old Questions

The recent launch of three new magnetometer satellites (the Danish Oersted, Argentina's SAC-C, and Germany's CHAMP mission, all of which have NASA involvement) is providing a renewed opportunity to investigate ways to separate temporal and spatial variations of the earth's magnetic field. This separation is difficult because any one measurement of the magnetic field is actually an observation of the combined contributions from the internal main (core) magnetic field, from the ionosphere and magnetosphere, and from sources within the crust. A comprehensive modeling approach, described elsewhere in this section, is one approach that has proven useful in

separating the different components of the total field. But having multiple satellites making measurements at the same time from different orbital locations also helps in the separation of time-variable contributions from the longer term, more permanent components of the field. One product of this improved analysis capability is a much better representation of the lithospheric or crustal fields. This has, in particular, led to a better definition of the boundaries of the continental cratons, as shown in the Figure below.

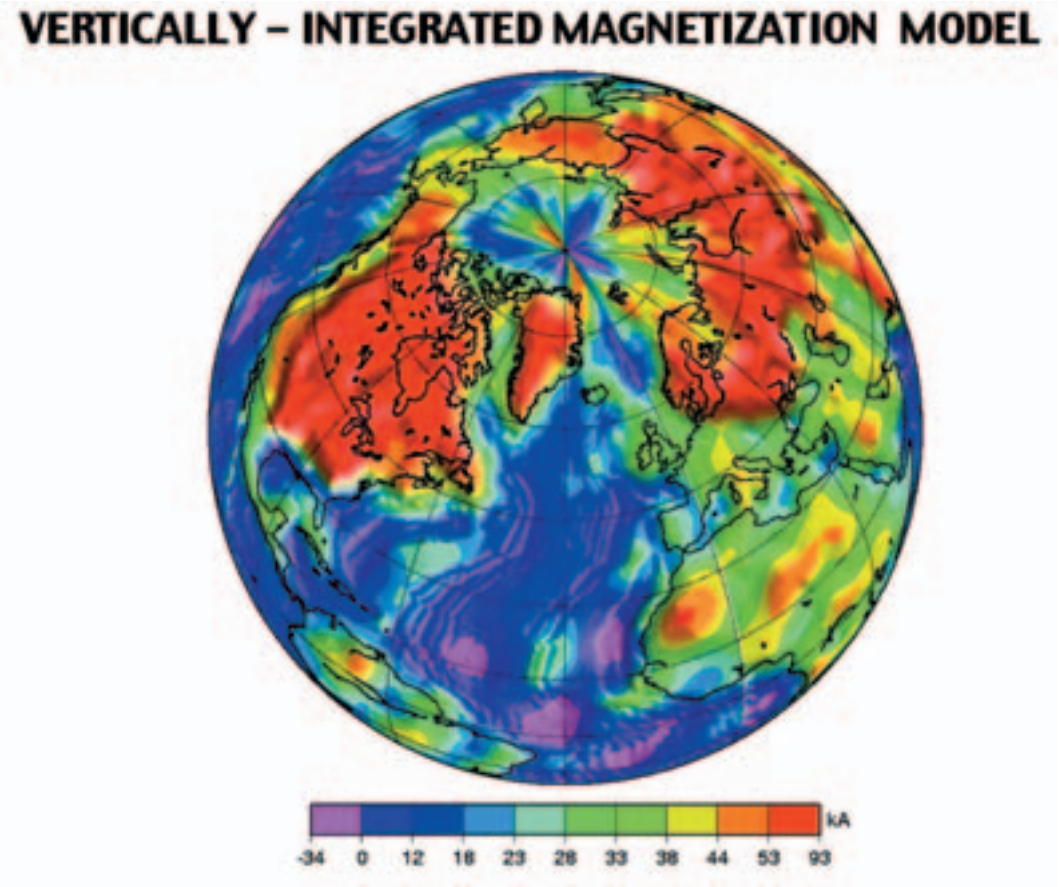

Figure 4.

Figure 4 shows a vertically-integrated model of the induced and remanent magnetization of the Earth's crust that explains the new satellite magnetic field observations. The model also incorporates information from surface magnetic field observatories in addition to the satellite data, and uses seismically-derived estimates of the thickness of the crust. Areas of negative magnetization are due to orientations in directions oblique and opposite to that of the present earth's field. Positive (induced) magnetizations generally align with the present day field.

The model shows in color long-wavelength magnetization features, which are dominated by the continent-ocean crustal thickness and composition contrast (e.g., compare North America and the Atlantic Ocean). Short-wavelength features shown by shaded relief are mostly sea-floor spreading anomalies. In a paper in Geophysical Research Letters, Purucker and colleagues suggest that the very large total field magnetic anomalies centered over Kentucky and the south-central United States are the manifestations of the magnetic edges of the continental craton along the southern boundary of North America. That is, their strong magnetization is due to the difference in magnetic properties and thickness between continental and oceanic crust.

The current generation of satellites include several which, in the future, will dip to lower altitudes, which will improve the spatial resolution of anomalies such as those shown in Figure 4. This should allow scientists to address even more localized questions, such as the age and heat flow of the central Greenland crust (see Figure 4), now the site of rapid ice flow (Fahnestock et al., Science, Dec. 14, 2001). While Greenland is typically classified within the same cratonic zone as the Canadian shield, ice cover masks all but the borders of Greenland. Recent seismic surface-wave observations and preliminary analysis of the current low-altitude satellite magnetic field observations suggest that only the northern and southern edges of Greenland are underlain by ancient, cold crust. Future lower altitude magnetic field observations should help refine this model of the Greenland crust.

Contact: Michael Purucker, Geodynamics Branch, purucker@geomag.gsfc.nasa.gov

Satellite Altitude Magnetic Anomaly Study of the Kiruna, Sweden Iron-Ore Deposit

Previous studies of satellite altitude (~400 km) crustal magnetic data, mainly from the Magsat mission, have revealed several significant (>15 nT) anomalies over known ore bodies in Russia, the United States and the Central African Republic. Additional satellite data is now available from the Danish Oersted satellite, and is becoming available from the newly launched German CHAMP mission. We recently investigated another of the world's largest known iron ore deposits in the area around Kiruna, Sweden, by looking at the relationship between satellite-altitude magnetic and aeromagnetic data of northern Sweden and the regional geology/tectonics of the Kiruna iron ore district. Figure 5 compares the satellite-elevation crustal anomaly field from Magsat with aeromagnetic data from the NORDKALOTT (Unified study by geological surveys of Norway, Sweden and Finland) upward continued to the same altitude.

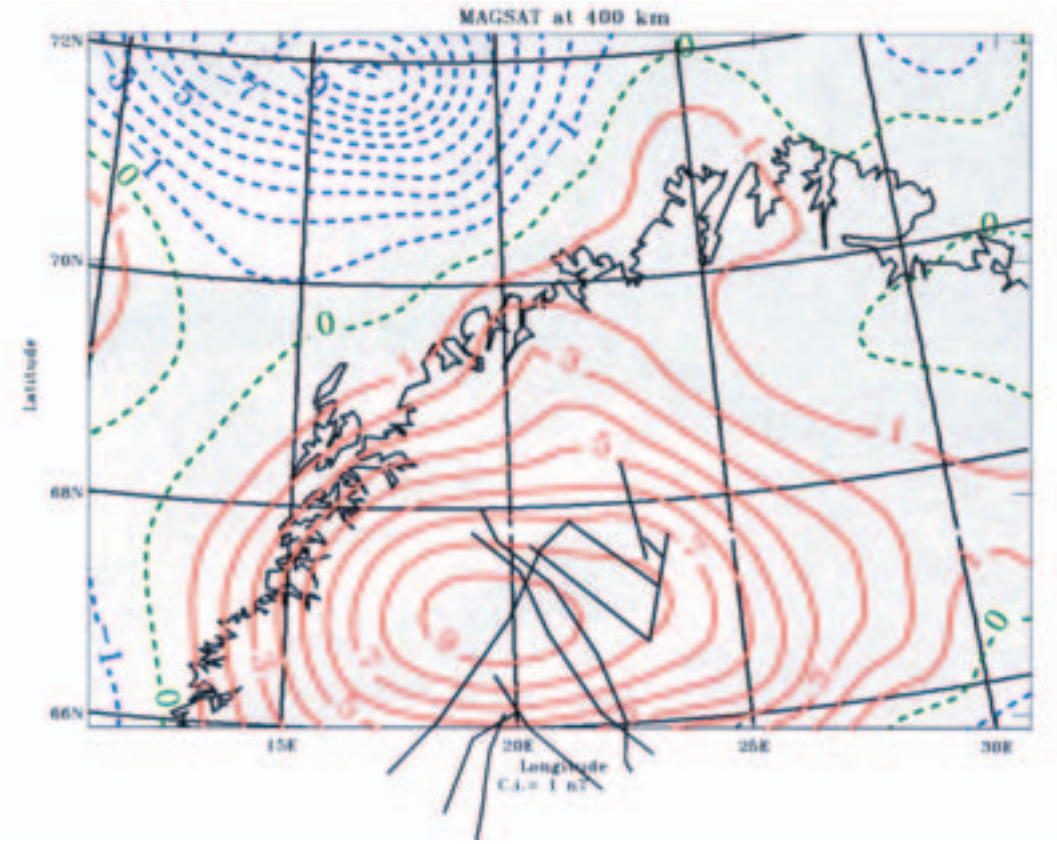

Figure 5.

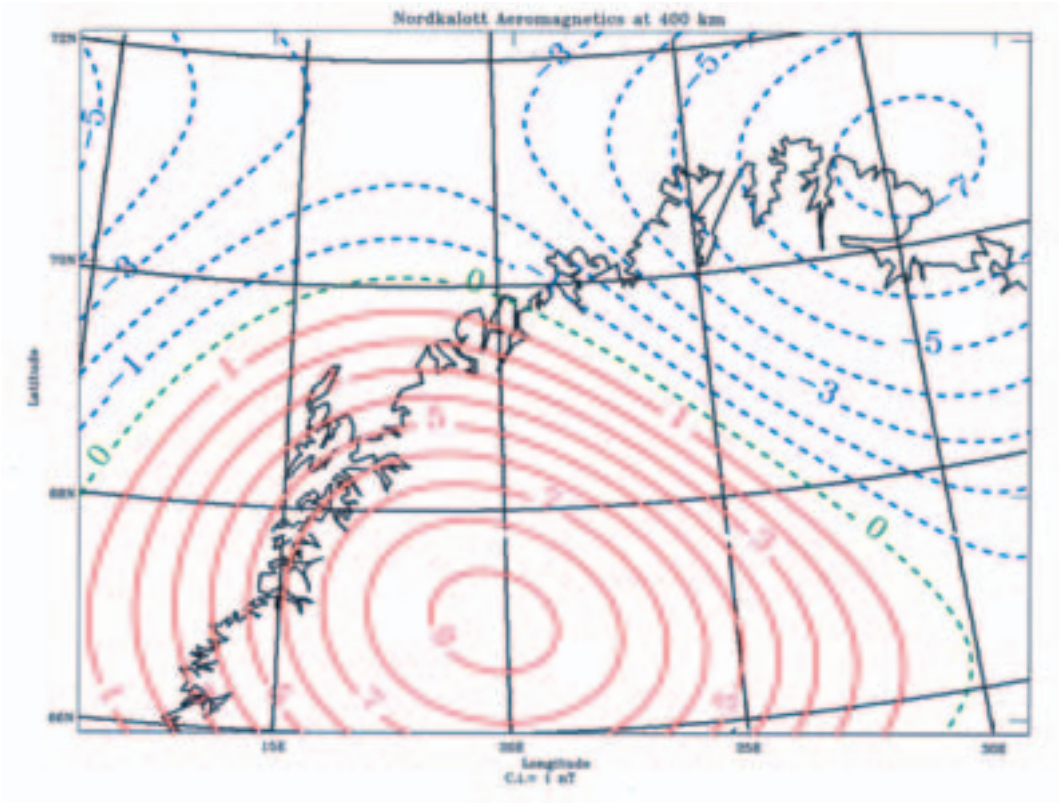

Figure 6.

In the Magsat map (Figure 5) the marine regions surrounding Norway are represented by predominately negative anomalies. The land area is dominated by a positive bulls-eye anomaly (the Kiruna anomaly) with a maximum value (>9 nT) centered 67 deg. N latitude and 20 deg. E longitudes near the city of Kiruna, Sweden. Extensive aeromagnetic surveying has been done across this region and these extremely detailed magnetic data reveal a concentration of high near-surface anomaly values (>6000 nT). The Kiruna region is the center of a complex nexus of magnetic highs. The mathematically upward-continued aeromagnetic data (Figure 6) shows these NORDKALOTT data at 400 km altitude have virtually the same anomaly pattern as the Magsat map. It is particularly noteworthy that the positive magnetic anomalies in both the satellite and upward continued aeromagnetic data are coincident and have the same value. This means that these data are both sensing the same anomalous magnetic body and that the Earth's main field has been correctly and completely removed from both data sets.

We made an estimate of the depth-to-source of the magnetic body from an analysis of these satellite magnetic anomaly data. The method used was originally developed by D. Ravat and P. Taylor and is based on the property that the rate of decrease of the anomaly amplitude with distance from the source is a known function. This method, which is best suited to nearly circular, isolated, large amplitude anomalies, yielded a depth of between 20 and 30 km for the source of the anomalous mass responsible for the Kiruna anomaly. Since the thickness of the Earth's crust in the Kiruna area is known to be less than 46 km this would place the magnetic source body in the mid to lower crust.

The major fracture zone of this region, based on geologic mapping, are superimposed on the Magsat anomaly map (Figure 5). The intersection of the major fracture zones lies very near the center of the Kiruna anomaly. It is, therefore, interesting to speculate that the anomalous magnetic mass causing the satellite-altitude anomaly is not only deep-seated but may also be related to the fracture zone pattern. It has been suggested by others that major lineaments play a role in

the emplacement of the ore deposits of Northern Sweden and that major mineralization of the upper crust is controlled or localized by large and deep fractures in the crust. The fracture zones could provide migration routes allowing lower crustal material to be emplaced in the upper crust.

Contact: Patrick Taylor, Geodynamics Branch, ptaylor@ltpmail.gsfc.nasa.gov

Geomagnetic Field and Geodynamo Modeling

The question of why the Earth possesses an (internal) geomagnetic field has been asked since Sir Gilbert in the 17th century. It wasn't until the 20th century that a consensus was reached: The Earth's outer core is a molten alloy of mostly iron plus a small percentage of lighter constituents. In much of the Earth's history, the planet cooled slowly to form a solid inner core, and latent heat was released and lighter constituents were depleted into the outer core. The buoyancy force then drives convection, generating and maintaining the geomagnetic field via a geodynamo process.

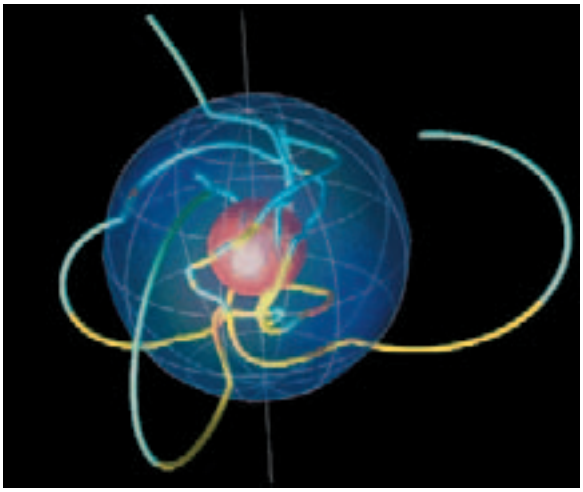

Figure 7: A snapshot of one magnetic field line through the numerical Earth's core from our numerical model MOSST. The red sphere represents the solid inner core, the blue opaque surface represents the core-mantle boundary (CMB). The orange segments indicate the field lines leaving the center, while the blue segments indicate those approaching the center.

We have developed a Modular, Scalable, Self-consistent, Three-dimensional (MOSST) numerical model to simulate core dynamics and geodynamo processes. This model is based on the Kuang-Bloxham model developed in 1999, with improvement in (1) implementation of three-dimensional angular momentum variation of the inner core, outer core and mantle, aiming at the studies of core-mantle interaction and Earth's rotation variation; (2) implementation of lower mantle heterogeneity in the model, aiming at the effect of thermal and magnetic heterogeneity on magnetic field secular variation and on core-mantle coupling; (3) transformation of the reference frame from a mathematical uniform rotation frame to the mantle reference frame for tasks (2); (4) modularization of numerical code to facilitate future geophysical plug-in applications and computational efficiencies.

Figure 7 shows a magnetic field line across the Earth's interior generated by MOSST. The zonal field line segments (e.g. toroidal field) is generated by stretching the meridional line segments (e.g. poloidal field) in zonal directions; the poloidal field, in turn, is generated by folding and twisting poloidal field line segments. Our research focuses on the physics of geodynamo action, the force balances inside the core, and the spatial and temporal behaviors of the magnetic field, targeted to predicting geomagnetic field secular variation, and studying the force-response of the solid Earth-core systems.

In 2001, we have studied (1) the effect of thermal heterogeneity on magnetic secular variation, solving for the magnetic field and the core flow with a heterogeneous thermal boundary condi-

tion based on seismic tomography of the lower mantle; (2) laboratory dynamos, obtaining numerical solutions for the experimental settings, to help design experimental dynamos; (3) prediction of geomagnetic field secular variation (on decadal timescales for geomagnetic field modeling, and on timescales of several thousands years for archeomagnetic and paleomagnetic studies) (See also the Core Flow and Core-Mantle Coupling entry in the Global Geophysical Fluids and Their Mass Transports section).

Contact: Weijia Kuang, Space Geodesy Branch, weijia.kuang.1@gsfc.nasa.gov

The South Atlantic Anomaly

The geomagnetic dipole axis of the Earth is offset from its rotation axis in the direction of the northwest Pacific. Because of this the geomagnetic field strength is relatively weak in the diametrically opposite position-- in the western South Atlantic Ocean. The geomagnetic field strength controls dangerous particle flux and radiation in the near Earth environment. Spacecraft and humans in low Earth orbits (a few hundred to 1000 km altitude) can suffer severe radiation damage when passing through this area. Instruments on spacecraft such as the Hubble Space telescope, Topex, Oersted, Shuttle, etc. have been affected by this radiation. This radiation will limit the time astronauts can spend on the Space Station. During severe magnetic storms the radiation can be deadly for astronauts on Extra Vehicular Activity.

This radiation originates, largely, from the corona of the sun and reaches low Earth orbit within one or a few hours. The science of "Space Weather" is concerned with attempts to predict the radiation environment of the Earth. So far predictions have not been very successful.

Measurements of the geomagnetic field in space define the focus of this radiation zone. The changes in the geomagnetic field strength with time indicate that the South Atlantic Anomaly is covering a larger and larger area and getting more intense, i.e. the field strength in this region is getting less as the years go by. There are no known ways to shield against this intense radiation.

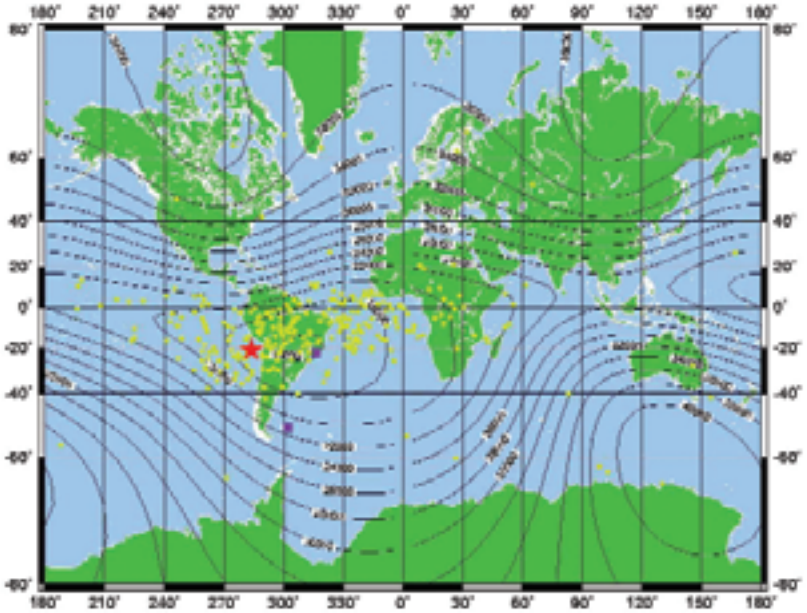

Figure 8. Red star shows where Modis had a problem in June, 2001. Yellow dots show where Topex had problems during 1992-1998.

Contact: James Heirtzler, James.R.Heirtzler.1@gsfc.nasa.gov

Geomagnetic Field

The geomagnetic field is described analytically by a spherical harmonic series. The amplitude of the various terms in the series is given by a set of coefficients, of various degrees and orders. Using these coefficients one can construct a power spectral curve. This interesting curve has two distinct parts. The much larger, short wavelength part is believed due to the Earth's main field at the core-mantel boundary and the lower amplitude, shorter wavelength part due to magnetized rocks of the Earth's crust. The longer wavelengths of the crust are hidden by the field of the main field and, conversely, the short wavelengths of the Earth's main field are hidden by the field of the crust.

We would like to know the full spectrum of crustal anomalies to study the tectonic of the crust. Several investigators have tried to discover the longer wavelengths due to the crust. Voorhies has shown that one can simulate the shorter crustal field, statistically, as randomly oriented dipoles over the surface of a sphere. Purucker and others have shown that if you assume the continents are magnetized a certain way one can build a full crustal anomaly spectra.

There are some alternative avenues that can be investigated. One would attempt to find how to separately estimate the main field and remove that, so as to leave the long wavelength crustal field. Another would be to review large area aeromagnetic surveys over known magnetic rocks to see how one separates main field from crustal field in these areas, and use that as a guide for other areas.

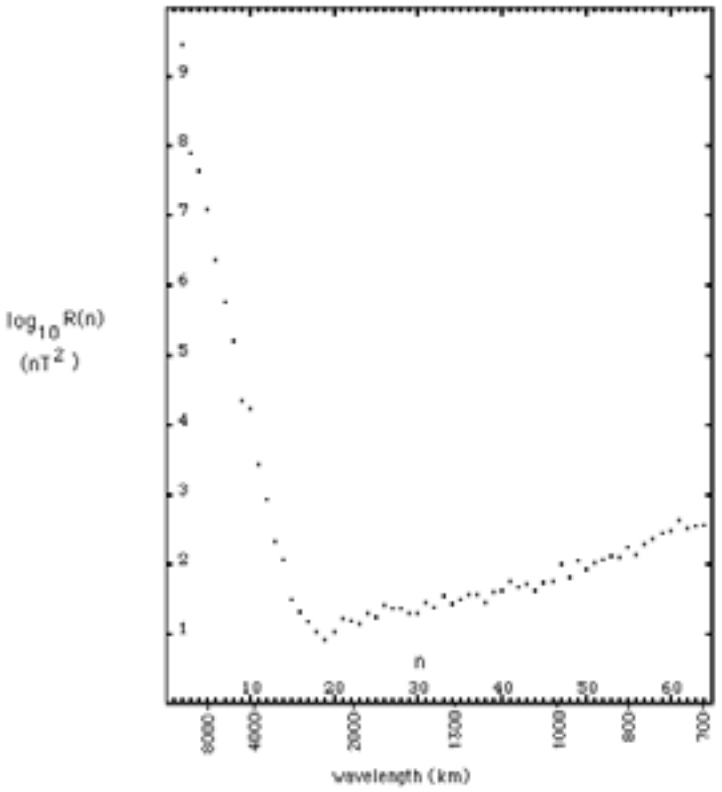

Figure 9. Geomagnetic field spectra as a function of spherical harmonic parameter n. The approximate wavelength is shown.

Contact: Jim Heirtzler, James.R.Heirtzler.1@gsfc.nasa.gov

Geomagnetic time variations in the Indian Ocean

To know the time variations of the geomagnetic field one needs to measure the field at the same place at two different times. This is easy to do with fixed land geomagnetic observatories, but these are widely spaced and do not cover the oceans. Although satellites do provide a measure of the secular variation of the field with track crossings or modeling the field at various times, they cannot provide a secular variation map with the necessary spatial resolution. Clusters of repeat magnetic stations on land show that the main field can change quasi-erratically over distances of a few hundred kilometers. Repeat stations have not been made over much of the land surface but the indication is that there may be cells of secular variation, where the variation in one cell may be different from that of an adjacent one. This information is keenly important to understand what causes the magnetic field of the Earth.

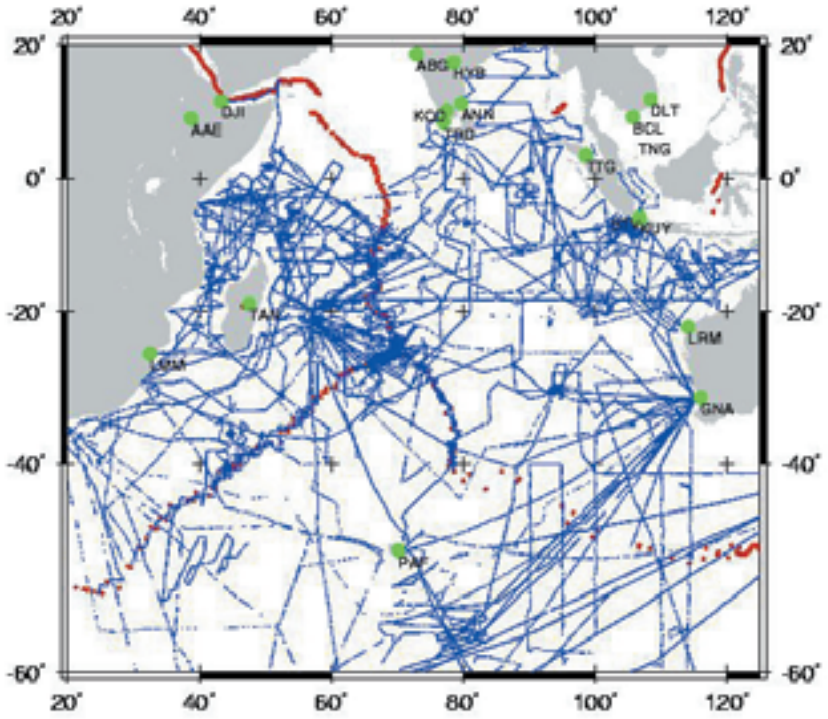

Figure 10. Ships tracks in the Indian Ocean, 1960-1980, where ships towed magnetometers. Track crossings yielded secular variation. Red dots define the mid-ocean ridge and trenches. Green dots are geomagnetic observations.

During the 1960's, 1970's, and 1980's there were more than 200 ship cruises which measured the geomagnetic field strength in the Indian Ocean. 75 of the longest of these were used to study results at track crossings. The accuracy of magnetic field readings by ships is usually within a few nanoteslas and the position is usually known to within a few hundred meters.

The general conclusion is that an apparent secular variation determined in this way may show a relatively large difference from the secular variation determined on a nearby track crossing or from nearby land observatories. Values found for the western Indian Ocean are more nearly like values from observatories there. There is a tendency for secular variation values to be more negative than from satellite results. This study does not preclude cells of secular variation although their limits cannot be prescribed.

Contact: Jim Heirtzler, James.R.Heirtzler.1@gsfc.nasa.gov

Crustal Deformation

GPS field measurements of point positions taken over several years provide crustal motions that are used to investigate the subduction zone process, especially where large earthquakes are a significant hazard. Of particular interest are shallow dip subduction zones where both earthquakes can be great and mountain building extensive. Active folds and faults on Kodiak Island, Alaska were identified using Landsat imagery, DTED and kinematic GPS elevation data. Anomalous motions not easily explained by either current plate motion or as long term post-seismic effects have been observed in the Kenai Peninsula area of Alaska. Crustal motion data has been used along with visco-elastic modeling to estimate the thicknesses of the converging Pacific and Australian plates near New Zealand, as described below. Ongoing studies of paleolakes have concentrated on Lake Bonneville and Lake Lahonten in the Western US where unusual upper mantle structure appears to exist. In these lake rebound studies GPS measurements provide the elevation of past shorelines and bio-stratigraphic markers provide a time reference that permits reconstructing the rebound history following loss of the water. On a global scale, the satellite-laser ranging network has been measuring the inter-plate tectonic velocities as well as vertical deformations at the stations, refining the plate tectonic model and contributing to better definition of the terrestrial reference frame.

Crustal Deformation and Earthquake Hazard at Kodiak Island, Alaska

The Kodiak Islands are located in the eastern Aleutians of Alaska and lie approximately 140 to 250 km from the Alaska-Aleutian trench. The Pacific plate is subducting beneath the North American plate near Kodiak Island at a rate of about 57 mm/yr. Since Kodiak Island lies within the southern extent of rupture from the great (M=9.2) 1964 Prince William Sound earthquake, we might not expect a large earthquake to occur in this region in the near future. But there is still a significant earthquake hazard in this region. The faults located above the plate interface could slip in large earthquakes. In fact, geologic work done by a co-investigator (G. Carver, Humbolt State University) shows that there are numerous crustal faults across the Kodiak Islands which have slipped in earthquakes in the last 100,000 years.

To quantify the rate of ongoing crustal strain, we established geodetic sites at a range of distances from the trench, and in addition established some coverage parallel to the trench, on the portion of the island accessible by roads. Changes in the rate and orientation of short-term strain across the northern, populated part of Kodiak Island have been estimated from GPS measurements made by us between 1993 and 2001. This field observation program included, in 1995, 1997, and 1999, an educational outreach program with Kodiak Island High School, funded in part by a GSFC Director's Discretionary Fund (DDF). Students participated in setting up observing sites, recording data, and analyzing the results. Although most of these GPS observations were made using temporary portable stations, in 1999 a permanent GPS site (KODK) was established (using support from the DDF) that is now part of an international, global GPS network. KODK is run and maintained by Kodiak Island High School Earth Science teacher Eric Linscheid. A description of this collaborative research program with NASA by Linscheid can be viewed at http://www.koc.alaska.edu/nasa/index.html.

Figure 11 shows a shaded relief digital elevation map of the northeastern segment of Kodiak Island. The location of GPS sites in which horizontal velocities have been estimated are shown. Both orientation and magnitude of the horizontal motions are displayed. The location of the Kodiak launch facility is given by ^ and the city of Kodiak by #.

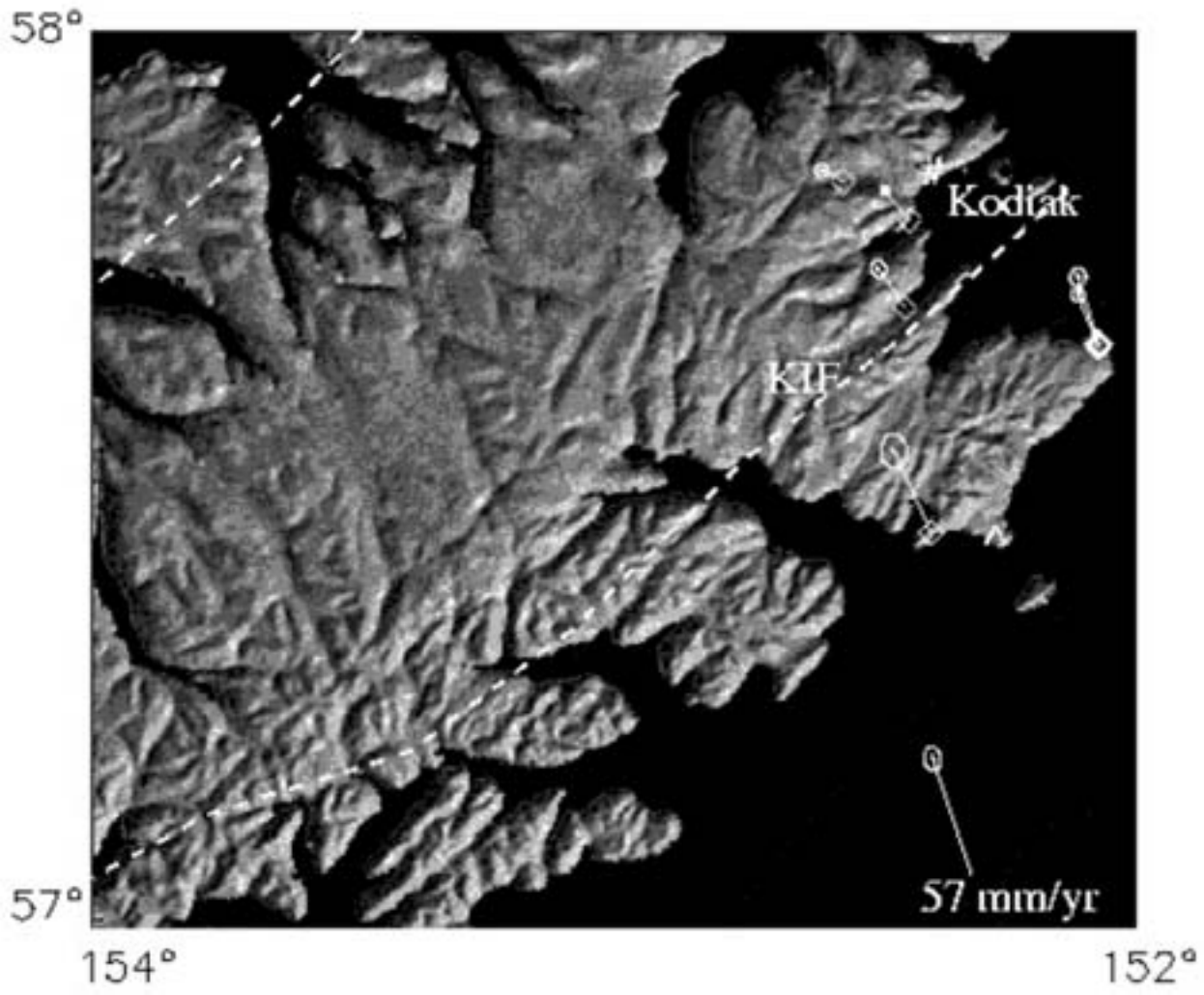

Figure 11.

The rate of ongoing crustal deformation across the Island ranges from up to 20 mm/yr along the eastern coast near the Kodiak Launch facility to 7 mm/yr east of the city of Kodiak. Locking of the plate interface at shallow depths is the process exerting the greatest influence on the horizontal, interseismic rate of deformation shown in Figure 11. Most of the deformation can be accounted for by this mechanism. Note in Figure 11 that the orientation of the short-term deformation rates of the sites located near the east coast of Kodiak Island are similar to the plate motion vector, as expected for a locked main thrust zone. The orientation of site vectors west of the fault "KIF", however, are rotated counter clockwise (more westerly). These results suggest that, in addition to eventual thrust faulting on the main plate interface and crustal shortening, some strike-slip motion may occur on faults within the overriding plate.

Contact: Jeanne Sauber, Geodynamics Branch, jeanne@steller.gsfc.nasa.gov

Tectonic Plate Coupling and Elastic Thickness from Space Geodetic Measurements of Crustal Movements

Measurements of crustal movements in seismic zones provide insight into earthquake processes and properties of the Earth's crust and mantle. Cohen and Darby (2001) recently showed that geodetic measurements of crustal movement, can be used to simultaneously determine the strength of coupling between interacting tectonic plates (a measure of how large an earthquake might occur in the region) and the effective elastic thicknesses of the lithospheric plates (a measure of the depth range over which the earth is mechanically strong enough to support stresses without significant viscous flow).

In the past lithospheric thicknesses have been determined by examining the deformation of the earth in response to long time-scale loading. For example, measurements of the bending of tectonic plates under seamounts (underwater volcanoes) or sedimentary basins have shown that oceanic plates typically have an elastic thickness between 10 and 50 km and continental plates have similar or greater elastic thicknesses. An important aspect of these determinations is that the applied stresses persist for very long times, 1 million to 100 million years.

In the case of the earthquake cycle, however, stress accumulation and release takes place over much shorter time: 100 to 1000 years. It is possible that flow in the higher viscosity portions of the earth may not occur and tectonic plates may have a greater effective elastic thicknesses. Cohen and Darby investigated this possibility. A dense set of GPS-derived crustal velocities were used in combination with an elastic-viscoelastic model of crustal deformation to determine the coupling and elastic thicknesses near the Hikurangi trough at southern North Island, New Zealand, a part of the Australian-Pacific plate boundary region shown below (Figure 12).

Figure 12.

At the southern Hikurangi Trough the Pacific Plate approaches the Australian plate with a relative velocity of ~39 mm/yr. The approach is highly oblique, with the angle between the relative plate motion and the normal to the Hikurangi Trough being about 60 degrees. The GPS-derived crustal velocity field for this region, published recently by Darby and Beavan (2001), and a finite element model of the obliquely convergent plate boundary, are shown below (Figure 13).

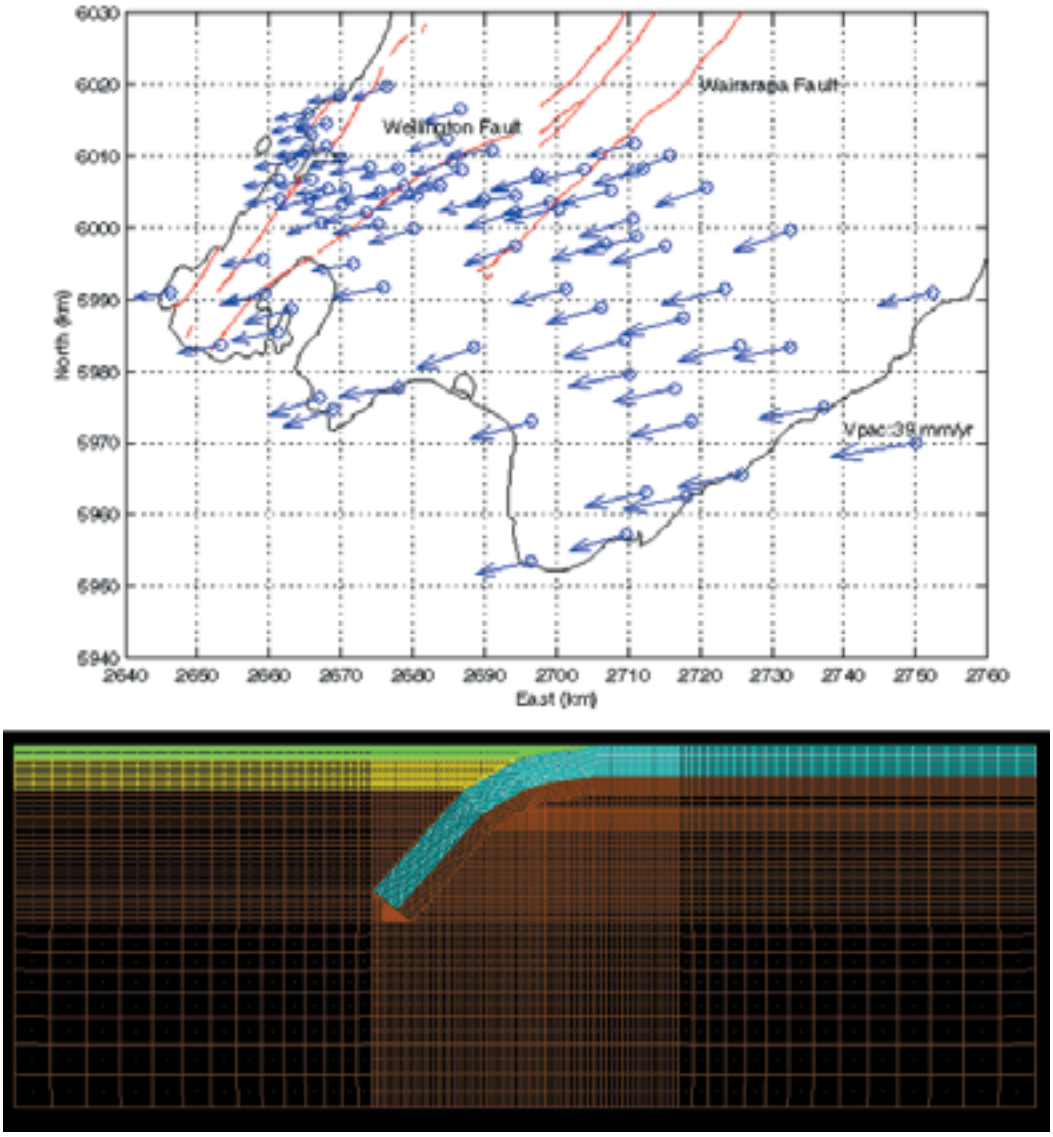

Figure 13.

An important feature of southern Hikurangi region is that, although it is very active seismically on a geological time-scale, there has been no major earthquake since 1855. Thus, any transient response to the last earthquake has long since dissipated and the crustal velocities can be described using a steady-state model whose behavior depends on the plate coupling and plate elastic thicknesses. For given values of plate thickness, the coupling is obtained by mathematical inversion techniques applied to the finite element model and the GPS data. The thicknesses are then systematically varied to find a best fit between observed and predicted velocities (as measured by the reduced chi-squared parameter) as well as the range of model parameters that are statistically consistent with the observations. Figure 14 shows the set of reduced chi-squared

contours derived by Cohen and Darby, using a seismological constraint that the Young's modulus of the Australian crust is a factor of two smaller than the Young's modulus of the mantle and Pacific Plate.

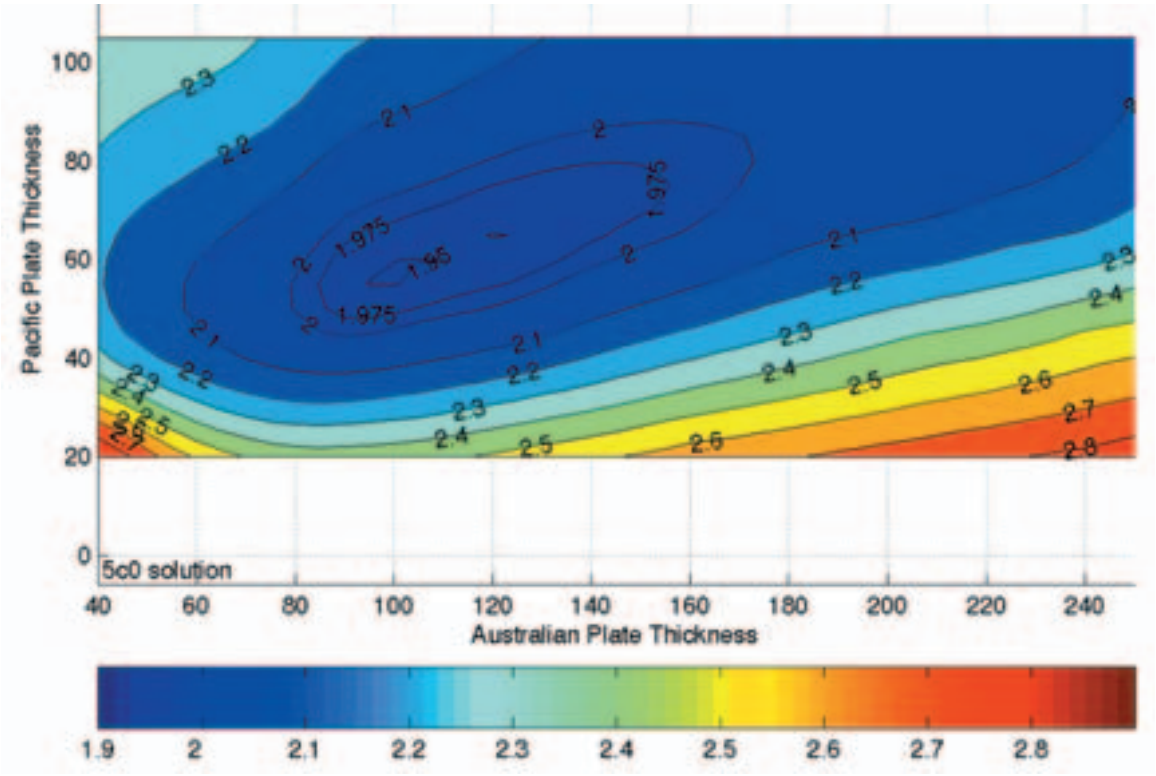

Figure 14.

From this Figure and the associated analysis, Cohen and Darby concluded that:

(1) The "best" value for the thickness of the Pacific and Australian plates are, respectively, about 45-65 and 100-125 km (but the range of acceptable values, as indicated by the blue region in Figure 14, is large). Alternatively, smaller thicknesses were obtained when the Young's modulus contrast was increased above the values derived from seismic velocity data. There are no estimates of long-term plate thicknesses in this region of New Zealand, but estimates of the thickness of the Australian plate at the Wanganui basin (200 km to the northwest) indicate a value of about 15 km. The geodetic results suggest that the apparent elastic thickness in response to earthquake stress is, as suggested above, greater than the thickness associated with long time-scale geologic (plate motion) processes.

(2) The results explain why simple infinite elastic half-space models of interseismic strain accumulation seem to "work", i.e. provide a reasonable fit to the data, even though the plates do have finite thickness. The continental plate is thick, although not infinitely so and the oceanic plate is stronger than the continental plate. Both of these conditions suppress the surface effects of viscous flow at depth.

(3) The trench normal component of the crustal velocity field is much more diagnostic for discriminating between model parameters than the trench parallel component. This result has implications for planning future ground and space based observations of crustal motions in this kind of tectonic setting.

(4) The coupling coefficient (which can take on values between 0 and 1) is > 0.8 to depths of 20-

25 km. This indicates that the plates in this region are currently strongly coupled. The coupling strength at very shallow depths cannot be estimated because there are no geodetic observations over the shallow part of the zone (which lies in the ocean). However, the estimates of coupling at seismogenic depths (where earthquakes are generated) are virtually unaffected by this ambiguity. This an important conclusion for seismic hazard estimation.

Because some of the aspects of this work were surprising and have potential importance for both earthquake hazard studies and for basic tectonic modeling, efforts are now underway to determine whether the results for New Zealand are replicated elsewhere.

References:

Cohen, S.C., and D.J. Darby, Tectonic plate coupling and elastic thickness derived the inversion of geodetic data using a steady-state viscoelastic model: Application to southern North Island, New Zealand, J. Geophys. Res. (submitted), 2001.

Darby, D.J. and J. Beavan, Evidence from GPS measurement for contemporary interplate coupling on the southern Hikurangi subduction thrust and for partitioning of strain in the upper plate, J. Geophys. Res., 106, 30881-30891, 2001.

Contact: Steven C. Cohen, Geodynamics Branch, scohen@carnoustie.gsfc.nasa.gov

Satellite Laser Ranging Measurements of Vertical Motion

For over three decades, the global SLR network has provided precision orbit determination, Earth orientation and station motion resolution to the scientific community, tracking a growing number of satellites with an evolving network of stations. The SLR-defined horizontal velocity models of the late 1980's first showed that the relative velocities of stations on the stable interiors of tectonic plates were about five percent slower than those expected from the geophysical models of that era. This observation supported the 1994 revision of the Potassium/Argon-defined paleomagnetic time scale based on astro-geochronology. The latest velocity field defined by the SLR network in Figure 15 shows the agreement with the prevailing model at a scale which illustrates the centimeter per year velocities of the tectonic plates.

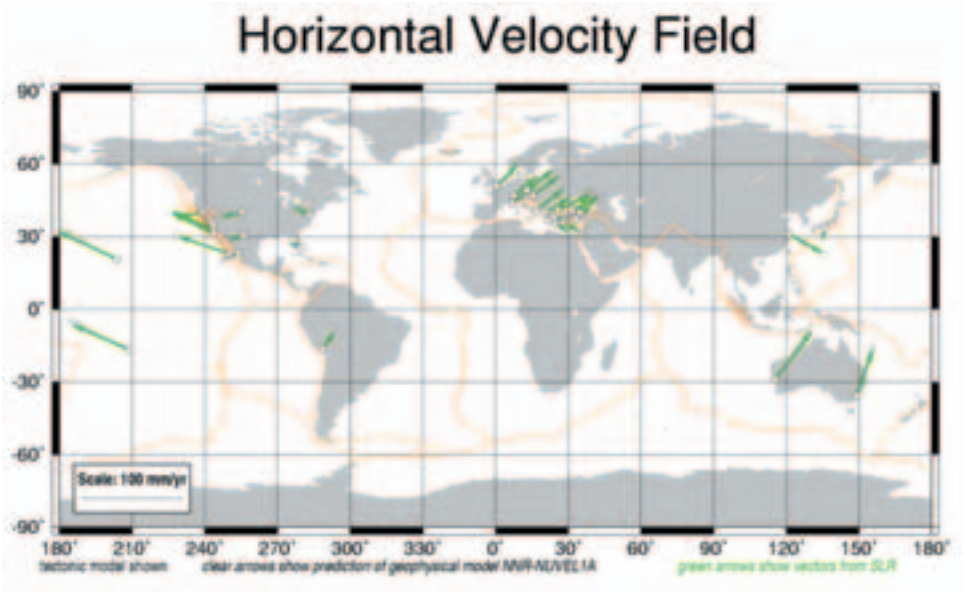

Figure 15. Comparison between the SLR velocity model and the geophysical model.

The ability of the SLR systems to accurately define Earth scale can also be used to monitor vertical movement; in particular the effect of post-glacial rebound (PGR) from Laurentian and Fenno-Scandian ice loading. This is known to affect polar locations at a level which is an order of magnitude less than the tectonic plate velocities, and at an even lower level of less than two millimeters per year outside the region of glaciation.

The twenty year record of vertical position at SLR stations tracking the LAGEOS satellite contains signals with periods between hours and years, as well as the long-term effects of crustal movements and post-glacial rebound. On-going advances in overall system accuracy, in conjunction with improved satellite, Earth, orbit perturbation and relativity modeling now allow us to use the SLR measurements to detect these subtle motions.

The sites capable of PGR model assessment are shown in Figure 16. They all lie in the region of fore-bulge collapse, for which the Fenno-Scandian model predicts subsidence in Europe of about one mm/year. On the other hand, the Laurentian model predicts a subsidence of more than two mm/year at the Goddard Geophysical and Astronomical Observatory, which is a strong signal for results that reach an accuracy of better than 1/2 mm/year for these observations. Most of the other stations in the SLR network exhibit vertical motion less than 1/2 mm/year as expected.

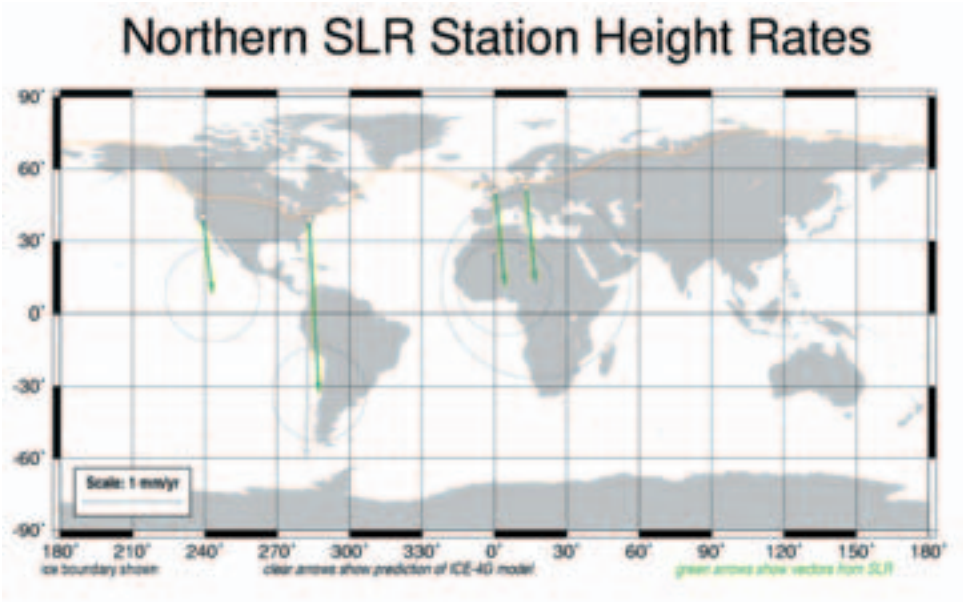

Figure 16. Comparison of SLR fore-bulge collapse values with the geophysical model.

Independent measures of PGR from space geodetic instruments will further the knowledge of coastline dynamics allowing more precise measures of present-day sea level changes. Continuing measurements of plate boundary deformation provides observational constraints necessary to address fundamental questions about the vertical and horizontal structure of the lithosphere, to understand plate-driving forces, and to clarify the behavior of the viscosity and dynamics of the upper mantle as it contributes to lithospheric deformation. Horizontal motion associated with post-glacial rebound is an order of magnitude less than in the vertical, although it is actually more sensitive to possible vertical variations in mantle viscosity. That sub-millimeter per year accuracy requirement remains as a challenge for future analysis of the SLR observations.

Contact: Ronald Kolenkiewicz, Space Geodesy Branch, Ronald.Kolenkiewicz.1@gsfc.nasa.gov

Topography and Surface Change

Airborne and spaceborne laser altimetry provide the basis for studies of areas where geological hazards exist (such as earthquakes, volcanoes, coastal erosions). In cooperation with USGS and local agencies, an intense study of the Puget Sound area in Washington State has revealed new details of previously unknown faults and better characterization of other landforms (e.g., beach terraces) related to active faulting. Many of these are hidden beneath dense canopy which airborne lidar can penetrate to provide information on both canopy structure and the "bare Earth" structure. Calibration and validation studies for the future laser altimeter instrument GLAS on ICESat have been ongoing and calibration sites in Alaska, Washington State and in the Western United States have been selected to help cover the major kinds of surfaces (mountainous glacial, faulted vegetated, flat dessert) the lidar will measure. Technology development is focusing on imaging lidar capability, such as single photon counting, scanning and swath mapping. Planning is underway for a third Shuttle Laser Altimeter flight to demonstrate this capability.

To enable such high-precision measurements requires the capability of precision orbit determination of the satellites, which brings a unique set of challenges and possibilities. New software are being developed and have been successfully applied, to obtain optimal solutions for orbit, instrument calibration parameters, and biases, in conjunction with the present state-of-the-art gravity model for the Earth (see Precise Orbit Determination section below).

New versions of a Digital Tectonic Activity Map have been produced, and these have become very popular outreach items on the World Wide Web. Also, as described below, a major new book on the role of satellites in "Exploring Space, Exploring Earth" will be published in the summer of 2002.

Puget Sound Faults and Earthquake Hazards

The densely populated Puget Lowland of western Washington occupies a dynamic geologic setting in the North American plate above the Cascadia subduction zone. Oblique plate convergence along the subduction zone subjects the Lowland to damaging earthquake and volcanic hazards and helps create landslide-prone topography in the poorly consolidated materials typical of active convergent margins. Traditional remote-sensing technologies are of limited utility in identification and assessment of these hazards, due to the difficulty in imaging the ground surface through the dense cover of vegetation. Indeed, the subtle tectonic landforms associated with recent earthquake deformation are essentially invisible beneath the forest canopy.

"Finding active faults and tectonic landforms in densely forested regions using Airborne Laser Terrain Mapping (ALTM), Puget Lowland, Washington" is an ongoing collaboration between the USGS (Sam Johnson, PI) and the Geodynamics Branch which addresses this problem. The program is funded by the Solid Earth and Natural Hazards programs of NASA HQ. Mid-way through the project, the following have been accomplished:

(1) The project has fostered a partnership between the USGS, NASA and seven local government agencies, forming the Puget Sound Lidar Consortium (PSLC). The PSLC has pooled resources to acquire 4800 km^2 of ALTM data in 2000 and 2001, and is scheduled to collect an additional ~2500 km^2 of data in 2002.

(2) Discovery of five previously unknown linear scarps up to 6 m high in the ALTM "bald Earth" imagery that are interpreted as surface ruptures of large earthquakes, based on the results of trenching across two of the scarps. The ALTM imagery also enables detailed elevation measurements of uplifted and tilted shoreline terraces bordering Puget Sound that reveal actively growing folds produced by slip on the faults.

(3) The USGS and NASA, together with the Terrapoint, LLC, have developed new algorithms to derive "bald Earth" topographic maps in heavily forested terrain (see Figure 17) and have made major improvements in data acquisition and quality control procedures.

(4) ALTM images have proven to be an essential tool in regional landslide hazard assessment.

An example of the ALTM data acquired along a river valley is shown in perspective views of the canopy top and the underlying "bald Earth", derived by filtering the data to remove laser returns from vegetation and buildings (Figure 17). The images are produced from digital elevation models at 1.8 m spatial resolution and depict an area 2.1 x 1.3 km in size. No vertical exaggeration is applied. The "bald Earth" image reveals a previously unmapped landslide deposit that was hidden beneath the vegetation cover.

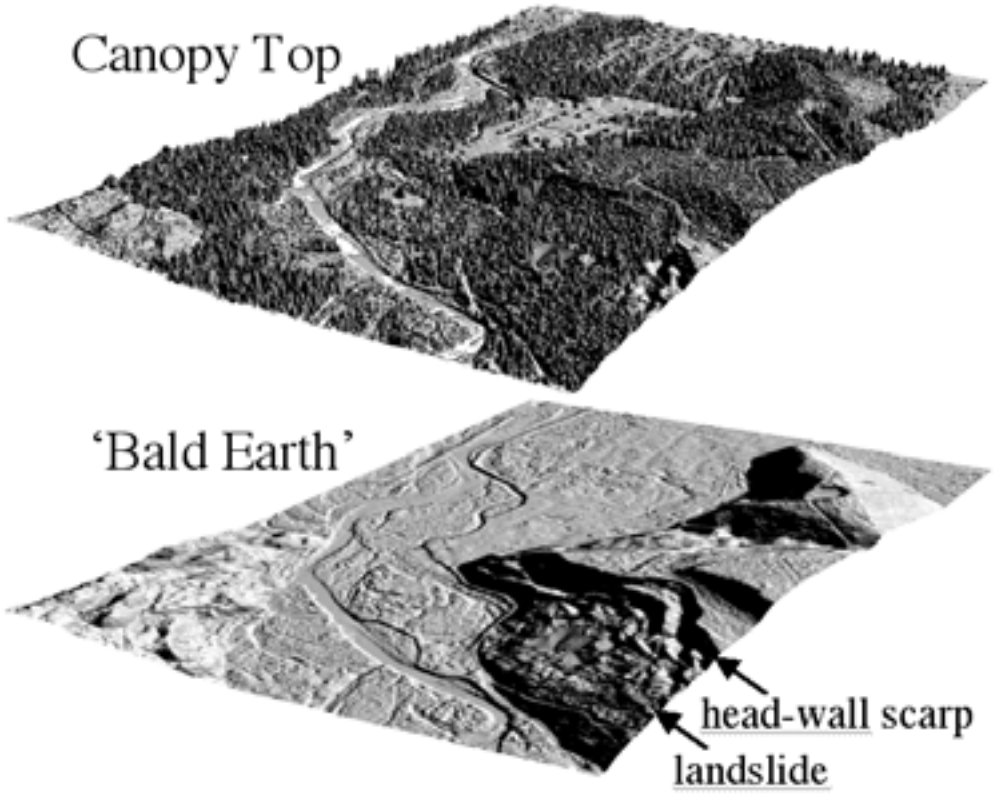

Figure 17.

Contact: David Harding, Geodynamics Branch, harding@core2.gsfc.nasa.gov

ICESat Laser Altimetry: Calibration Techniques for Precision Geolocation for ICESat-Waveform and Profile Matching to Digital Elevation Models

In the thirty years since the launch of the Skylab radar altimeter, satellite altimetry has proven to be a powerful tool for mapping the topography of the Earth and other planets. To fully exploit the data obtained from an orbiting altimeter, it is necessary to calibrate certain parameters not only before launch but also after the altimeter is in orbit. In preparation for the launch of the ICESat

mission, ICESat science team member Jack Bufton and his LTP co-investigators (D. Harding, S. Luthche, D. Rowlands and J. Sauber) have developed a number of calibration techniques for the ICESat laser altimeter. These include the integration of multiple tracking data types with planned pointing maneuvers over oceans, as well as matching waveforms and profiles to land DEMs (Digital Elevation Models) [Rowlands et al., 2000]. The analysis of residuals for geolocated laser footprint tracks can assess the relative accuracy and reproducibility of the resulting geolocation. These analyses do not make possible the assessment of the absolute accuracy or systematic errors of a geolocation result, however.

Comparison of geolocation results to accurate DEM's does provide a means to assess the absolute accuracy and systematic errors of the laser footprint position, and to evaluate alternate geolocations methods. The comparison can be done based on differencing elevation profiles or waveforms with respect to an accurate DEM. In profile matching, the elevation for each footprint along a profile is differenced with respect to the corresponding DEM elevation. With the ability of laser altimeters to digitize the backscattered energy (and therefore produce waveforms), the waveform matching approach potentially has greater sensitivity in assessing footprint geolocation than the profile matching. Waveform matching is accomplished by minimizing the residual between within-footprint surface height distributions as recorded by the observed waveform and a simulated waveform derived from an accurate DEM.

The waveform matching approach is being assessed prior to launch in order to establish the DEM characteristics required for validation purposes. We are conducting sensitivity studies with various DEMS. The studies consider DEM resolution, accuracy, extent, vegetated versus non-vegetated, rugged versus smooth topography, and uniform versus spatially varying reflectance. One of the DEM's that has been used is a 1.8 m resolution DEM of a 2350 sq km area of western Washington State acquired for the Puget Lowland Lidar Consortium. Results of airborne lidar studies in that vegetated area are described elsewhere in this section. To assess ICESat performance over Alpine glaciers we are also using a DEM from part of the Bagley Ice Field and Seward Glacier in southern Alaska.

References:

Rowlands, D.D., C.C. Carabajal, S.B. Luthcke, D. J. Harding, J.M. Sauber, and J.L. Bufton, Satellite Laser Altimetry: Orbit Calibration Techniques for Precise Geolocation,

The Review of Laser Engineering, vol. 28(12), pp. 796-803, December, 2000. Contact: Jeanne Sauber and David Harding, Geodynamics Branch, jeanne@steller.gsfc.nasa.gov

"Exploring Space, Exploring Earth: New Understanding of the Earth"

A book which summarizes the impact of space research on solid earth geophysics and geology is now in production and will be published by Cambridge University Press in 2002. The book is written from the unique perspective of Paul Lowman, the first geologist hired by NASA (in 1959) who has been involved in both space exploration and study of the Earth from orbit. This dual career provided access to almost all aspects of geological and geophysical research carried out by NASA and GSFC scientists.

A foreword by Neil Armstrong summarizes classic efforts to determine the size and shape of the Earth in ancient Greece. The first major chapter reviews space geodesy, a field founded by the late John A. O'Keefe (to whom the book is dedicated) with discovery of the "pear-shaped earth" from Vanguard tracking data in 1959. The next chapter covers crustal magnetism as revealed in data from satellites such as Magsat, the launch of which in 1979 propelled Goddard to the forefront in this new field of study. Remote sensing from Earth orbit follows, with extensive exam-

ples of Landsat imagery and that from other satellites, including Terra (see Figure 18).

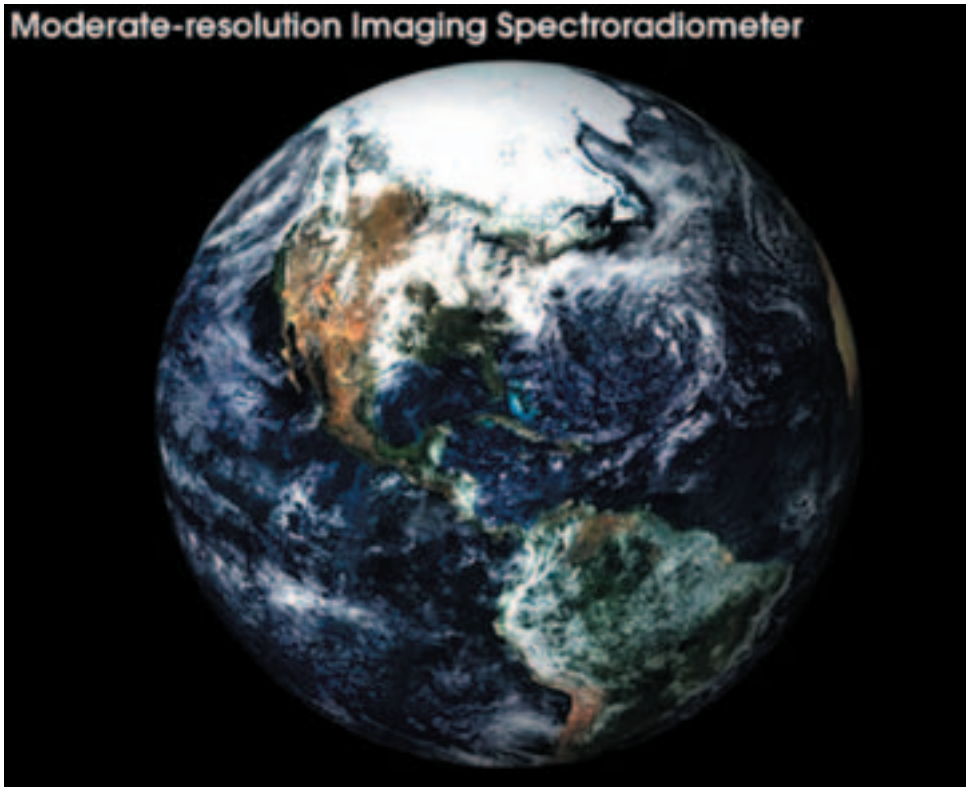

Figure 18.

To this point, the book has been primarily focused on the direct results of space research in geology and geophysics. Later chapters cover a wider range of topics that apply, perhaps less directly, to the study and understanding of the Earth. Among these are impact cratering and comparative planetology as they relate to evolution of the Earth's crust. The final chapter discusses the effect of life on terrestrial tectonics. This is interpreted through the Gaia Hypothesis, in which the Earth is thought to have various parameters, such as temperature, regulated by life. The book describes a "biogenic theory of tectonic evolution," in which the broad structure of the earth is the result of biologically-promoted sea-floor spreading and related phenomena superimposed on a crustal dichotomy formed by catastrophic impacts on the early Earth. The final line of the book describes the Earth as it might be reported by an interstellar visitor: "It is unique, a uniqueness that may be due primarily to its life. "

"Exploring Space, Exploring Earth" is a synthesis of scientific progress over many decades from many contributors, but also provides a comprehensive summary of the achievements of scientists and engineers at Goddard Space Flight Center.

Contact: Paul Lowman, Geodynamics Branch, lowman@core2.gsfc.nasa.gov

Mars Geology and Geophysics

The Mars Orbiter Laser Altimeter (MOLA) on board the Mars Global Surveyor (MGS) mapped the topography of Mars until the end of June, 2001, producing more than 600,000,000 precision ranges to the surface and clouds of the planet. The MOLA Science Team released in 2001 a Gridded Data Product of the topography of Mars, at a resolution 64 pixels/degree (better than 1 km) and accuracy of 1 meter with respect to Mars' center of mass. MOLA data is the basis for numerous studies of Mars, of both its topography and its gravity field. Discovery of a very large population of buried impact basins below the plains in the northern lowlands has provided important constraints on the origin of the crustal dichotomy and the age and nature of the lowland crust. As described below, it appears the lowlands formed extremely early in Martian history, which has implications not only for crustal evolution but perhaps also for the possibility of life. Accumulating evidence for extremely young volcanic flows and features on Mars, observed not only by high resolution images but also shown by their fresh topographic character as revealed by MOLA data, raises the possibility that Mars may still be, at least locally, warm and active. Constraints on eruption rates and inferences of volcanic style have also been made, supported by laboratory and theoretical work constrained by terrestrial data on known flows. Much of this work has been carried out in collaboration with students from various high schools and universities, and has benefited enormously from in-house graphics software development using IDL. A program GRIDVIEW, as described below, has reached a mature state in which staff and even short-term visitors can rapidly study and analyze MOLA gridded data to address a wide variety of problems.

Experience with magnetic field satellites in low orbit around the Earth (e.g., Magsat) has been applied to the study of crustal magnetic anomalies discovered on Mars. Techniques for representing the anomalies in terms of dipole sources were used to produce an improved description of the anomaly field. A comparison of the spectral characteristics of the Earth and Mars fields dramatically shows the difference between the mostly induced crustal anomalies of the Earth and the remanent anomalies on Mars, and emphasizes the much greater strength (and inferred magnetization) of the martian sources.

The tracking of the MGS spacecraft provide data for new Martian gravity field models, which represent a quantum leap from previous models derived from tracking data of earlier spacecraft. Called MGM-1025, the state-of-the-art model solutions, complete to spherical harmonic degree 70, revealed the gravity field of the planet in unprecedented detail. It also provided the foundation for the MGS precise orbit determination (POD, using the software GEODYN, see section below), which in turn enables the solution of the altimetry data provided by MOLA instrument discussed above.

Ancient Lowlands on Mars

The BIG problem in martian geologic evolution is the origin of Mars' fundamental crustal dichotomy: the separation of the crust into two quite distinct "hemispheres". The southern parts of Mars are generally high and heavily cratered, an indication of their great antiquity. The northern lowlands are 3-5 km lower and covered by plains which, based on their much smaller number of craters, must be much younger that the highlands.

The origin of this crustal dichotomy is a problem of both how and when it occurred. Some have suggested formation of the lowlands occurred in the middle period of martian history (the Hesperian epoch) while others believe the dichotomy dates to the Noachian, or early portion of Mars history. How the crust of Mars became separated into these two distinct provinces has been a matter of controversy for as long as the dichotomy has been recognized. Explanations have ranged from purely exogenic (a single giant impact or several very large impacts) to purely endo-

genic (internally driven processes including mantle convection, sub-crustal erosion, or perhaps plate tectonics). One problem with understanding the origin of the dichotomy is that the nature of the lowland crust below the plains was previously unknown.

Frey and coworkers showed that MOLA data reveal the presence of what are most likely buried impact basins below the visible surface of Mars (Frey et al., 1999, 2001). These "Quasi-Circular Depressions" (QCDs) are generally not visible in imaging data but well shown by stretched color and contoured MOLA data. A search for these in the relatively young lowlands revealed a very large number (644) larger than 50 km in diameter (Figure 19). Of these, only 90 were visible in Viking imagery.

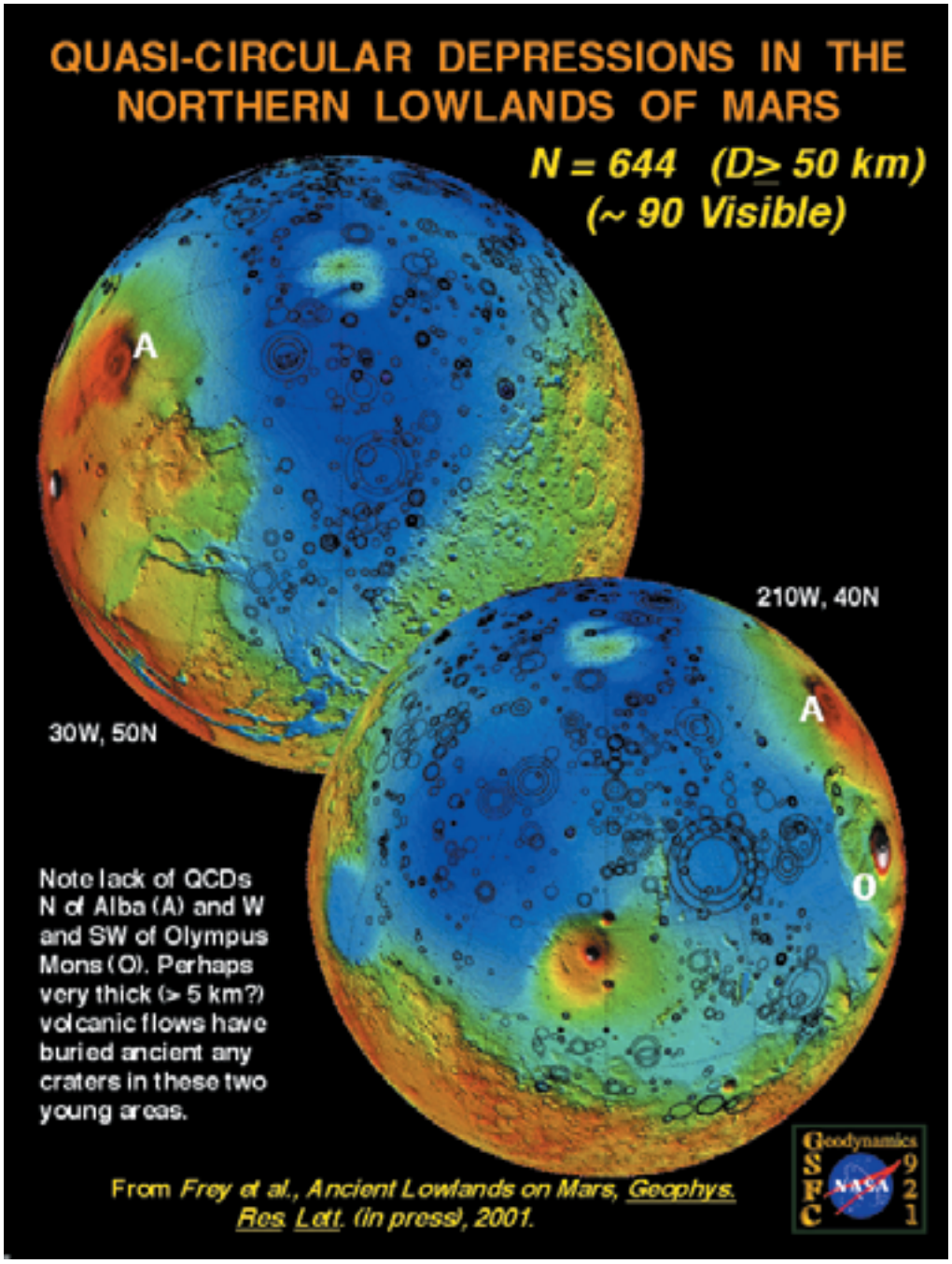

Figure 19.

That means that 85% of the population lies below the plains and that underlying crust is very old. It also implies the plains are relatively thin, so that relic topography still shows through. Cumulative frequency curves (cumulative number larger than a given diameter per unit area versus diameter) show that the buried lowland surface (below the plains) is older than the visible highland surface (but not as old as the buried highland surface). Furthermore, comparison with crater counts done on smaller areas of designated geologic units whose relative stratigraphy is known suggest the buried lowland crust is Early Noachian in age, dating from the earliest time period in martian geologic history, the time of intense cratering. But when did it become low? Unless there is some way to lower an already cratered surface without destroying the craters (that today we see as the buried QCDs), the lowlands must have been lowered during the period of intense cratering, as indicated in Figure 20.

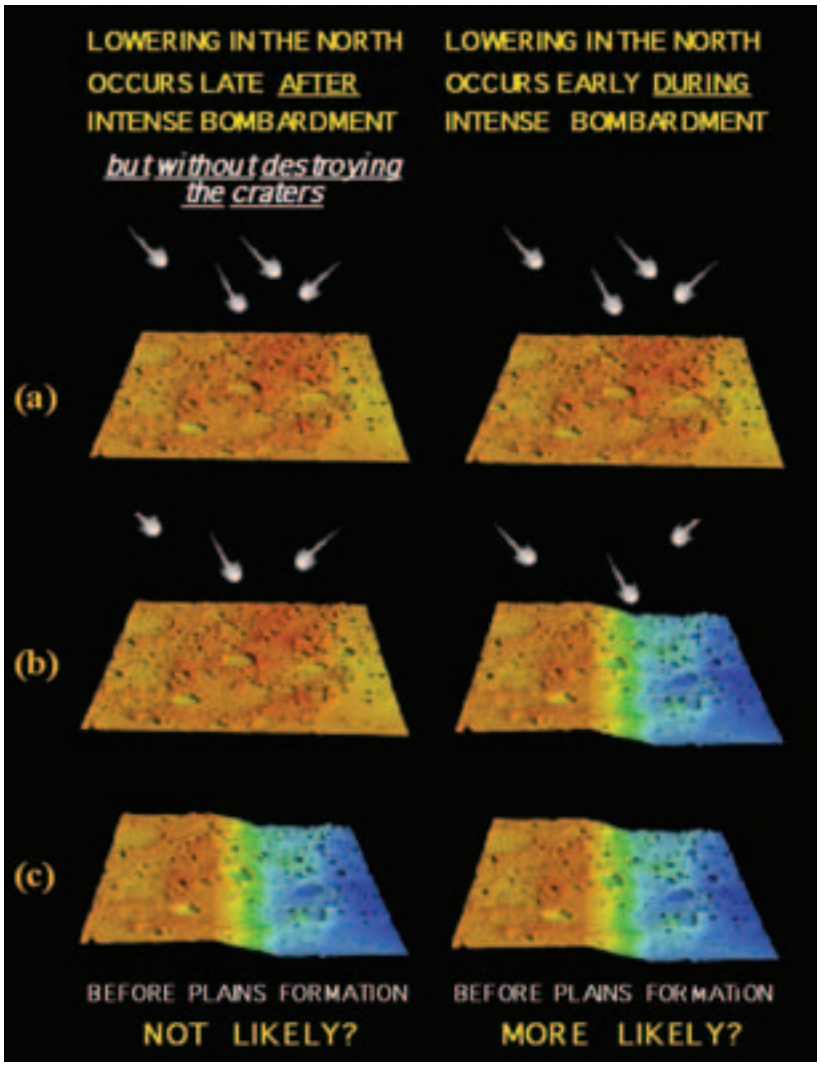

Figure 20.

This constraint on the lowlands is only temporal, but it may limit the likely mechanisms that can form the lowlands (and therefore the crustal dichotomy). It certainly favors processes which occur early and quickly (such as large scale cratering), and may make longer-lived processes such as whole mantle convection and plate tectonics unlikely.

There are implications of this work that go beyond the question of the martian crustal dichotomy. It is sometimes assumed that the oldest terrains on Mars date from its origin 4.6 billion years ago.

If buried impact basins were found in these very old units, the oldest known terrains would then have to be younger than 4.6 billion years ago. Also, it appears there was a northern lowland essentially throughout martian history. That means that at whatever early time conditions on Mars permitted water to run across the surface, there was a basin into which the water could drain. So there may well have been an early (shallow) ocean on Mars, with all the implications that can have for the possibility of life.

This work was supported by the Mars Global Surveyor Project.

References:

Frey, H., S.E.H. Sakimoto and J. H. Roark, Discovery of a 450 km diameter, multi-ring basin on Mars through analysis of MOLA topographic data, Geophys. Res. Lett., 26, 1657-1660, 1999.

Frey, H.V., J.H. Roark, K.M. Shockey, E.L. Frey and S.E.H. Sakimoto, Ancient lowlands on Mars, Geophys. Res. Lett. (in press), 2002.

Contact: Herbert Frey, Geodynamics Branch, frey@core2.gsfc.nasa.gov

New Perspectives on the Enigmatic Medusae Fossae Formation, Mars

One of the most enigmatic formations on the surface of Mars is called the Medusae Fossae Formation (MFF). Its young age, distinctive surface texture, localized setting, and lack of obvious source have prompted a variety of proposals concerning its origin. Mars Orbiter Laser Altimeter (MOLA) data in conjunction with high resolution Mars Orbiter Camera (MOC) images from the Mars Global Surveyor (MGS) mission have provided important information on the extent, volume, roughness, orientation and superposition relationships that help limit the likely nature of the MFF.

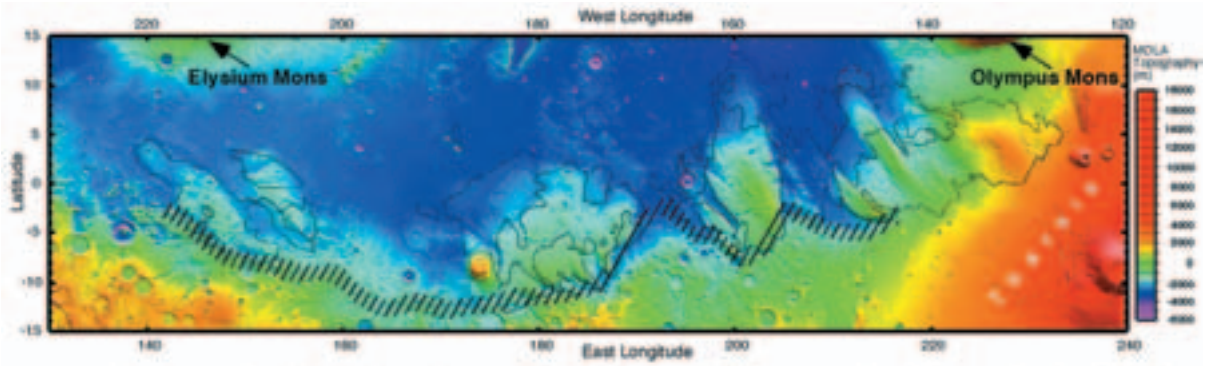

Location map for Medusae Fossae Formation (MFF). Base map is MOLA topography. Scale is on the right. Outlined areas are location of MFF deposits based on earlier Viking image mapping. Hatched region is the crustal dichotomy boundary separating old cratered terrain to the South from younger smooth plains to the North. Our studies indicate the MFF may have had wider extent than shown by the above map, but the deposits may be thinner than previously assumed.

Figure 21.

The MFF is a wind-scoured deposit located near the equator of Mars between the Tharsis and Elysium volcanic centers at 130^{o} -240^{o} E and 15^{o} S to 15^{o} N. Located along the major crustal dichotomy boundary (Figure 21), it overlies both old cratered highlands and young plains-forming units, which include very young volcanic flows and small cones. At large scales the formation appears smooth, but at smaller scales there are lineations that appear to be wind-eroded features (see Figure 22 and Figure 23). Overall the MFF has a MOLA pulse width roughness 2-3 times that of the Mars global average.

Earlier studies based on Viking imagery led to a variety of hypotheses for the MFF, including ignimbrites or ash flows, carbonate platforms, shoreline terraces, rafted pumice deposits, paleo-polar deposits, and uplifted and exhumed ancient terrain. Geologic mapping earlier identified three distinct units (upper, middle and lower members) of the formation, but more detailed images available from MOC have shown multiple layers and cohesive caprock overlying much more friable (easily eroded) material. Studies by Bradley et al. (2001) using MOLA and MOC data have now reduced the likely origins to two quite different but atmospherically-related possibilities: volcanic airfall or aeolian deposits.

In particular, MGS data have shown that the MFF is draped over but does not always fully mask peaks and valleys in older terrain. There is clear indication that ancient fluvial systems underlie the MFF but also that MFF material appears to deflect some channels, suggesting a complex interplay between two quite distinct processes. MOLA topography has significantly reduced the estimates of the thickness of the MFF from an earlier 3 km to about 1 km on average, suggesting only about half the volume previously believed. On the flip side, the areal extent of MFF materials in the past may have been much larger than what currently survives.

Although some researchers have resurrected the suggestion that the MFF is similar to polar layered terrain units and may represent paleo-deposits of this unit (located near the present-day equator!), the MOLA topography does not support this.

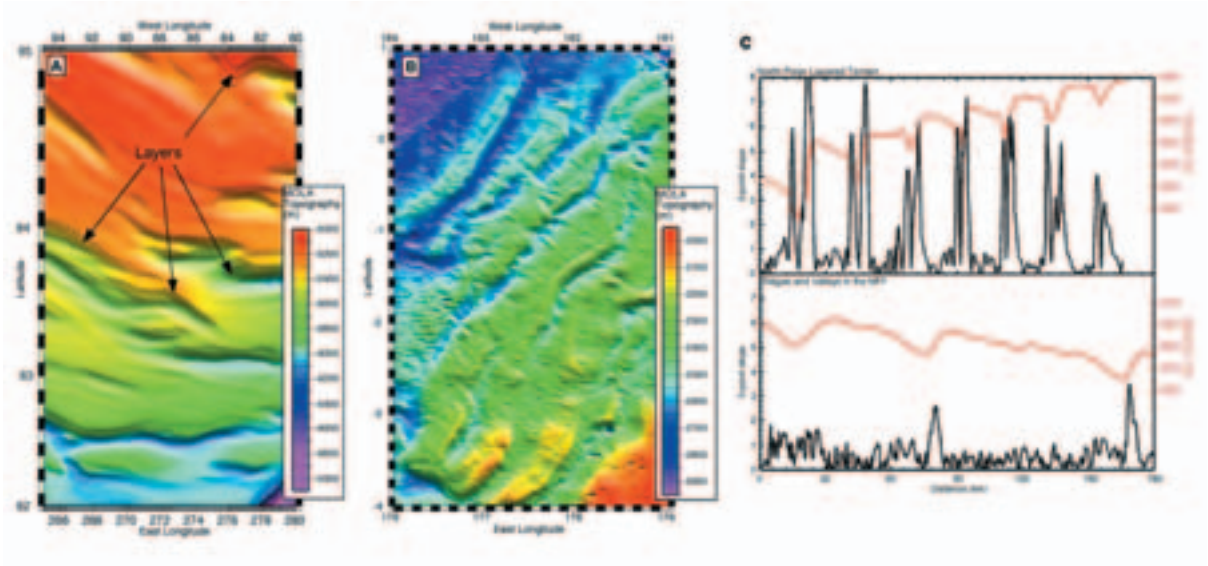

Figure 22.

In particular, the width, depth and wall slopes of valleys in the MFF materials (Figure 22b) are quite different from those of valleys in polar layered terrain (Figure 22a; also Figure 22c). Intervalley roughness is much greater in MFF materials and the valley spacing much more irregular than for polar layered terrains. On the basis of these quantitative comparisons it appears unlikely the MFF are paleo-polar layered terrains.

Yardangs (irregular grooved ridges produced by wind erosion of weakly consolidated sediments) suggest multiple episodes of wind-related deposition and erosion in the MFF. They have a variety of orientations, including bi-directional patterns where the deposits are thin, but the lack of a consistent pattern overall suggests neither wind direction nor underlying topography alone controls their emplacement. But the observation of a common angle between intersecting sets of yardangs in some areas of the MFF (Figure 23) does suggest that material properties such as jointing may control their orientation in these areas.

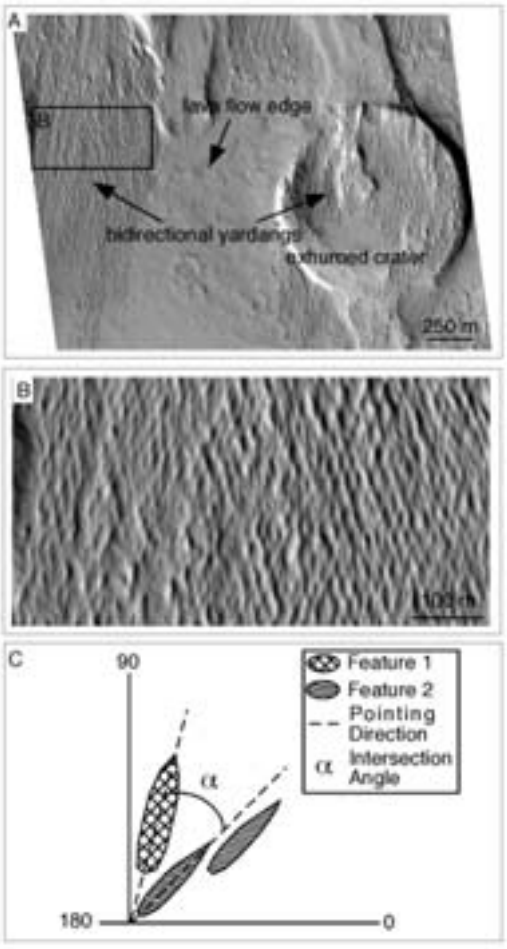

Figure 23.

The new data provide little support for some of the suggested origins of this unusual deposit. In particular, the lack of widespread horizontal layering virtually eliminates ideas such as carbonate platforms, paleo-shorelines or other water-related origins. As described above, paleo-polar deposits like present-day polar layered terrains are also not viable. The two most likely remaining candidates are volcanic airfall deposits such as ashes and tuffs or non-volcanic aeolian deposits such as loess. Volcanic airfall is most consistent with the whole range of characteristics of the MFF, especially presence of widespread resistant (to erosion) zones, ability of MFF to drape pre-existing topography but also to apparently deflect development of a fluvial channel, widespread occurrence of yardangs with different orientations, and apparent evidence for jointing.

References:

Bradley, B.A., S.E.H. Sakimoto, H. Frey and J.R. Zimbelman, The Medusae Fossae Formation: New Perspectives from Mars Global Surveyor, J. Geophys. Res. (Planets) in press, 2002.

Contact: Susan Sakimoto,UMBC/GEST at the Geodynamics Branch,
sakimoto@core2.gsfc.nasa.gov

Recent Floods and Volcanism in the Cerberus Plains, Mars

The Cerberus Plains on Mars are a smooth low area just north of the planet's dichotomy boundary, located along the equator between the two large volcanic centers of Elysium and Tharsis. A long series of sub-parallel fissures called the Cerberus Rupes stretches from Elysium across the plains to their center. Based on studies done using 1970's vintage Viking Orbiter data, explanations for the Plains included deposits laid down by water, a dry lakebed, or simply lava flows. Since Mars Global Surveyor arrived in 1997, and began mapping in 1999, the area has been under renewed scrutiny which has taken advantage of the much higher resolution imagery and elevation data now available.

Detailed images from the Mars Orbiter Camera (MOC) have revealed fresh-appearing, young lava flows, possibly less than 10 million years old (based on crater counts). Mars Orbiter Laser Altimeter (MOLA) data have provided stunning, detailed topography. Susan Sakimoto has used the topography to trace young lava flows across the plains back to their sources at the Cerberus Rupes fissure, and to characterize the range of vent types observed in the region. The region is mostly lava-covered and clearly not simply a lakebed. Sakimoto has also found that the volcanic flow rates are similar to those expected for plains volcanism regions on Earth. This work was reported at the annual Geological Society of America meeting (Sakimoto et al., 2001), and was reviewed in Science, (Kerr, 2001).

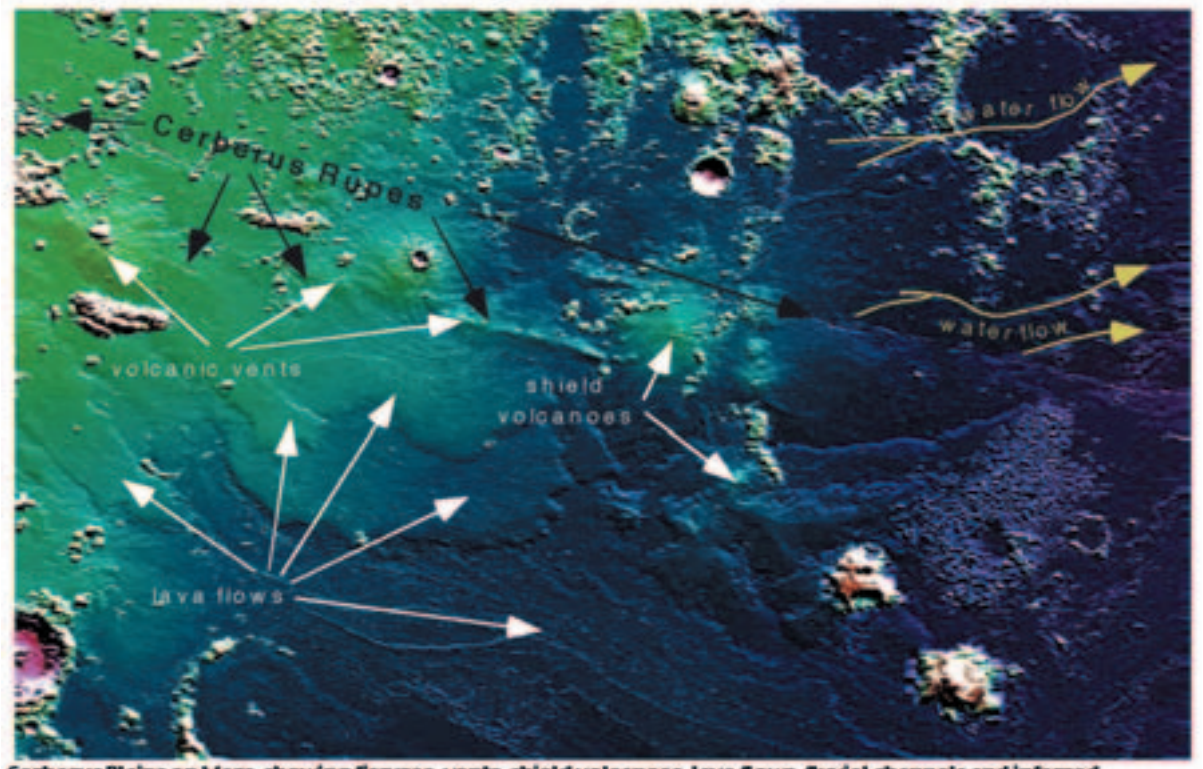

Cerberus Plains on Mars, showing fissures, vents, shield volcanoes, lava flows, fluvial channels and inferred directions of flows of both water and lava. Elevation shown by color (dark blues and purples are lows; greens are higher elevations).

Figure 24.

The lava flows in Cerberus (Figure 24) are topographically some of the best preserved on the planet. This makes them excellent candidates for modeling what types and rates of lava might have flowed through the observed channels. This modeling work is funded by the NASA Mars Data Analysis Program. As a terrestrial validation of lava flow models, Sakimoto is also working

with Dr. Tracy Gregg at the University at Buffalo using a combined approach of analytic models, laboratory simulations, field data, and computational fluid dynamics simulations (Sakimoto and Gregg, 2001). Figure 25 shows the excellent agreement reached so far with the field velocity measurements matched by channel model predictions of lava flow velocities.

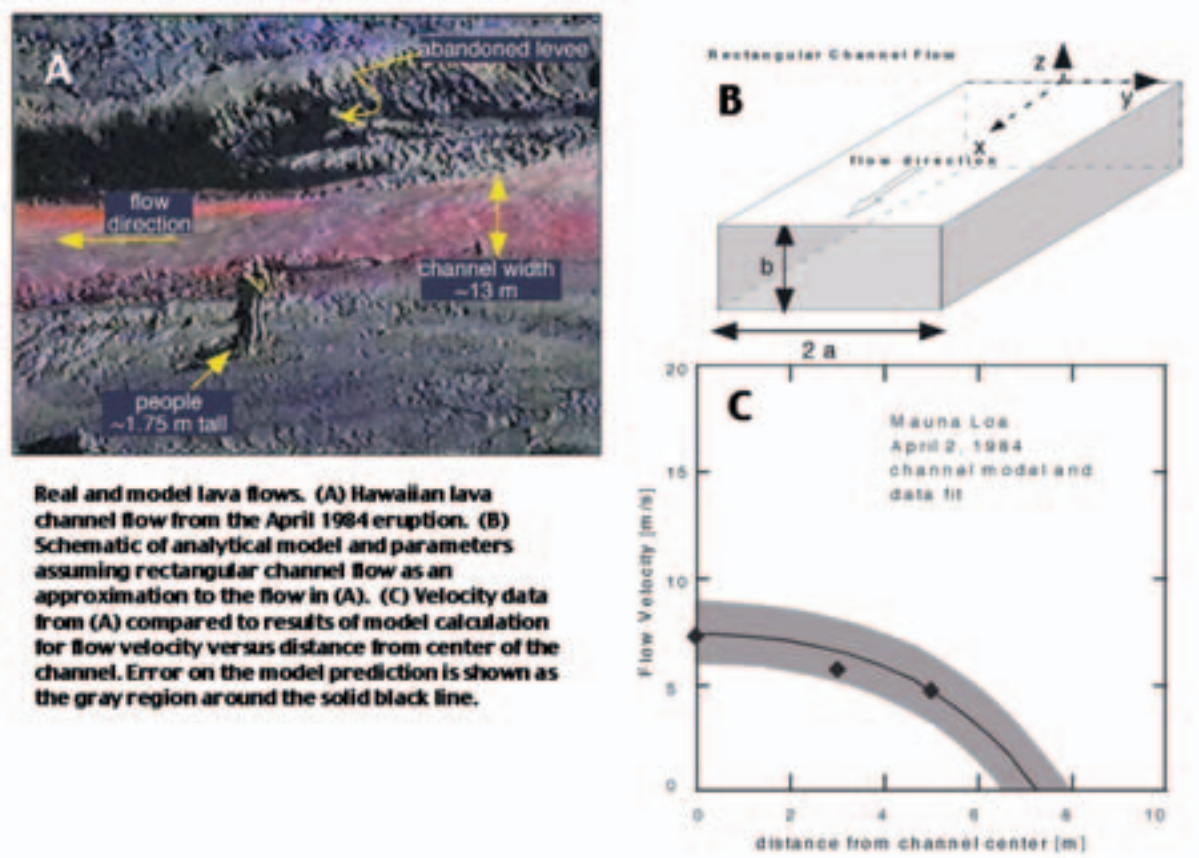

Real and model lava flows. (A) Hawaiian lava channel flow from the April 1984 eruption. (B) Schematic of analytical model and parameters assuming rectangular channel flow as an approximation to the flow in (A). (C) Velocity data from (A) compared to results of model calculation for flow velocity versus distance from center of the channel. Error on the model prediction is shown as the gray region around the solid black line.

Figure 25.

Sakimoto and collaborators are extending this terrestrial work into related flow field and shield analyses with the help of a NASA-funded Space Grant collaboration with Scott Hughes and Glenn Thackeray on a study of the Snake River Plains volcanism. The Snake River Plains serves as both as a terrestrial field case study, and as a basis for comparison for the Cerberus and other volcanic fields on Mars.

One of the more interesting terrestrial/planetary comparisons related to this work is in the realm of lava-water interactions, which many consider prime sites for life. Sakimoto, in collaboration with Devon Burr (a NASA Graduate Student Research Fellow at the University of Arizona), and her advisor Alfred McEwen, has shown that water likely also originated from the Cerberus Rupes, flowed across the western plains in the recent geologic past, and then debauched onto permeable lavas, where it may still exist as shallow ground ice (Burr et al., 2001, 2002). The story of the lava-water interplay for this region is expected to have very interesting implications for the preservation of hydrothermal environments late into martian history, since these are some of the youngest lava and water flows yet found on the planet. Sakimoto and Burr suggest that the fissures, water and lava flows are the surface manifestation of subsurface magma that has kept the local subsurface warm for tens of millions of years. As the magma rises towards the surface, it probably encounters and helps release subsurface water. This erupts onto the surface before or

after the lavas to create the intermingled lava and water channels and flows so clearly seen in the recent topography and images.

Since much of this activity is thought to be geologically recent (based on impact crater counts by other researchers), magma may well still be present at depth. The Cerberus fissures could erupt again. Given that the local conditions (likely warm and wet) are both interesting and perhaps hospitable for possible subsurface life, this region is one of four sites in consideration as a landing site for one of the two Mars Exploration Rovers scheduled for launch in 2005.

References:

Burr, D. M., A.S. McEwen, S.E.H. Sakimoto, Recent aqueous floods from the Cerberus Rupes, Mars, Geophysical Research Letters, 29, 1, 10.1029/2001GL 013345, 2002.

Burr, D., A. McEwen, S. Sakimoto, Recent Aqueous Floods From the Cerberus Rupes, Mars, Eos. Trans. AGU, 82(47), Fall Meet. Suppl., Abstract P22A-0537, 2001.

Sakimoto, S.E.H. and T.K.P. Gregg, 2001,Channeled flow: Analytic solutions, laboratory experiments, and applications to lava flows, Journal of Geophysical Research-Solid Earth, Vol. 106., No. B5, p. 8629-8648.

Sakimoto, S.E.H., S.J. Riedel, D. Burr, Geologically Recent Martian Volcanism and Flooding in Elysium Planitia and Cerberus Rupes: Plains Style Eruptions and Related Water Release? Presented at the Fall GSA meeting, Boston, Nov 5-8, 2001.

Kerr, R., Life-Potential, Slow, or Long Dead, Science, vol 294, p1820-21, 2001.

Contact: Susan Sakimoto, UMBC/GEST at the Geodynamics Branch,
sakimoto@core2.gsfc.nasa.gov

GRIDVIEW: Interactive Software for Analyzing Gridded Data

The Geodynamics branch has over the last several years developed a scientific visualization tool called GRIDVIEW that can be used by researchers and students alike to study gridded data sets. The program was created originally because researchers within the Laboratory needed a way to quickly and easily view and study the newly acquired topographic profile and gridded data from the Mars Orbiter Laser Altimeter (MOLA), one of the instruments on the Mars Global Surveyor satellite. The software was created with IDL (Interactive Data Language, from Research Systems, Inc.) and has evolved over several years to become a highly versatile yet user-friendly analysis tool. It is currently used by researchers and students in the US and other countries, including, Great Britain and Japan.

GRIDVIEW features a variety of functions and capabilities, some of which are described below, and uses simple pull-down menus for function selection by point-and-click. The program is extremely easy to use. After given a short (< 30 minutes) introduction to the program's capabilities, high school and undergraduate students have been able to use this tool to analyze the topographic characteristics of Mars in support of several education and research projects currently ongoing in the Geodynamics Branch. A graphical mouse driven interface allows the user to rotate a planetary globe (Figure 26a) and zoom into areas of interest and view the data in numerous ways (Figure 26b, 26c). Color representations of the data can be interactively stretched and manipulated to highlight specific details in the data (Figure 26b, 26c). A profile picking and display tool provides interactive options for distance, height and slope measurements along the profile (Figure 26d).

Examples of GRIDVIEW Functions

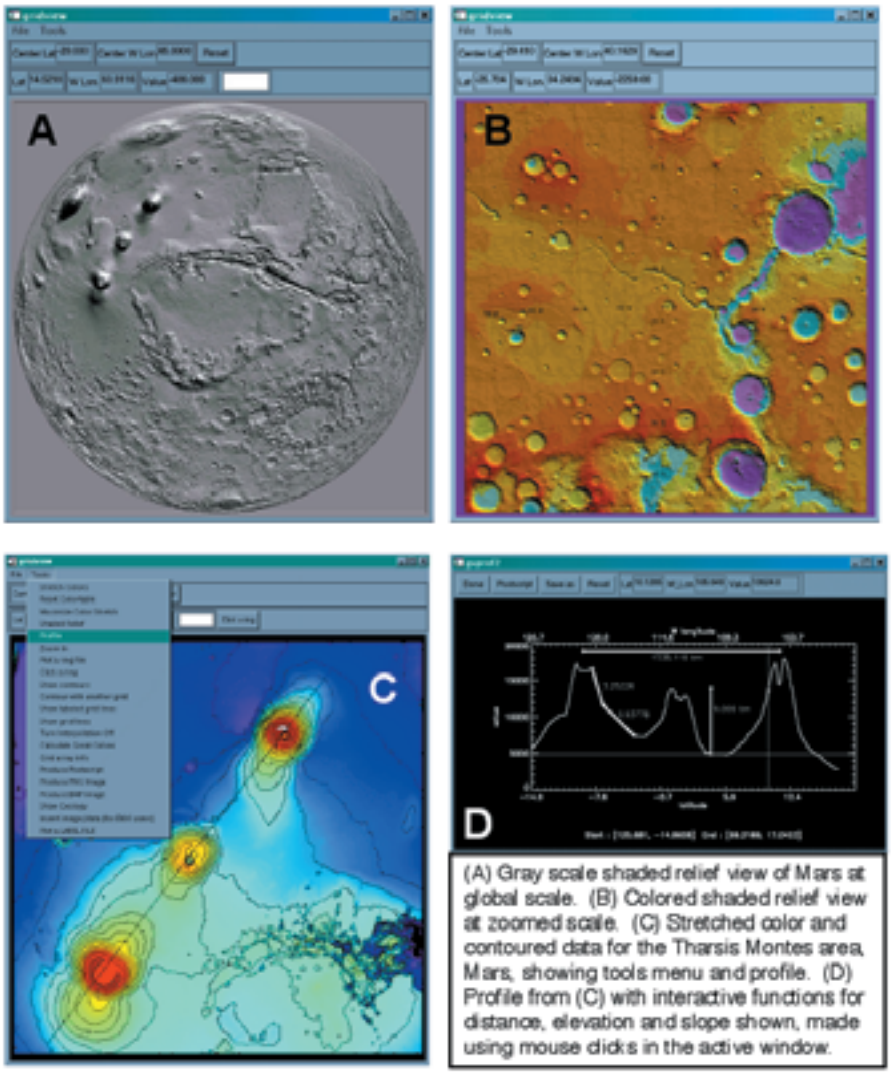

Figure 26.

A list of the major features available includes:

Global Rotation and Zooming

Selectable Color Representation of Data

Shaded Relief Viewing Options

Latitude / Longitude / Data Value Tracking

Color and Contrast Stretching

Contouring

Profiling

Interactive Distance, Height and Slope Measurement Tools

Basin Center and Diameter Measurement (Circle Fitting)

Plotting Basin Ring Files

Overlay Contours of other Data Sets

Postscript and Image Figure Output

The combination of color stretching and contouring capabilities of GRIDVIEW to highlight subtle details of the data has made it a very powerful tool for mapping and discovering previously unknown buried basins on Mars. This is described elsewhere in this report ("Ancient Lowlands on Mars"). In addition, GRIDVIEW is routinely used to measure heights and slopes of small volcanic features, depths of craters, channels and canyons, and geographic correspondence between different features (geologic units, gravity anomalies, magnetic anomalies, topographic features). It has also become a valuable tool for investigations of the crustal dichotomy boundary, characterization of geologic formations, calculation of sediment fill in and around large craters, and measurement of the thickness of volcanic flows and debris aprons.

The program was specifically designed to work with MOLA topography data but can be used to analyze any gridded data. It has been used in the Geodynamics branch to study gravity and magnetic data as well as Earth topographic data. Although development continues and additional features may be added, the utility of the program is so great that we have made it available to anyone wishing to use it. GRIDVIEW requires the installation of IDL software from Research Systems, Inc. (http://www.rsinc.com) and will run on any computer system supported by IDL (Windows, Mac, UNIX). The program is available for download on the web at http://core2.gsfc.nasa.gov/mola_pub/gridview .

Contact: James Roark, SSAI at the Geodynamics Branch, roark@core2.gsfc.nasa.gov

Magnetic Spectra of Earth and Mars

It has been known for decades that the Earth's crust contains magnetic anomalies, regions that, in the presence of the Earth's strong internal magnetic field, take on enhanced magnetic intensity or regions that were magnetized as they cooled and now preserve a remanent magnetization. These were first mapped in detail from orbit by NASA's Magsat in 1980, and more recently by the Danish Oersted and German CHAMP missions. It was only in the last few years that crustal magnetic anomalies were discovered on Mars by Mars Global Surveyor (MGS), but that has turned out to be one of the major findings and surprises of that mission. Techniques previously developed for the study of Magsat crustal anomalies have been used to better represent and help study the anomalies on Mars. One of these techniques is a spectral method that allows a separation of the contribution from crustal sources from that due to the main core field of the Earth.

When astrophysicists measure light from a distant star, they can break up the starlight into its component colors, creating a spectrum from long wavelength red to short wavelength blue, by passing the light through a mechanical prism. Similarly, when geophysicists measure a planet's magnetic field, they can break up the field into long and short wavelength components by running the data through a kind of digital prism called "spherical harmonic analysis." And just as astrophysicists can learn much about a star's surface and interior from its optical spectrum, geophysicists can infer something about a planet's crust and core from its magnetic spectrum.

The Earth's magnetic spectrum is determined from measurements made at magnetic observato-

ries on the surface, from aeromagnetic data, and from global surveys by orbiting satellites. Recently, satellite data has also become available for Mars. Thus it is now possible for the first time to compare the magnetic spectra of two different terrestrial planets, and to use techniques that separate out the core and crustal components as has traditionally been done for the Earth. This comparison is shown in Figure 27, which plots magnetic power (actually mean square magnetic induction) versus harmonic degree, a measure of the wavelength scale. Wavelength decreases from left to right along the horizontal axis. Dots and crosses show the actual magnetic spectrum of Earth and Mars, respectively. The curves are fits to specific types of source models, as described below. The Earth's magnetic spectrum has two distinct branches: a powerful, long-wavelength, rapidly decreasing (with harmonic degree) core-source magnetic field, caused by electric currents in its liquid iron outer core. The second flatter branch is due to a shorter-wavelength crustal-source field, caused by magnetization of crustal rock. These two branches cross at about degree 14. For the Earth we find best fitting fields from a core of radius 3512 + 64 km (very similar to the seismologic core radius of 3480 km), and from a crust represented by a shell of random dipolar sources at radius 6367 + 14 km, near Earth's mean radius of 6371.2 km.

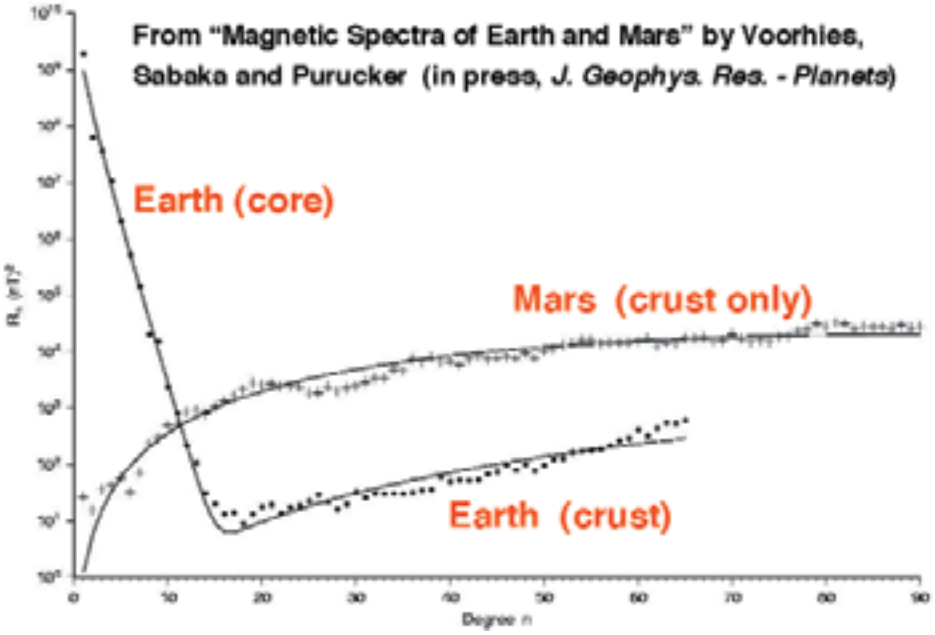

Figure 27.

The spectrum for Mars has no sign of a core-source field. This is consistent with the lack of direct observation of a global field by MGS. There is only a field from crustal sources, represented here by a shell of random dipoles, but now at radius 3344 + 10 km, and with sources about 10 times stronger than Earth's. The shell radius is about 46 km below Mars' mean radius of 3390 km, and agrees well with the mean depth of Mars lithosphere inferred by independent modeling of MGS topography and gravity data. Our results indicate Mars has a thicker, more intensely magnetized crust than Earth. This may in part be due to an iron-rich crustal magnetic mineralogy for the Red Planet, magnetized in the past by a now defunct core-dynamo.

Contact: Coerte Voorhies, Geodynamics Branch, voorhies@geomag.gsfc.nasa.gov

Valles Marineris May Provide a Key to Understanding Early Mars

On the Earth, magnetic field observations and in particular crustal magnetic anomalies can be used for a variety of studies, including geologic reconstructions, plate tectonic interpretations, and resource exploration. Crustal anomalies on the Earth are of two kinds, those induced by the present-day main core field and remanent anomalies produced when magnetic rocks cooled in the presence of the past magnetic field. The alternating pattern of anomalies that flank mid ocean ridges on the Earth and which characterize the seafloor spreading part of plate tectonics are of the latter type.

There exists a debate as to whether Mars ever experienced plate tectonic processes such as produce seafloor spreading on the Earth. The discovery by Mars Global Surveyor (MGS) of a strongly magnetic crust on Mars and the pattern of the anomalies seen has been interpreted by some as evidence for an early episode of plate tectonics on that planet. Whether or not this is so, techniques developed for the interpretation of crustal magnetic anomalies on the Earth, including those seen at satellite altitude by Magsat and other satellites, can be applied to the magnetic anomalies on Mars. These martian anomalies are of the remanent type since there is no present-day intrinsic field to induce anomalies of the sort known on Earth.

Figure 28 shows two recent magnetic maps of Mars derived using these techniques. The anomalies have a pattern strongly suggestive of faulting and perhaps offset along faults along a major tectonic structure. The Vallis Marineris on Mars is a series of large, fault-bounded canyons which have been compared with major rift structures on the Earth. The pattern in the magnetic maps, especially the abrupt truncation of the anomalies at the wall of the canyon, supports the idea that the Valles Marineris canyon is a tectonic graben. The maps also suggest that highly magnetic source rocks exist at the intersection of Coprates and Capri Chasmata, on the northeast corner of the canyons, and there is a good possibility that these magnetic rocks may be exposed along the fault wall.

It is generally accepted that the magnetic anomalies on Mars are very old. It is also likely that the Valles Marineris, though formed in the middle part of martian history, exposes much older rock, as suggested by the extensive layering revealed by the Mars Orbiter Camera on MGS. If so, the possible exposure of ancient highly magnetized rocks in the Valles Marineris may provide important clues to the early tectonic evolution of Mars and the nature and demise of the martian core dynamo.

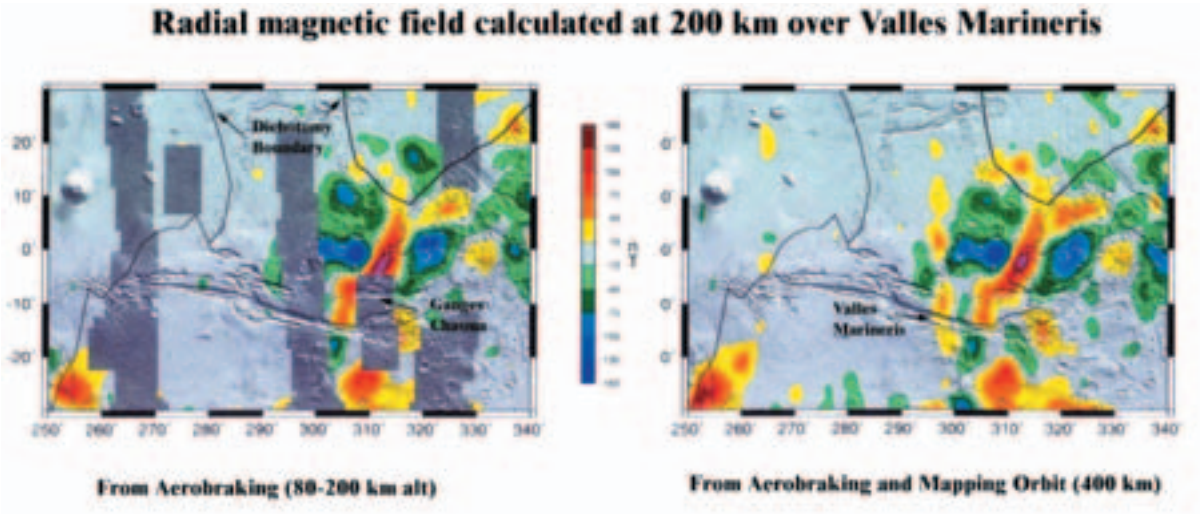

Figure 28.

Contact: Michael Purucker, RSTX at the Geodynamics Branch, purucker@geomag.gsfc.nasa.gov

Geopotential Solutions from Mars Global Surveyor Tracking Data

Prior to the arrival of the Mariner 9 and Viking Orbiter missions at Mars, knowledge of the Mars gravity field was limited to estimates of the Mars gravitational constant (GM, or the universal constant of gravitation multiplied by the planet mass), and the planet's oblateness. Estimates were obtained from studies of the motions of the natural satellites of Mars or from flybys of Mars by Mariner 4 and Mariner 6. The first insights into the unique character of the Mars gravity field came from the analysis of the Mariner 9 and Viking Orbiter tracking data, obtained by NASA's Deep Space Network (DSN). These analyses showed that the Mars gravity field was much rougher than that of the Earth with total variations in the geoid of up to 2000 m (compared to no more than 200 m for the Earth). A strong geoid high was detected over the Tharsis region of the planet. In addition, using some of the lower altitude (300 km periapse) Viking Orbiter tracking, different investigators have identified the large gravity anomalies associated with Olympus Mons and other martian volcanoes, such as Elysium, and the Tharsis Montes (Arsia, Pavonis and Ascraseus Mons). Although a strong mascon was detected in the Isidis basin, Mars was not found to have the same mascon basins as the Moon.

The tracking data from the Mars Global Surveyor (MGS) spacecraft differ in two fundamental respects from the earlier data obtained from the Viking Orbiters and Mariner 9. Firstly, MGS was located in near-circular, polar, and low-altitude (400 km) orbit, whereas the previous satellite missions were placed into eccentric orbits whose periapses only coarsely sampled the equatorial regions of the planet. Secondly, MGS obtained data using an X band system (~8 Ghz), compared to the S band tracking (~2 Ghz) used by the older spacecraft. The X band systems are less sensitive to noise from the solar plasma and the Earth ionosphere, and consequently the data quality is superior (0.1 mm/s compared to ~1-3 mm/s with the historic S band data).

The MGS spacecraft entered the mapping orbit in February 1999, and has been tracked continuously by the DSN. The radiometric tracking data and the Mars Orbiter laser altimeter data have been used in the derivation of solutions to 80x80 in spherical harmonics. We employ sophisticated modeling to account for all the forces that act on the spacecraft orbit, including third body gravity perturbations, and non-conservative force effects such as solar radiation pressure, atmospheric drag, and planetary radiation pressure and process the data in our least squares orbit determination batch processor (GEODYN). These new solutions revealed the geopotential of the planet in unprecedented detail [cf., Goddard Mars Model-2B]. The GMM-2B model included data only through February 29, 2000, or for the first year in the mapping orbit. The most recent data, especially those collected in late 2000 and early 2001 were obtained when the MGS orbit orientation angle wrt. the line of sight was optimum for gravity measurements. We have reprocessed all the available MGS tracking data through July 2001, including the data from the Science Phasing Orbits (prior to arrival in the Mapping orbit). The data were processed with the updated planetary rotation and pole orientation constants derived from Pathfinder and MGS data, as well as other improvements in the non-conservative force modeling. The new geopotential model, MGM-1025 (for Mars Gravity Model 1025) shows greater power in the spectral band from degree 60 to 70 (see Figure 29). The correlations of the gravity field with MOLA derived topography are improved with respect to GMM-2B. For GMM-2B the average correlation (to degree 70) was 0.72, whereas for MGM-1025 the average correlation is 0.76. We have almost exhausted the signal in the tracking data, and fit five day arcs to 0.10 to 0.15 mm/s. The signatures of small volcanic features such as Amphitrites Patera (an ancient volcanic shield, 62^{O}E, 58^{O}S), and Apollinaris Patera (175^{O}E, 10^{O}S) are now clearly visible in the gravity anomaly maps. A mascon is apparent in the Argyre basin. The signature of the Valles Marineris canyon system appears prominently in the new gravity model anomaly maps. In future, detailed joint studies of both the topography and the gravity can be expected to reveal new insights into the structure and evolution of the planet Mars.

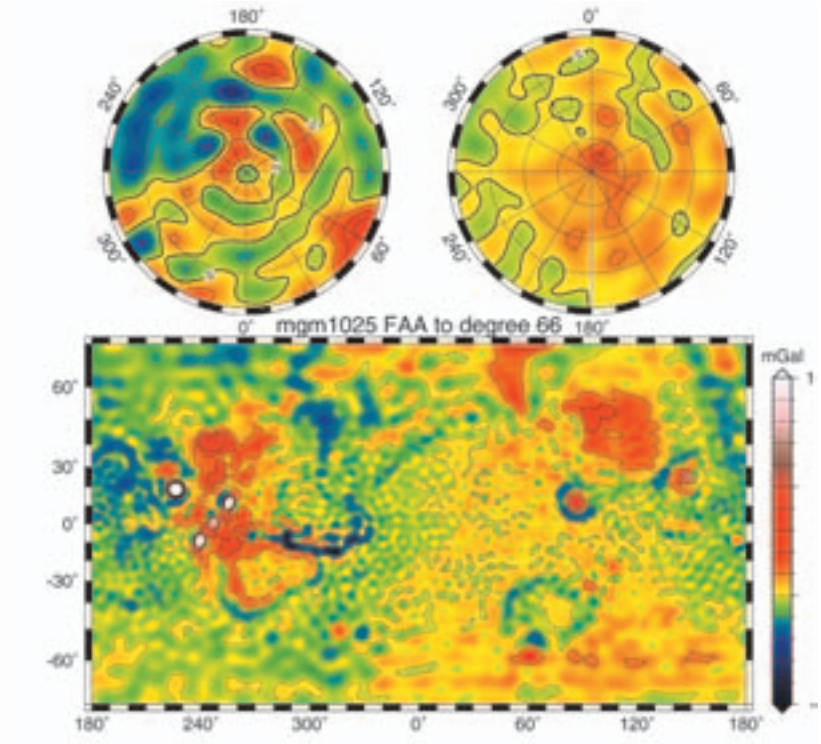

Figure 29. Free Air Gravity Anomalies of the MGM1025 gravity solution depicted to degree 66. The anomalies are shown on a mercator projection for the central latitudes, and on polar stereographic projections for the northern (upper left) and southern (upper right) polar regions.

Contact: Frank Lemoine, Space Geodesy Branch, Frank.G.Lemoine.1@gsfc.nasa.gov

Topography and Gravity of Mars

MOLA has completed its altimetric mapping of Mars, with 1 m vertical accuracy. Figure 30 shows color-shaded topography in four hemispheres centered at 0, 90, 180, and 270 degrees East (L to R, T to B). Higher elevations are shown by warmer hues, lower elevations by cooler hues. On the right, the planet is tilted by 22.5 degrees to reveal the ice-rich north and south polar deposits.

The Mars Orbiter Laser Altimeter (MOLA) mapped the topography of Mars until the end of June, 2001, producing nearly 600,000,000 precision ranges. The MOLA Science Team released in 2001 a Mission Experiment Gridded Data Product of the topography of Mars, at a resolution 64 pixels/degree (better than 1 km) and accuracy of 1 meter with respect to Mars' center of mass. A comparison with a previous digital elevation model provided by the US Geological Survey shows differences of ~1 km RMS, with some greater than 5 km. Many new features with modest topographic relief have been identified, and first-order structures such as the Utopia and Hellas impacts are now measured.

Cartographic control on Mars has been problematic, with errors of 5-15 km. MOLA has provided the Mars Geodesy and Cartography Working Group with a new control network that will be used by future orbiters and landers, whose positions are accurate to within 100 m. Such precise measurement is made possible by the careful analysis of gravity, tracking data, and spacecraft modeling conducted by members of GSFC Space Geodesy Branch.

Ongoing work to improve the knowledge of the gravity field and its time-varying components in combination with the topography of Mars is leading to improved understanding of the history, internal structure, and dynamics of the red planet.

MOLA has embarked this year on a systematic effort to measure the radiometric flux from Mars at 1064 nm wavelength, using enhancements to the original mapping software. These measurements will complement those by infrared spectrometers aboard the Mars Global Surveyor spacecraft.

The MOLA team has now measured the elevation changes from seasonal accumulation and sublimation of CO_2 snow at Mars' poles, a technically challenging accomplishment. Together with the analysis of small variations in the gravity field due to seasonal mass transfer, this provided an estimate of the density of the 1-2 m thick seasonal ice deposits and improves our understanding of the Martian climate.

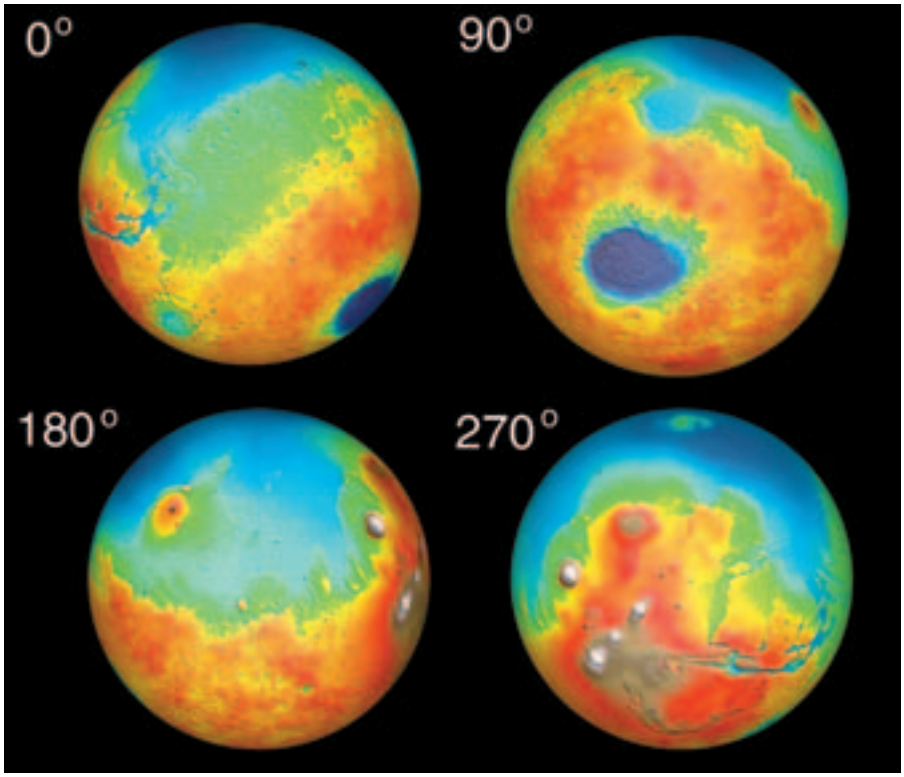

Figure 30. The topography of Mars revealed by Mars Orbiter Laser Altimeter measurements taken during the primary and extended mapping missions of Mars Global Surveyor.

Contact: Greg Neumann, Space Geodesy Branch, neumann@tharsis.gsfc.nasa.gov

Orbital-Rotational-Climatic Interactions

There is important coupling between the tilt of the axis (obliquity) of the non-spherical (oblate) solid but deformable Earth and its orbital motion that plays into the long term change in climate. Obliquity-oblateness feedbacks exist which can be important. Frequency modulation of the obliquity may be a significant forcing on changing the insolation and therefore the climate of the Earth. Similar effects exist on other planets. For Mars, for example, there are possible long term secular changes in the size of the polar cap. And sublimation and freezing of atmospheric constituents on planetary satellites like Triton and Charon are yet more examples of this interplay.

The diurnal and seasonal Yarkovsky re-radiation effect may contribute to the evolution of asteroid and meteroid orbits and could help populate the near-Earth space with small objects. Also, tidal dissipation and how it changes with and helps change orbital eccentricity is an important source of thermal energy for Mercury, which may help explain how that small and slowly rotat-

ing body still maintains an internal (core) magnetic field.

Yarkovsky Effects and the Orbital Evolution of Asteroids and Meteoroids

Ivan Osipovich Yarkovsky (1844-1902), a civil engineer who worked on scientific problems in his spare time, first proposed an effect which now bears his name. Writing in a pamphlet around the year 1900, Yarkovsky noted that the diurnal (day-night) heating of a rotating object in space would cause it to experience a force. This force, while tiny, can lead over time to large secular effects in the orbits of small bodies, especially meteoroids and small asteroids. In particular, the orbits of the meteoroids evolve towards resonances where gravitational effects of other planets cause them to be delivered into Earth-crossing orbits and eventually to Earth.

Yarkovsky's effect is a radiation force, and is the photonic equivalent of Fred Whipple's rocket effect. The basic idea behind Yarkovsky's diurnal effect is shown in Figure 31, which shows a spherical meteoroid in a circular orbit about the Sun. For simplicity the meteoroid's spin axis is taken to be perpendicular to the orbital plane, so that the Sun always stands above its equator. Insolation heats up the sunward side; the heat is ultimately re-radiated into space by the meteoroid (typically in the infrared part of the spectrum, unless the meteoroid is very close to the Sun). When it leaves the meteoroid, an infrared photon carries away momentum p according to the relation $p = E/c$, where E is energy, and c is the speed of light. Because more energy (and therefore more momentum) departs from the hotter side of the meteoroid than the colder side, the meteoroid feels a net kick in the direction away from the hotter part.

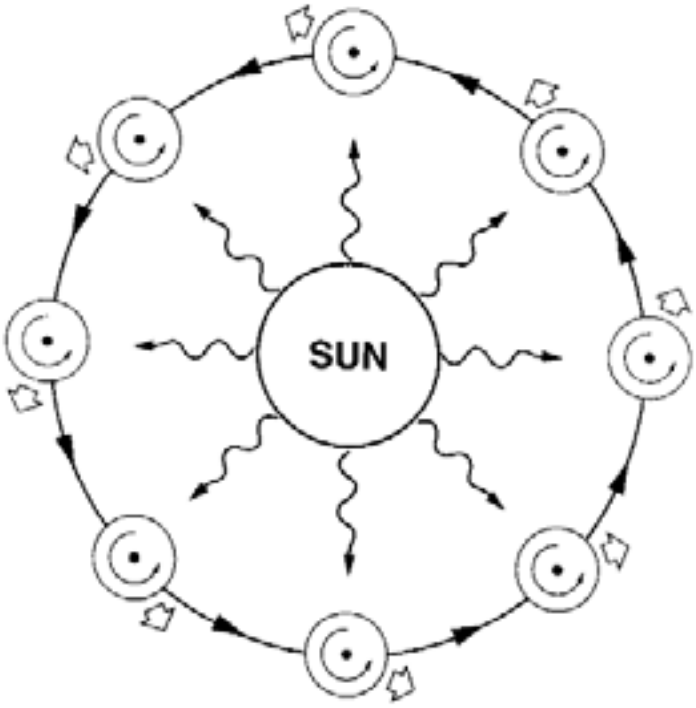

Figure 31.

If the meteoroid had no thermal inertia, then the temperature distribution would be symmetrical about the sub-solar point and the meteoroid would experience only a net force radially outward from the Sun. The only consequence of this force would be to weaken the Sun's gravitational grip on the meteoroid. However, all bodies do have some thermal inertia, which causes a delay in

heating and cooling of its material. The hottest part of the meteoroid is actually its afternoon side rather than the sub-solar (noontime) point. This is similar to the Earth, where afternoon is the warmest time of day, instead of noon. As a result, the force on the meteoroid has both a component radially outwards from the Sun and also along-track.

This along-track component causes a long term increase in the size of the orbit for the direct or prograde sense of rotation shown in Figure 31. But the sign of the diurnal Yarkovsky effect depends on the sense of rotation. If the meteoroid shown in Figure 31 rotated in the backwards or retrograde sense, then the orbit would shrink instead of expand. The important point is that over time the tiny Yarkovsky force can profoundly change the orbit of meteoroids, affecting the number that finally strike the Earth. The effect, of course, is generally greater for smaller bodies (unless they are so small they lack significant temperature gradients across them).

Nearly a century after Yarkovsky wrote his pamphlet a second Yarkovsky effect was recognized. While searching for the cause of the secular decay of the orbit of the LAGEOS Earth satellite, we realized that in general there had to be a seasonal effect in addition to Yarkovsky's original diurnal effect. The seasonal effect applies not just to Earth satellites like LAGEOS, but also to meteoroids and asteroids orbiting the Sun.

The seasonal Yarkovsky effect is illustrated in Figure 32. As in Figure 31, a spherical meteoroid is assumed to be in a circular orbit about the Sun, but in this case the spin axis lies in (not perpendicular to) the orbital plane. It is the component of force lying along the spin axis which gives rise to the seasonal effect. When the meteoroid is at the bottom of the figure, the Sun shines most strongly on its northern hemisphere. As with the diurnal effect, there is a delay in cooling due to thermal inertia, so the northern hemisphere is hottest further on in its orbit. For a body without thermal inertia the along-track force is periodic and averages to zero when integrated over one revolution about the Sun, but for real objects the average of the along track force is non-zero and leads to secular changes.

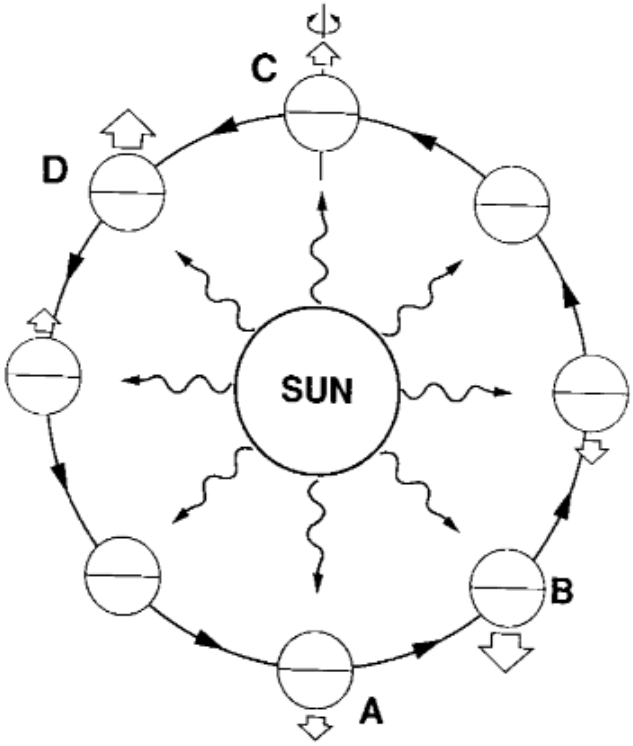

Figure 32.

For small orbital eccentricities (orbits that are nearly circular), the average along-track force always opposes to the motion of the meteoroid; it acts like drag and causes orbital decay. Unlike the diurnal Yarkovsky effect, the seasonal Yarkovsky effect is independent of the sense of rotation of the meteoroid; reversing its spin does not change the effect's sign.

These Yarkovsky effects may be an important mechanism by which meteoroids and small asteroids reach orbital resonances. Once the bodies reach the resonances, the eccentricities are rapidly pumped up so that after a few million more years their orbits cross that of the Earth, and they may fall to the ground to be picked up as meteorites. The drift times due to these effects for stony meteorites are on the order of 20 million years, in good agreement with the cosmic ray exposure ages.

These results are in press as a chapter in the book ASTEROIDS III, to be published by the University of Arizona Press, with W. F. Botke, D. Vokrouhlicky, D. P. Rubincam, and M. Broz as co-authors.

Contact: David P. Rubincam, Geodynamics Branch, rubincam@core2.gsfc.nasa.gov

Obliquity Modulation of the Incoming Solar Radiation

For several decades, geophysicists have been trying to develop a physical understanding of how the 100-Kyr cycle in the ellipticity of the Earth's orbit around the Sun shifts the pattern of insolation, triggering the growth and decay of great ice sheets in the high latitudes of the Northern Hemisphere. This effort has encountered great difficulty: The 100-Kyr orbital eccentricity cycle is too small in magnitude and too late in phase to produce the 100-Kyr climate cycle during the last 1 million years. This is one of the most perplexing and enduring puzzles in science. The second puzzle is how to explain the ice sheet cycles in the Northern Hemisphere from 1 to 2 million years ago when the global ice volume and deep sea temperature varied at an almost metronomic 41-Kyr period of the Earth's obliquity. Thirdly, we still do not understand why the 100-Kyr ice age cycle became dominant about 0.9 million years ago.

Numerous hypotheses and models have been proposed to explain these climate puzzles. Proposed explanations have invoked: (1) Stochastic resonance of orbital eccentricity forcing. (2) Internal oscillations of the climate system near the 100-Kyr period that can get phase-locked to orbital eccentricity forcing. (3) High nonlinear response of climate system to weak forcing by the orbital eccentricity. (4) Variations in the inclination of the Earth's orbital motion. (5) A climate system with three steady states and a set of pre-defined rules for moving between them. However, the physical mechanism of the climate cycles remains a scientific mystery.

In a paper published last year (Liu, 2001), it was shown, from a dynamics point of view, that the 100-Kyr periodicity of the ice age is not due to orbital eccentricity at all. Numerical climate models were used to demonstrate that frequency modulation of the Earth's obliquity (tilt of the rotation axis with respect to the orbit plane) is responsible and accounts for major climate changes during the past 2 million years (See Figure 33). Calculations of the variation in solar energy flux at the top of the atmosphere showed that the insolation flux deficit is the physics behind the ice age glaciation. According to this idea, it is unnecessary to invoke internal feedbacks such as ocean circulation and atmospheric CO_2 concentrations in the Earth system to understand the climate cycle puzzles. Results from model simulations are in good agreement with geological climate records for the past 2 million years and extension of the model simulations reveals that the current warming trend of the climate is almost over and will give way to a small ice age.

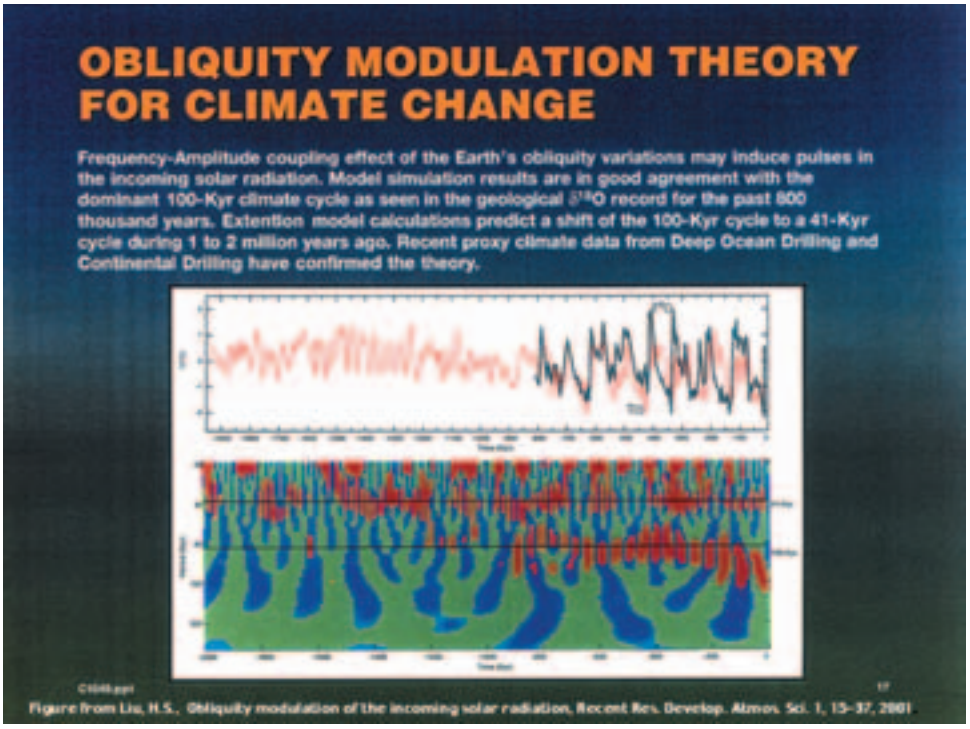

Figure 33.

Reference:

Liu, H.S., Obliquity modulation of the incoming solar radiation, Recent Res. Develop. Atmos. Sci. 1, 15-37, 2001.

Contact: Han Shou Liu, Geodynamics Branch, liu@core2.gsfc.nasa.gov)

Tidal Dissipation in Mercury

Two outstanding characteristics of Mercury are its high density and its strong internal magnetic field. The high density suggests a very large fraction of the planet is in the form of an iron core, which is difficult to explain in terms of its likely origin. Thermal history models for the planet suggest that the iron core of Mercury is likely to be frozen solid at present, in which case there should be no active dynamo to maintain its known magnetic field. Tidal dissipation may provide an answer to both of these puzzles.

Tidal dissipation within the planet Mercury is highly variable in both space and time, but may contribute significantly to the overall thermal budget of the planet. Tidal dissipation is the process by which periodic gravitational deformation of one body by another is converted to heat. The intensity of tidal dissipation depends on the material properties of the deforming body and the intensity of the gravitational interaction. Tidal dissipation in the planet Mercury has previously been recognized as having played a role in the planet's capture into a 3:2 spin-orbit resonance (see below), but has generally been ignored as a currently viable heat source. The present work suggests that such dissipation may in fact be far more important than previously realized, and may help explain why Mercury has a present-day main (core) magnetic field.

The path of the Sun, as seen from Mercury, is rather unusual. This is due to a combination of two factors, the 3:2 spin-orbit resonance (in which Mercury complete 3 rotations for every 2 orbits),

and the high eccentricity of the orbit. The rotation rate is quite uniform, but the orbital angular rate changes significantly, with higher rates near perihelion and lower rates around aphelion. Though the rotation rate is 3/2 the average orbital rate, the instantaneous ratio varies throughout the orbit. For all orbital eccentricities in excess of 0.191059, the maximum orbital rate exceeds the rotation rate, and the Sun (as seen in the Mercury sky) makes a small retrograde (backwards) motion for part of the Mercury day. The exact path depends on the eccentricity of Mercury's s orbit, which at the present time is 0.206 (highest of all the planets). Due to exchange of angular momentum with the other planets, Mercury's eccentricity fluctuates significantly on time scales of 1 million to 10 million years (Figure 34), and has been as low as 0.1 and as high as 0.4 within the past 20 million years. In some simulations of the long term dynamical evolution of the solar system, the eccentricity of Mercury has been calculated to exceed 0.7 several times within the past 109 years. At e = 0.8685, the orbits of Mercury and Venus intersect and a chance of collision becomes possible.

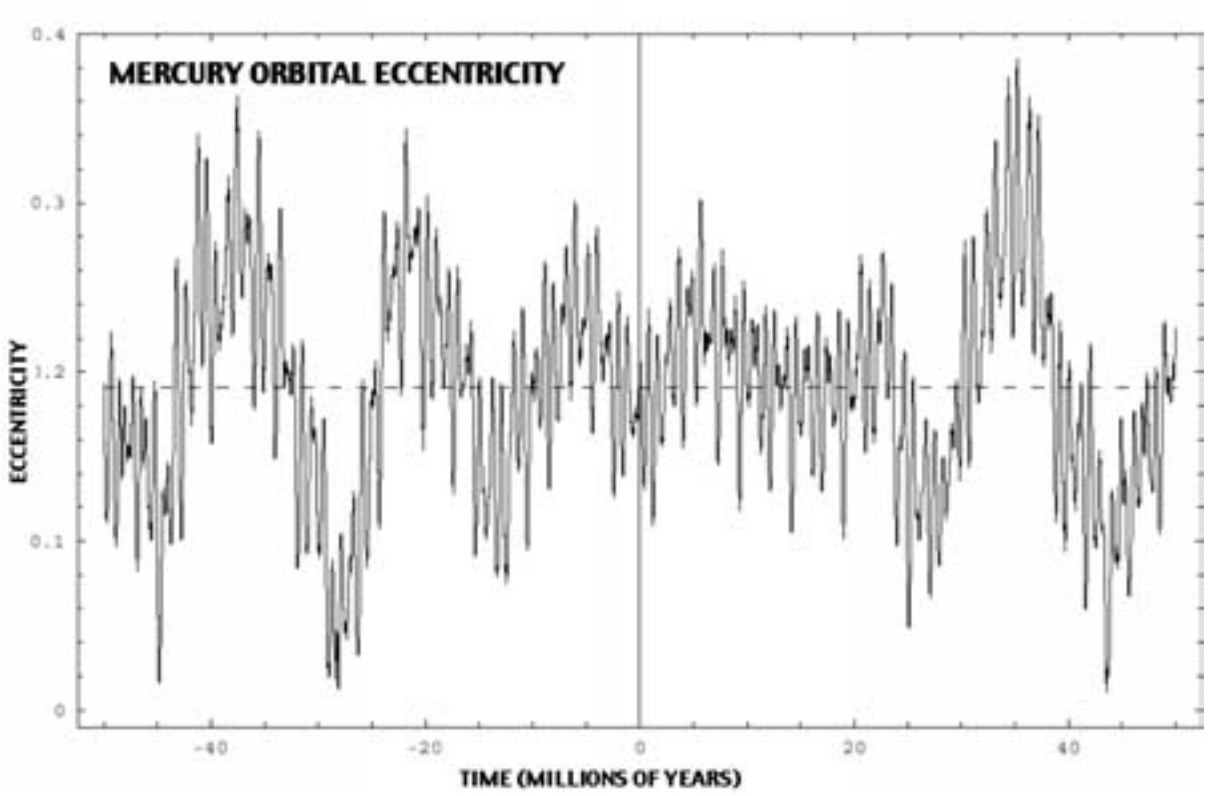

Figure 34.

The two points on the equator of Mercury where the Sun is directly overhead at closest approach (perihelion) receive the most radiative heating, and also the most tidal heating. If the orbit were perfectly circular (e=0), the sub-solar point on Mercury's surface would move at uniform rate, and the associated peak in tidal potential would remain constant in amplitude. As the eccentricity increases, the potential at the sub-solar point varies over the orbit, and the rate of motion of the sub-solar point along the equator becomes more irregular. So tidal effects becomes more variable.

The internal structure of Mercury is largely unknown, and as a result, details of the dissipation pattern and intensity are still quite uncertain. However, using conservative estimates of the density, rigidity, and viscosity structure for Mercury, it appears that the current global rate of dissipation is in the vicinity of 3×10^{12} Watts. This is about the same as for the Earth, but significantly less than for Jupiter's tidally heated and highly volcanic moon, Io (10^{14} Watts).

The dissipation rate depends strongly on orbital eccentricity, and so changes as the eccentricity evolves. Figure 35 illustrates that dependence for a particular model of internal structure, assuming a 50 km thick elastic lithosphere, a 500 km thick viscoelastic mantle with a viscosity of 1021 Pa s (similar to the Earth's mantle), and a fluid iron core. These material properties are highly uncertain, but are believed to be representative. The dissipation rate is nearly constant for eccentricities at or below the present value, and then exhibits a dramatic increase as the eccentricity increases.

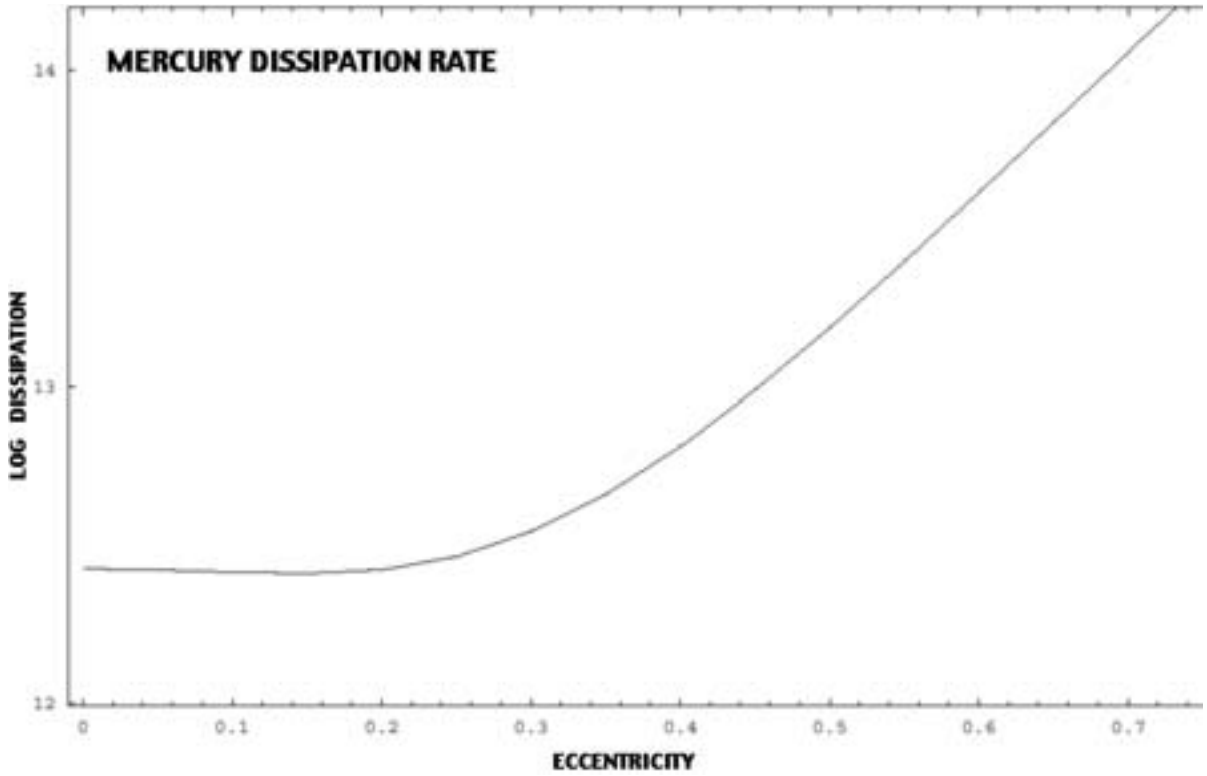

Figure 35.

Episodes of extremely high orbital eccentricity may have lead to tidal heating rates large enough to evaporate away significant amounts of volatile constituents. This could account for the observed high density, as has been suggested to explain a similar larger-than-expected density for Io. Tidal dissipation may also provide the thermal energy to keep the core liquid and convecting, and thereby maintain the magnetic field.

Contact: Bruce G. Bills, Geodynamics Branch, bills@core2.gsfc.nasa.gov)

Precise Orbit Determination, Gravity Field, and Terrestrial Reference Frame

Precise orbit determination (POD) is a major area of activity in the Laboratory. For four decades GSFC has maintained the world's leading expertise in POD for Earth-orbiting satellites and planetary spacecraft, as well as its operational and scientific derivatives. For operational applications, as with satellite-laser-ranging and radar and laser satellite altimetry, POD enables important science investigations that would otherwise be impossible. It also serves as the source data for the definition and maintenance of the terrestrial reference frame, which is a fundamental requirement for almost all precise space geodetic measurements today and in the future. In scientific applications, recovery of the Earth's global gravity field directly from POD data from various satellites has been a major effort over the decades. LTP is the birthplace of the world's state-of-the-art grav-

ity field models for Earth (NASA/TP 1998-206861, Lemoine et al.)and Mars (see Mars Geology and Geophysics section above), which are continually refined as new data and new data types become available. In addition, the most precise POD, using satellite-laser-ranging techniques, has clearly revealed the long-wavelength time-variable gravity signals, which is source data for studies of global geophysical fluids (see the next section).

Precision Orbit Determination (POD)

TOPEX POD: The Space Geodesy Branch computes the precise orbit ephemerides that are used on the geophysical data records (GDRs) of the TOPEX/POSEIDON mission. TOPEX has been returning altimetry data almost continuously since October of 1992. Since then the Space Geodesy Branch has computed more than 300 ten-day "cycles" of TOPEX orbits each with an accuracy of better than 3 centimeters radially and better than 15 centimeters in total position. The routine production of these highly accurate orbits has been a major factor in TOPEX/Poseidon mission success.

The TOPEX orbits that we compute have contributed and will continue to contribute to the success of other radar and new laser altimetric missions. TOPEX altimetry can be used to form inter-mission "crossovers" with altimetry from these other missions. Information gleaned from the inter-mission crossovers will allow these other missions to benefit from the TOPEX data. TOPEX has become the standard for altimetric reference frames. Additionally, we have plans to use TOPEX orbits and altimetry to link the reference frames of space-based laser altimeters such as VCL (Vegetation Canopy Lidar) and ICESat (Ice Cloud and Land Elevation Satellite).

GEOSAT Follow On (GFO) is a radar altimetric satellite. The satellite belongs to the Navy, but the data is available to the scientific community. By an agreement with the Department of the Navy and NOAA, the Space Geodesy Branch is funded to compute the precise orbit ephemeredes for GFO. The GPS receivers on GFO have not been performing at a usable level and we are one of the very few groups capable of achieving near TOPEX level accuracy for GFO without GPS tracking. This is in part due to our dynamic crossover capability. GFO-GFO dynamic crossovers are routinely used in our GFO orbit solutions and were also used to "tune" a gravity field for GFO. Figure 36 shows the reduction in TOPEX-GFO crossovers when our tuned GFO gravity field is used. Our GFO orbits have enabled scientific research across government agencies and also across laboratories in GSFC's Earth Sciences Directorate.

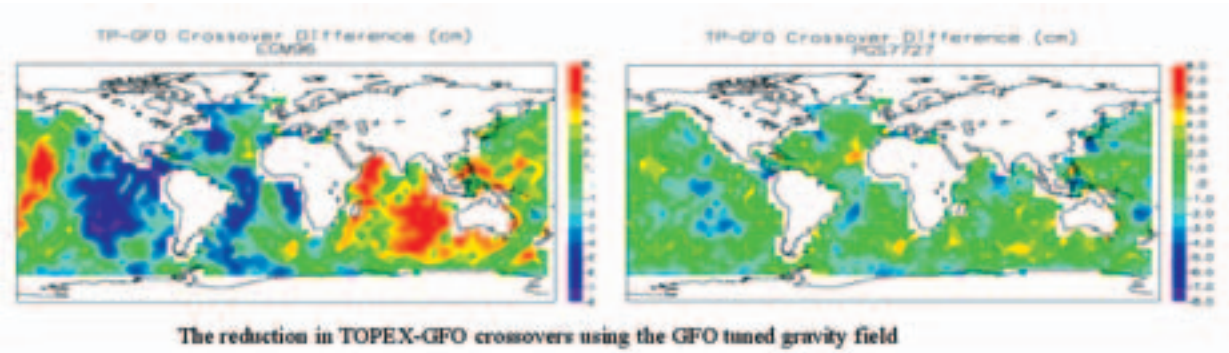

Figure 36.

POD for Laser Altimetry (SLA, MGS, VCL, ICESat): Orbit determination for laser altimetric satellites brings with it a unique set of challenges and possibilities. Laser altimeters require on-orbit calibration of instrument parameters such as pointing and ranging biases. In the Space Geodesy Branch we have developed an approach that simultaneously determines the orbit of a

satellite along with the laser altimeter instrument parameters from a combined reduction of navigation tracking and laser altimeter range data. In preparation for future space-based laser altimeter missions, this approach has been successfully applied to the reduction of Shuttle Laser Altimeter (SLA-01 and SLA-02) mission tracking and altimeter ranging data. A significant improvement in SLA surface return geolocation and shuttle orbit accuracy has been achieved (e.g. Figure 37). We have applied these techniques to extensive VCL and ICESat pre-launch calibration simulations and error analyses. These analyses have resulted in the design and development of specific instrument calibration strategies and techniques (e.g. ocean sweep maneuvers and dynamic crossover analysis) that will play an important role in the VCL and ICESat missions.

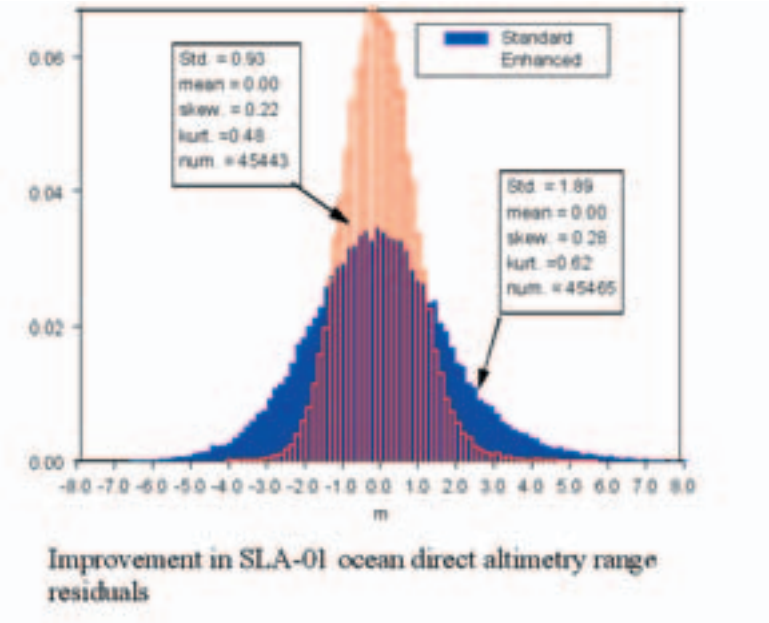

Figure 37.

Mars Global Surveyor is another laser altimetric mission where we have successfully applied our combined approach to orbit determination and altimetric calibration. Our orbit solutions were an important part of the topographic mapping of Mars. As part of the orbit determination process the Space Geodesy Branch has also developed the GMM-2B Mars gravity model (see Figure 29 in the from Mars Global Surveyor Tracking Data section).

POD for Earth Gravity Modeling (CHAMP and GRACE): The Space Geodesy Branch has a very long history of extracting Earth gravity information from the analysis of satellite motion. With the launch of CHAMP (The Challenging Mini-satellite Payload) in 2000 and the recent launch of GRACE (The Gravity Recovery and Climate Experiment) the techniques by which gravity information is recovered from tracking data will dramatically change and the Space Geodesy Branch will help shape that change. These next generation gravity missions combine a new generation of GPS receivers, a high-precision three-axis accelerometer, and star cameras for the precision attitude determination. Accelerometer data will be used to separate gravity perturbations from non-gravity perturbations after on-orbit calibration of the accelerometer. For the CHAMP mission, precision orbit determination based on GPS and SLR tracking data will isolate the orbit perturbations, while GRACE will include inter-satellite ranging. The Space Geodesy Branch is currently processing the CHAMP GPS, SLR and accelerometry data for gravity model development. Our state-of-the-art GPS and SLR tracking data analysis is complemented by our innovative accelerometer data analysis capabilities which are being applied to the on-orbit calibration of the CHAMP accelerometer. The Space Geodesy Branch is one of two US groups to have demonstrated extensive accelerometer calibration expertise. Figure 38 shows a plot of calibrated accelerations from the CHAMP satellite in the cross track direction.

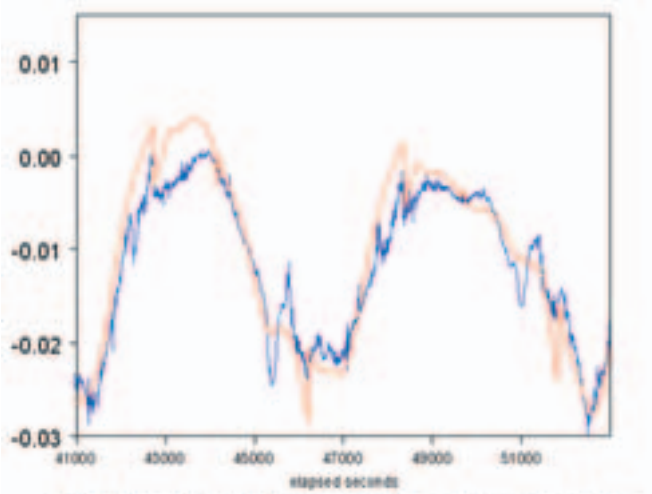

CHAMP calibrated cross-track accelerometer data (blue) vs. modeled accelerations (red)

Figure 38.

The GRACE mission consists of two satellites in low earth orbit separated by about 200 kilometers. There will be very precise (about 1 micron/second) intersatellite tracking between the satellites. The Space Geodesy Branch has developed a new orbital analysis technique to exploit this tracking. The technique allows orbit determination and gravity recovery in segments (arcs) only a few minutes long. Traditionally, orbit determination requires analysis in arcs that are at least a day in length. We have demonstrated that there is only slight degradation in gravity recovery (see Figure 39) induced by short arc analysis (as opposed to analysis using traditional length arcs). On the other hand short arc analysis opens up a wealth of applications that would be unavailable with the traditional approach.

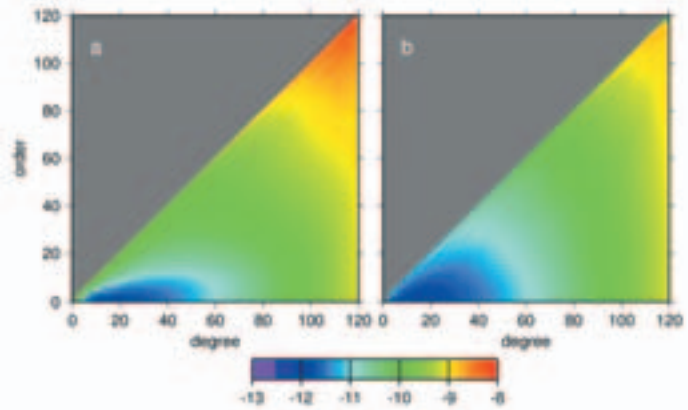

Formal errors for gravity simulations employing (a) short arcs and (b) long arcs. Colors show the logarithm of errors for fully normalized coefficients.

Figure 39.

Contacts: Scott Luthcke, David Rowlands, Frank Lemoine, Space Geodesy Branch, sluthcke@geodesy2.gsfc.nasa.gov, drowland@helmert.gsfc.nasa.gov, flemoine@ares.gsfc.nasa.gov

Terrestrial Reference Frame (TRF) from Satellite Laser Ranging (SLR) for Mass Transport in the Earth System

Satellite laser ranging (SLR) has monitored for a long time the continuous redistribution of mass within the Earth system through concomitant changes in the Stokes harmonic coefficients of the terrestrial gravity field. Our latest analysis of the 1993-present SLR data set from LAGEOS and LAGEOS 2 data for the IERS (International Earth Rotation Service) Terrestrial Reference Frame (ITRF) includes the weekly monitoring of such compound changes in the low degree and order harmonics. Along with the static parameters of the TRF we have determined a time series of variations of its origin with respect to the center of mass of the Earth system (geocenter). These estimates provide a measure of the total motion due to all sources of mass transport with the Earth system and can be used to either complement the estimates from the future missions or to validate them through comparisons with their estimates for the same quantities. The data were reduced using GSFC's GEODYN/SOLVE II software, resulting to a final RMS error of ~8 mm – close to the datanoise level.

Recent improvements in the analysis and modeling of very precise laser ranging observations to artificial Earth satellite targets warrant a new reduction of long series of observations from certain geodetic quality targets such as LAGEOS 1 and 2. These targets have traditionally provided the international community with the most precise definition of the origin and scale of the terrestrial reference frame (TRF). Since the establishment of the International Earth Rotation Service, satellite laser ranging (SLR) has been the key-technique in providing this information to the Service. The significance of such an improvement in the SLR analysis is due to the increased interest in the highly precise definition and monitoring of the height component. This derives from the need to precisely monitor the temporal variations in global scale and in the ability of the space techniques to realize with high fidelity the nearly instantaneous geocenter motion.

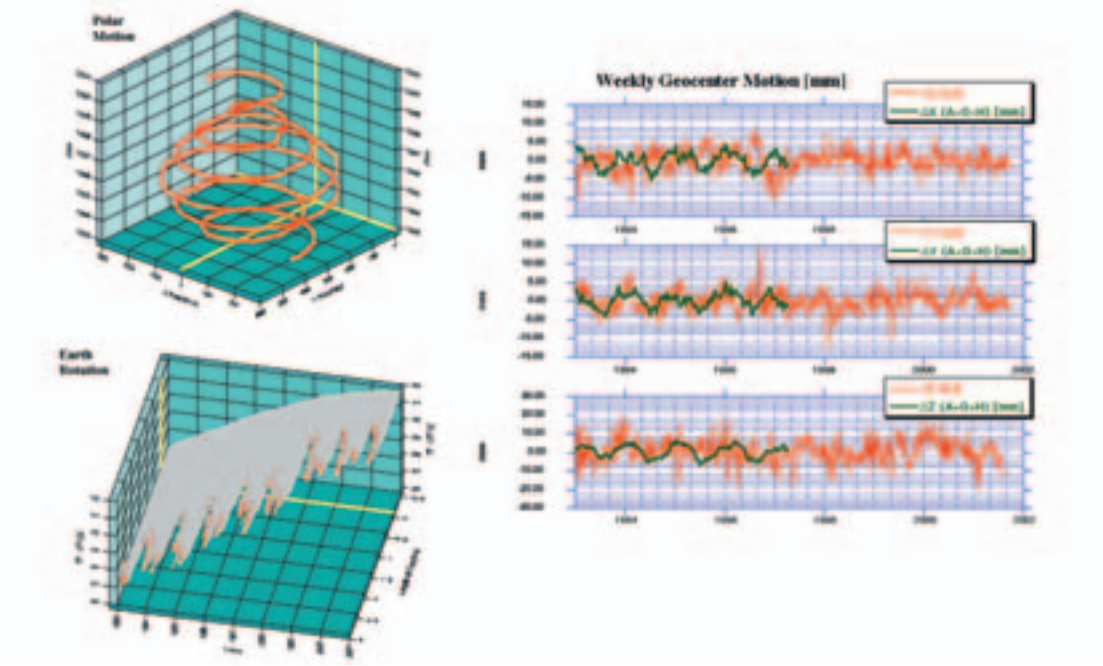

Figure 40. SLR defines the origin, scale, and relative orientation of the TRF used in monitoring v ery small variations in the kinematics of Earth caused by continuous mass transport of Atmospheric, Oceanic, and hydrologic origin. On the average, mass transport causes the origin of the TRF to "orbit" around the instantaneous center of mass (geocenter) within a region the size of a cherry.

The launch of new missions such as CHAMP and in the near future, GRACE, to monitor temporal variations in the long and medium wavelengths of the gravitational field associated with climate change, is the driving force behind this need for increased quality in the definition and mon-

itoring of the TRF. With this motivation in mind, we have used up-to-date information in the complete re-analysis of the 1993-2001 SLR data set from the two LAGEOS satellite targets, to produce the solution that is described here.

Our results for 2000 (Figure 40) were already contributed to IERS and included in the realization of the ITRF2000. This solution was one of the most consistent SLR contributions, with errors of 2.4 mm and 1.2 mm/y for the position and velocity vectors respectively.

Contact, Erricos C. Pavlis, Joint Center for Earth Systems Technology and Space Geodesy Branch, epavlis@helmert.gsfc.nasa.gov

Global Geophysical Fluids and Their Mass Transports

Large-scale mass transports in the Earth system produce variations in Earth's rotation, gravity field, and geocenter. Although relatively small, these global geodynamic effects have been measured by space geodetic techniques to increasing, unprecedented accuracy, opening up important new avenues of research that will lead to better understanding of global mass transport processes and the Earth's dynamic responses. In a real sense, the space geodetic techniques (including satellite laser ranging, very-long-baseline interferometry, the Global Positioning System, satellite altimetry) are employed as powerful remote-sensing tools in monitoring global mass transports in and among the atmosphere-hydrosphere-Solid Earth-core system components, or the "geophysical fluids".

Mass transports occur in the atmosphere-hydrosphere-solid Earth-core system (the "global geophysical fluids") on all temporal and spatial scales, and cause the following geodynamic effects: (1) variations in the solid Earth's 3-D rotation via the conservation of angular momentum and effected by torques at the fluid-solid Earth interfaces; (2) changes in the global gravitational field according to Newton's gravitational law; and (3) motion in the center of mass of the solid Earth relative to that of the whole Earth ("geocenter") via the conservation of linear momentum. These minute signals have become observable by space geodetic techniques with ever increasing precision/accuracy and temporal/spatial resolution.

Important research achievements in these areas conducted in our Laboratory during 2001 are reported here, highlighting the breadth of the related research field and its truly interdisciplinary nature.

Global Geophysical Fluids Center (GGFC) and Research Activities

Realizing the essentiality of strong interactions and collaborations among researchers worldwide, the International Earth Rotation Service (IERS) established in 1998 a GlobalGeophysical Fluids Center (GGFC) in our Laboratory after a thorough selection process. GGFC is headed by B. F. Chao of the Space Geodesy Branch. It in turn coordinates the activities of eight Special Bureaus (SB) established worldwide, including two in our Laboratory (SB for Tides and SB for Mantle, with substantial association with other SBs). Its role is to support, facilitate, and provide services to the worldwide research community in areas related to geodynamic variations that are caused by mass transport in the geophysical fluids.

Many fundamental geophysical processes involving large-scale mass transports that do cause measurable geodynamic effects -- although even they produce signals typically no larger than 1 part in 1010. The most prominent are perhaps weather effects, driven originally by solar radiation input, and related over much of the globe to the Earth’s rotational Coriolis force and modified by atmosphere-ocean and atmosphere-land interactions. The meteorological pressure systems

appearing on weather maps indicate that different masses of air move around the planet as part of the general circulation. The wind thus produced shows a variation on short timescales of these synoptic motions, but they are strong as well on longer scales related to intraseasonal, seasonal, and interannual oscillations. Interannual anomalies associated with El Nino/La Nina are of particular interest in this regard. Remarkably, the length of day showed a very clear strong signal during the recent 1997-98 El Nino event and in earlier ones as well.

Mass transport also occurs in the oceans where it is caused mainly by tidal forcing, surface wind forcing, atmospheric pressure forcing, and thermohaline fluxes. Satellite altimetry can measure changes in the sea surface height caused by these forcing mechanisms, and the GRACE mission (see below) will soon be able to measure changes in the ocean-bottom pressure. Numerical models of the oceanic general circulation allow the response of the oceans to these forcing mechanisms to be investigated in detail, and allow quantities such as the angular momentum associated with oceanic mass transport to be modeled and compared with Earth rotation measurements. Recent studies have shown that nontidal oceanic mass transport can measurably change the length of the day, and can also cause the Earth to wobble as it rotates.

Large mass transports/redistributions occur as tides at all tidal periods. The tides involve mass transports and angular momentum exchanges within the Earth system at periods ranging from subdaily to 18.6 years. Earth tides, ocean tides, and atmospheric tides all contribute to geodynamic variations, and all are readily observable with modern techniques. The Earth's body tide is responsible for large length-of-day variations at monthly and fortnightly periods; the ocean tides are the dominant cause of diurnal and semidiurnal variations in both rotational rate and polar motion. The geodetic measurements are stimulating improvements to all fluid and solid tidal models.

Redistribution of water mass stored on the continents occurs on a variety of timescales. Seasonal and shorter time scales involve precipitation, evaporation, and runoff, with storage of water in lakes, streams, artificial reservoirs, soil, and biomass. Over longer timescales, storage variations in ice sheets and glaciers signal climate change, while ground water storage changes take place in deeper aquifers. Some of these hydrological processes are fundamentally regulated by vegetation; but all are ultimately exchanged with and hence reflected in atmospheric water content and sea level in an intricate budget. Water mass redistribution involving these various reservoirs and mechanisms has been shown to have observable effects on Earth rotation, geocenter and gravity field changes. However, the variety of transport mechanisms and storage reservoirs makes the task of globally monitoring water storage on land an extremely challenging task. Indeed, this is considered to be a first order problem for the climate community, and is being pursued at every major climate research center.

The solid, but non-rigid, Earth is perpetually in motion as well. There are motions caused by external forces, including tidal deformation, atmospheric and oceanic loading, and occasional meteorite impacts. For internal processes, volcanic eruptions and pre-seismic, coseismic and post-seismic dislocations associated with an earthquake act on short timescales. On longer timescales, present-day post-glacial rebound, surface processes of soil erosion and deposition, and tectonic activity such as plate motion, orogeny, and internal mantle convection, all transport large masses over long distances. Finally, the entire solid Earth undergoes an equilibrium adjustment in response to the secular slowing down of the Earth's spin due to tidal friction.

Deeper in the solid Earth, the fluid outer core is constantly turning and churning in association with the geodynamo's generation of the magnetic field. The variation of the core angular momentum can evidently be inferred from surface observations of the geomagnetic field or modeled by physical hypotheses and the equations of motion that drive and govern the geodynamo and hence the core flow. This core angular momentum has been compared to the observed variations of the length-of-day at decadal timescales, while torques at the core-mantle and inner core boundaries

have been evaluated. The recent seismological finding of a differential rotation of the solid inner core is also under evaluation in this context.

In this sense, the entire Earth system consists of several geophysical fluid components. Various types of torques acting on the boundaries between the geophysical fluids exchange angular momentum among the fluids, thus exciting Earth rotational variations. These torques include: (i) frictional torque, in the form of wind stress over land and ocean surfaces, ocean bottom drag, and viscous stress at the core-mantle and inner core boundaries; (ii) pressure torque acting across topography that exists between atmosphere-land, ocean-land, and core-mantle boundaries; (iii) gravitational torque acting on density anomalies at distance; (iv) electromagnetic torque generated by the geodynamo that acts on the core-mantle and inner core boundaries. In addition, subtler interactions exist among the geophysical fluid components which would modify the Earth's response. Notable examples include mantle elastic/inelastic yielding under surface loading, the ocean's inverted-barometer behavior (or the departure from it), and the extent of coupling at the core-mantle and inner core boundaries. They are in general functions of the timescale under which the effect in question applies.

In 2001, in addition to the existing Special Bureaus, an eighth one, the SB for Loading, was established after a thorough proposal and selection process. GGFC has also conducted open meetings and sponsored special sessions at international conferences.

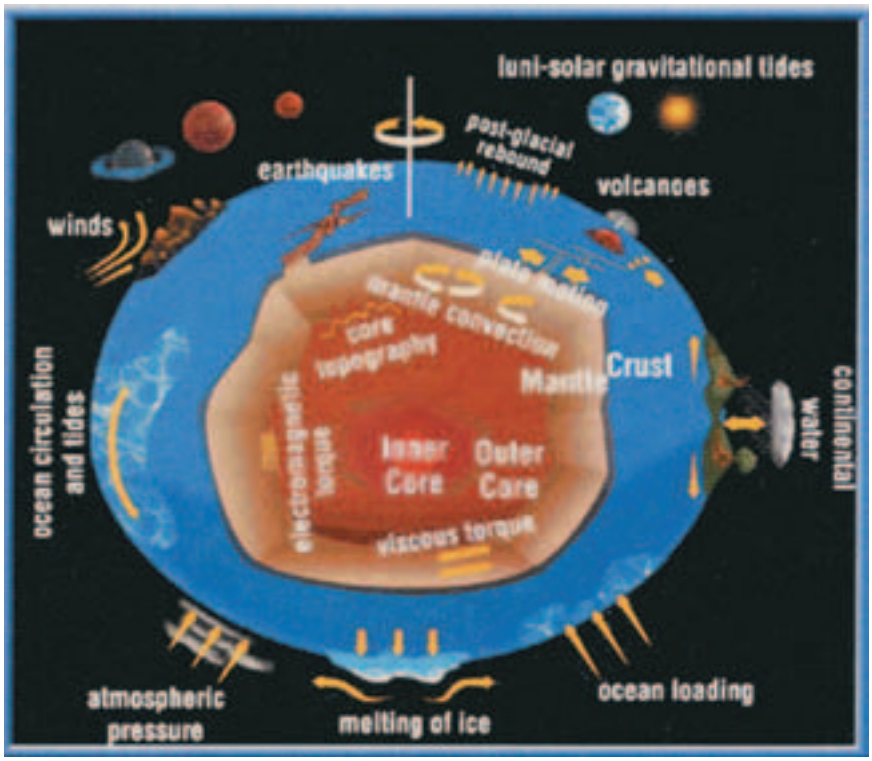

Figure 41: Cartoon that depicts large-scale mass transports in global geophysical fluids, that cause geodetically measurable geodynamic effects.

Contact: Benjamin Chao, Space Geodesy Branch, chao@bowie.gsfc.nasa.gov

Subdaily Tidal Variations in Earth Rotation

In the last few years our ability to measure daily and even subdaily variations in the Earth's rotation rate has markedly improved. There are some surprisingly strong rotation variations at these very rapid periods. An analysis of these variations shows that they have the same periods as the tides. Evidently, as tidal waters move about over the Earth, the Earth's rotation speeds up and down.

An example is shown in Figure 42, which displays rapid variations in the rotation rate (in terms of Universal Time) as observed by hourly measurements and as predicted by a numerical model of ocean tides. The measurements are from an intensive campaign of Very Long Baseline Interferometry (VLBI) observations. The ocean predictions (smooth curve) are from a global model constrained to agree with satellite altimeter measurements of tidal heights.

As can be seen, both diurnal and semidiurnal variations are present in UT, and they appear to be well predicted by the ocean model. There are two ways that the ocean tides can cause such rapid variations.

(1) As the tides move water around the globe, the varying sea levels change the moment of inertia of the earth. By conservation of angular momentum, the solid earth changes its rotation rate accordingly.

(2) As the tidal currents slow down or speed up, they exchange angular momentum with the solid earth, which is manifested in the rotation rate. Mechanism (2) is slightly more important for rotation rate variations; both mechanisms are about equally important for polar motion variations.

Our present work in this field builds on our 1994 Science paper (Ray et al., 1994). We are examining how the Earth's fluid core gets decoupled from the mantle during these rapid rotation variations. As our geodetic measurements and our ocean predictions improve, we hope to learn more about this core-mantle coupling.

One key aspect of improving our ocean model predictions involves obtaining better estimates of deep-ocean tidal currents. We have recently devised a large-scale, sparse, least-squares assimilation algorithm that inverts precise satellite-based tidal elevations (and any other possible information) to determine tidal current velocities. The procedure rigorously accounts for the ocean tide's self-gravitation and crustal loading, subtle forces that have surprisingly large effects on the tides. Acoustic tomography measurements of tidal currents are also proving useful. This work is described in Ray (2001).

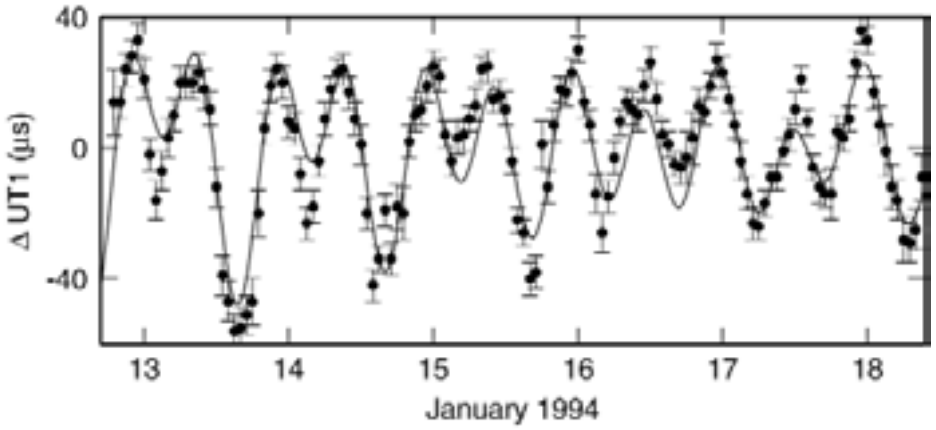

Figure 42. Rapid variations in Universal Time as measured by VLBI and as predicted by a numerical ocean model.

The way to understand Figure 42 is as follows: Consider the rotating Earth to be your clock. Such a clock keeps "Universal Time." Your clock is actually fairly inaccurate compared with atomic clocks, which since about 1955 have been our standard timekeepers. Figure 42 shows how your clock is first ahead and then behind an atomic clock. The UT clock will sometimes be as much as 50 microseconds ahead or behind atomic time. These errors are caused by the fact that ocean tides are changing the Earth's rotation rate. There are also longer period errors in the UT clock that are caused by other geophysical fluids, especially the winds.

References:

Ray, R. D., D. J. Steinberg, B. F. Chao, and D. E. Cartwright, Diurnal and semidiurnal variations in the Earth's rotation rate induced by oceanic tides, Science, 264, 830-832, 1994.

Ray, R. D., Inversion of oceanic tidal currents from measured elevations, Journal of Marine Systems, 28, 1-18, 2001.

Contact: Richard Ray, Space Geodesy Branch, Richard.D.Ray.1@gsfc.nasa.gov

Atmospheric Torques on the Solid Earth and Oceans Based on the GEOS-1 General Circulation Model

Output from the NASA/DAO GEOS-1 general circulation model has been used to compute atmospheric torques on the oceans and solid Earth for the period April 1, 1980 - November 30, 1995. The pressure torques due to polar flattening, equatorial ellipticity, and continental orography were computed. Wind stress torques over land and oceans were calculated as well as the gravitational torque due to the non-radial part of the Earth’s gravitational field. The computations include the axial component of torque, associated with changes in length of day (LOD), as well as the equatorial components, associated with motions of the Earth’s axis of rotation. Seasonal averaging and analysis was done for the various torque components.

Analysis of the seasonal means indicates the following: the equatorial torque vector rotates clockwise with the seasons (as seen from the North) on the equatorial plane. The pressure torque due to polar flattening and the gravitational torque are the largest contributors by far, with magnitudes ranging from 320 to 420 Hadleys for the torque associated with polar flattening and 145 to 200 Hadleys for the gravitational torque. They also control the annual harmonic equatorial budget with magnitudes of 280 Hadleys for the pressure torque due to polar flattening and 111 Hadleys for the gravitational torque.

Ocean wind stress ranks first (by power of variance) in the annual harmonic axial budget with a magnitude of 7 Hadleys. Global wind stress contributes more to annual variability of the axial component than mountain torque; their magnitudes are 9 and 3 Hadleys respectively.

It is of interest to ascertain what seasonal atmospheric pressure patterns are associated with the equatorial torque behavior. An example is presented in Figure 43, which shows the difference between the winter mean and the annual mean computed for the years 1981-1994. The seasonal means are based on 14 averages for each of the four seasons and 14 one-year averages. In general, the global pressure patterns show an inverse relationship between spring and autumn and between summer and winter. In particular the pressure field over the Asian landmass shows this pattern very dramatically.

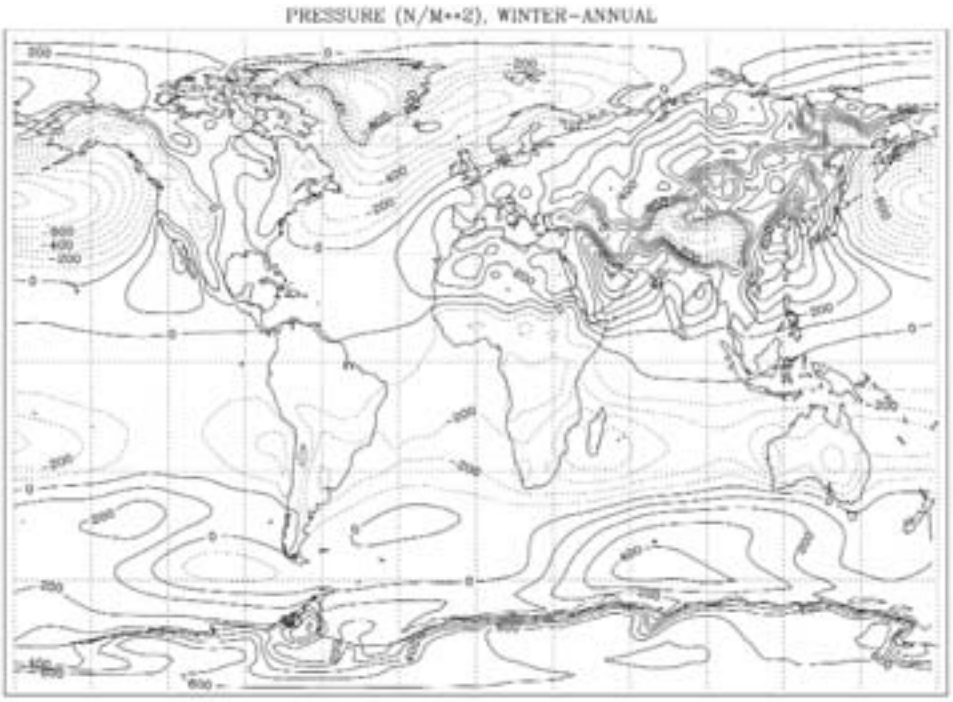

Figure 43. The difference between the mean winter pressure pattern and the mean annual pressure pattern. Annual mean computed for the years 1981-1994 (14 one-year averages). Seasonal means are based on 14 averages for each of the four seasons.

Contact: Braulio V. Sanchez, Space Geodesy Branch, Braulio.V.Sanchez.1@gsfc.nasa.gov

Time-Variable Gravity and Geophysical Cause

Temporal variations in the Earth's gravity field have been observed by studying the perturbations of orbiting satellites for over two decades. Our current efforts have examined the time-variable gravity signal from two different approaches using the SLR and DORIS data. The first approach has been the investigation of the long-term zonal rates. Comprehensive simultaneous solutions for the tiny annual variations and the long-term "secular" variation (i.e. a linear slope) superimposed upon the static zonal Stokes coefficients through spherical harmonic degree 5, in addition to the 9.3- and 18.6-year tidal amplitudes, have been estimated from tracking data for 9 spacecraft spanning the years 1979-1997 (in total) (Cox et al., 2000). The secular variations appear to be caused predominantly by post-glacial rebound—although our results indicate that possibly half of the post-glacial rebound effect can be offset by the effects of deglaciation and present-day Antarctic ice mass loss, both of which also have a substantial effect on the global water budget and sea level. The decadal geodynamic effects of artificial reservoirs appear to be at the threshold of observability; the recent results appear to support the predictions, that only about 1/3 of the actual mass had been represented in the estimates of major reservoir impoundments.

The level of misfit in the inverse solutions against the suite of geophysical models indicates that the geodetic observations (gravity zonal rates, polar drift rates, and sea level rates) are far from entirely explained using the existing modeling data available as of the last year or so. This situation is made worse by recent climatic changes (e.g., strong ENSO fluctuations) and the observed interannual variations in gravity field under consideration here—our solutions indicate that the inclusion of significant amounts of data from 1998 onward yield significantly different even-zonal harmonic solutions basically a reversal of trend since 1998. This has also been observed in yearly solutions for J2 through J4, where a change in slope is apparent somewhere between 1996 and 1998.

The second approach we have used involves the estimation of time-series solutions for the low-degree gravity field in a preliminary effort to understand and explain the apparent interannual signals (including the trend reversal) seen in the comprehensive and yearly solutions, and to better understand the annual signals. Time-variable gravity solutions at the yearly and shorter timescales have been generated and studied. The recovered annual signal exceeds the uncertainties out to degree 5 for the zonal harmonics, providing a spatial resolution of approximately 4000 km, enough to observe annual basin scale mass transport. Figure 44 shows the results for J2, after the inverted barometer ("IB") corrected atmospheric signal has been removed. In addition, an empirical residual annual term has been removed. There is a residual ENSO-period variation after the IB correction in the computation of the atmospheric gravity. Also shown are estimates for the Greenland+East Antarctic ice height change as sensed by radar altimetry, (provided by the Oceans and Ice Branch), and the global sea-level (GSL) change (assumed to be uniform over the ocean) derived from TOPEX/POSEIDON (T/P) data, both expressed as a J2 time series. As the figure shows, there is a significant deviation from the nominal rate occurring ca. 1998.

The J2 rates inferred from the observed GSL rate and the ice height rate do not explain the observed J2 rate. This is especially true if the nominal J2 rate of -2.9×10^{-11} per year reflects a long-term GSL rate of 1.8 mm/year. If the source is strictly within the oceans there has to be a redistribution of mass within the oceans, and possibly a redistribution of heat and salinity. As an example of the mass flux involved, imagine one fictitious scenario that increases J2—a uniform melting of the Greenland icesheet resulting in an eustatic sea level rise. It can be easily computed (3) that, for every 10^{-11} increase of J2, the required Greenland mass loss rate would be 102 gigatons (or cubic km in water volume), accompanied by a net global sea level (GSL) increase of 0.28 mm. To overshadow the PGR and produce the nominal J2 rates that we found, nearly seven times as much water per year would have to be involved, for a total (non-steric) GSL contribution of nearly 2 mm/yr. This is a global change of huge proportion never before experienced in short order in modern observations.

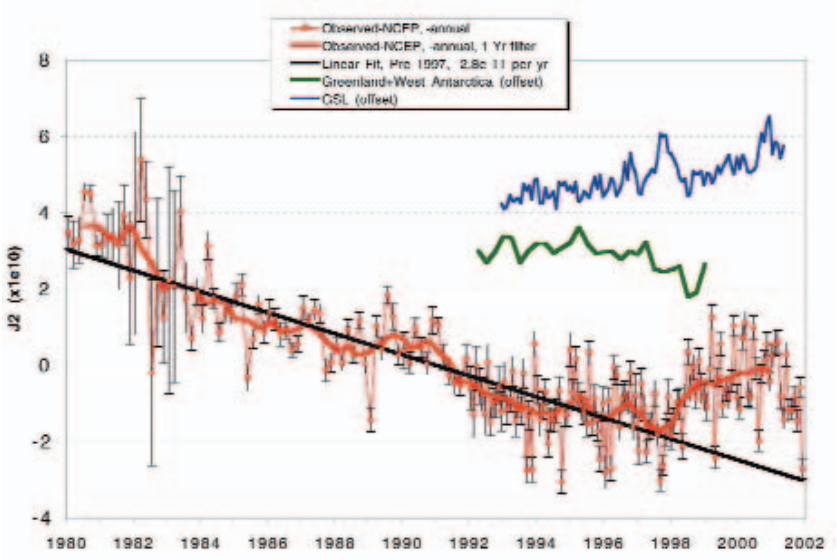

Figure 44. Observed J2 trend, after removal of IB corrected atmospheric gravity signal and a residual annual term. The black line is a weighted linear fit to the observed series through 1996. The equivalent J2 representation for global sea level (GSL), and the Greenland+W. Antarctic RADAR altimeter derived ice heights are also shown, and have been offset for clarity. Observed values prior to 1992 are 60-day values, after which they are nominally 30-day values. Error bars shown correspond to the formal uncertainty in the observed values. All values are $x10^{-10}$.

Contact: Christopher Cox, Space Geodesy Branch, ccox@stokes.gsfc.nasa.gov & Benjamin Chao, Space Geodesy Branch, Chao@bowie.gsfc.nasa.gov

Core Flow and Core-Mantle Interactions

Earth's outer core is the largest geophysical fluid system (in both volume and mass). It is always in convection, as evidenced by the presence of the geomagnetic field in much of Earth's history. Applying our MOSST geodynamo model output (described in the Geomagnetism section above), we study the interaction between the outer core and the solid mantle on various time scales. Figure 45 shows a snapshot of density anomaly distribution in the core. One can see a strong zonal flow (indicated by the zonal stretched fluid parcels), and an up-welling/down-welling convective flow (indicated by meridionally stretched fluid parcels). On very long timescales (~108 years), the properties of the lower mantle determine the core convection and geomagnetic field, which is the manifestation of the core responding to the forces from the mantle. On the extreme short timescale (years to decades), the solid mantle responds to the forces from the core.

Our current focus is the dynamics of core-mantle interactions that influences geodetic observables such as Earth's rotation in decadal length of day (LOD) variation. In past studies, limited to kinematic studies, we incorporated the dynamic core-mantle interactions within our numerical geodynamo model MOSST. Our accomplishments include (1) estimating the topographic (or pressure) core-mantle interaction, that are dynamically consistent with the core dynamics (the results are published on GRL and reported in several conferences); (2) estimating electromagnetic core-mantle coupling, in which the Lorentz stress and the magnetic torque on the CMB are simulated with a (varying) electrically conducting D"-layer (our manuscript on the research is accepted for publication and the results are also presented in IAGA/IASPEI joint assembly and in AGU meetings); (3) estimated effect of density anomalies on the gravitational core-mantle interaction; (4) initiation of studies on the effect of mass redistribution in the core on time-varying gravity field, and on the pressure loading at the CMB and mantle deformation (see also Geomagnetic Field and Geodynamo Modeling entry in the Geomagnetism section above).

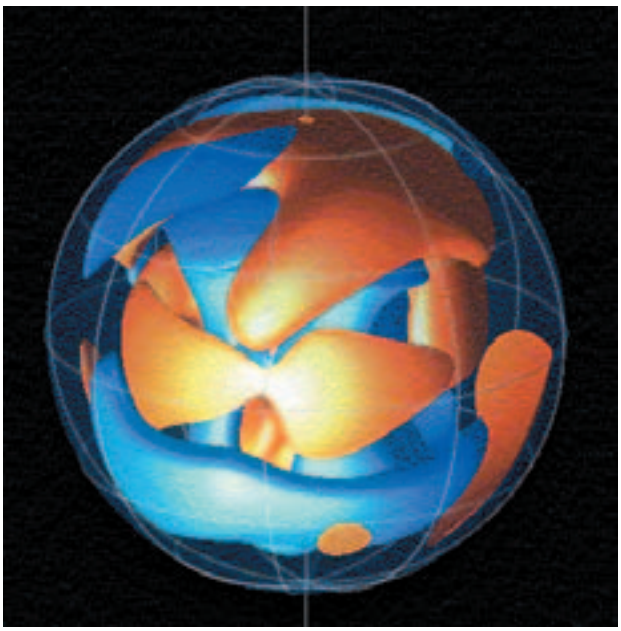

Figure 45. A snapshot of density anomalies from our numerical model MOSST Lighter fluid parcels (in orange) ascend from the inner core boundary to the core-mantle boundary spirally. Heavier fluid parcels (in blue) move in opposite direction.

Contact: Weijia Kuang, Space Geodesy Branch, kuang@bowie.gsfc.nasa.gov

Planetary Missions

Mars Orbiter Laser Altimeter - MOLA

MOLA is the Mars Orbiter Laser Altimeter, an instrument currently in orbit around Mars on the Mars Global Surveyor (MGS) spacecraft. The instrument transmits infrared laser pulses towards Mars at a rate of 10 Hz and measures the time of flight to determine the range of the MGS spacecraft to the Martian surface. Range measurements have been used to construct a precise topographic map of Mars that has many applications to studies in geophysics, geology and atmospheric circulation. MOLA also functions as a passive radiometer, and is currently measuring the radiance of the surface of Mars at 1064 nm.

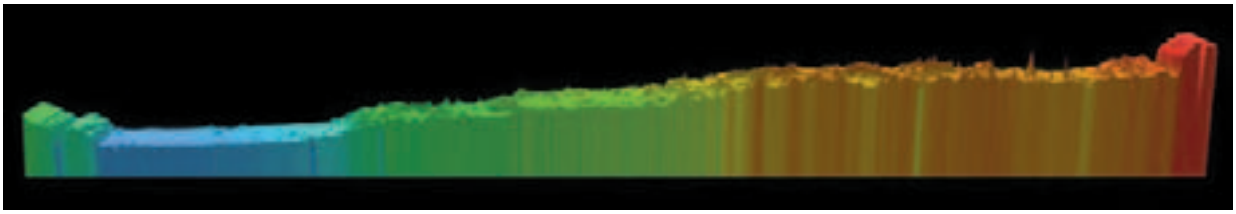

Figure 46.

Figure 46 is a pole-to-pole view of Martian topography from the first MOLA global topographic model [Smith et al., Science, 1999]. The slice runs from the north pole (left) to the south pole (right) along the 0° longitude line. The figure highlights the pole-to-pole slope of 0.036°, such that the south pole has a higher elevation than the north pole by ~6 km. This global-scale slope was likely present for most of Mars' history and controlled the surface and subsurface transport of water indicated by images of outflow channels and valley networks. The regional high (in orange) in mid-southern hemisphere latitudes corresponds to the western edge of the topographic annulus that encircles the massive Hellas impact basin. In the figure warm colors correspond to high elevations and cold colors correspond to low elevations. Note the exceedingly flat northern hemisphere in blue.

The Mars Global Surveyor spacecraft, launched November 7, 1996 by the National Aeronautics and Space Administration (NASA) and the Jet Propulsion Laboratory (JPL) of the California Institute of Technology, carries a remote-sensing instrument, MOLA-2, a laser altimeter with a range precision of 37 centimeters, and a profiling resolution on the Martian surface of ~300 m. MOLA's vertical accuracy is limited by the orbital determination for the spacecraft, and is currently at the sub-5-m level (~1-meter not including geoid error!) but is expected to improve further with advanced orbit reconstruction techniques.

The MOLA instrument is functioning as a passive radiometer and is routinely sampling the 1064-nm radiance of the Martian surface. Measurements are collected once a second and have a resolution of approximately 300 m x 3 km.

MOLA last collected altimetry data on June 30, 2001, when the instrument oscillator stopped. Without the oscillator the laser does not receive fire commands. At the time of the oscillator anomaly, MOLA had been in space for 1696 days, and had undergone 216 power-on/off cycles. The MOLA laser had fired 671 million times in space and MOLA had made about 640 million measurements of the Martian surface and atmosphere. Until the anomaly, the laser energy had been nominal and steady at about 20 mJ/pulse. The June 30 event was the first anomaly in MOLA's operation since the MGS launch in November 1996 .

To measure the radiance of the Martian surface, the MOLA receiver is used to measure optical

power at 1064 nm scattered by Mars within its receiver field-of-view. MOLA's passive radiometer mode was built into the instrument, but was previously used only to automatically adjust the settings of the ranging receiver thresholds. Passive radiances were collected throughout the MGS Mapping and Extended Mission, and these observations are only now being processed for scientific use. In the passive mapping mode, the instrument has been optimized for measuring radiance, and the instrument now has greater sensitivity than it did when used for ranging. Radiance measurements are being relayed back to Earth in the same manner as the altimetry data. These data will be processed and calibrated, and then released as soon as possible. The data will also be documented and archived by the NASA Planetary Data System.

Seasonal Variations of Snow Depth on Mars

Using topography collected over one martian year from the MOLA on the MGS spacecraft, there was measured temporal changes in the elevation of the martian surface that correlate with seasonal cycle of carbon dioxide exchange between the surface and atmosphere. The greatest elevation change (1.5 to 2 meters) occurs at high latitudes (above 800), whereas the bulk of the mass exchange occurs at lower latitudes (below 750 N and below 730 S). An unexpected period of sublimation was observed during northern hemisphere autumn, coincident with dust storms in the southern hemisphere. Analysis of MGS Doppler tracking residuals revealed temporal variation in the flattening of Mars that correlate with elevation changes. The combined changes in gravity and elevation constrain the average density of seasonally deposited carbon dioxide to be 901 +- 230 kilograms per cubic meter, which is considerably denser than terrestrial snow.

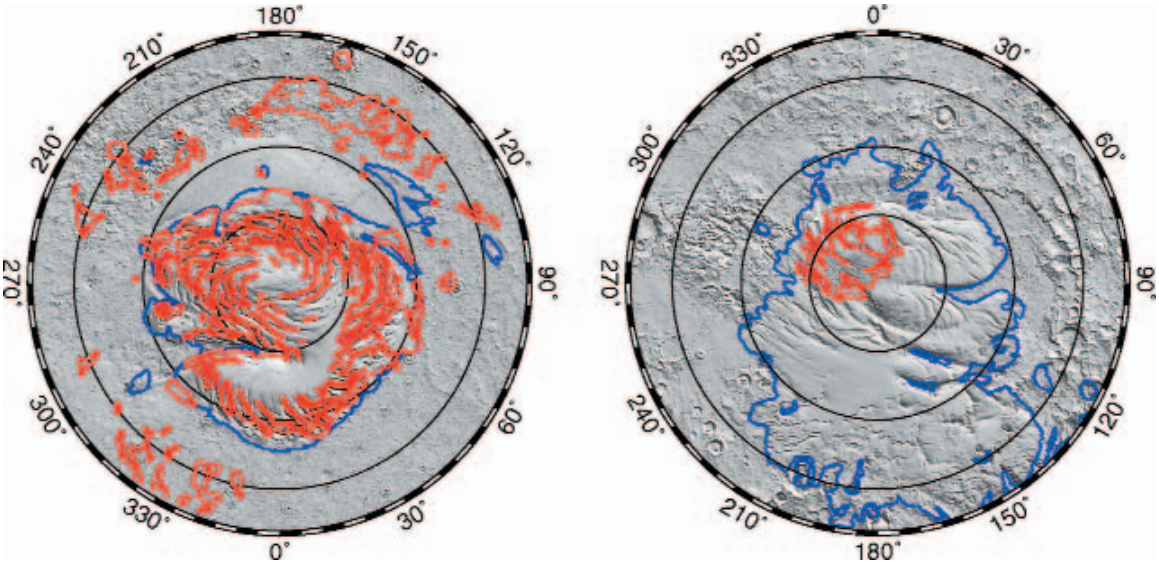

Figure 47. Shaded relief maps of (left) north and (right) south polar topography of Mars. The projection is polar stereographic from latitude 720 to the poles. The red contours in each hemisphere represent the approximate extent of the residual ice caps (demoted by high albedo); the blue contours trace regions of elevated polar layered terrains. Smith et al., Science, December 2001

Contact: David Smith, dsmith@tharsis.gsfc.nasa.gov

MErcury Surface, Space ENvironment, Geochemistry, and Ranging (MESSENGER)

Mercury holds answers to several critical questions regarding the formation and evolution of the terrestrial planets. As part of the Discovery Program of the NASA, the MErcury Surface, Space ENvironment, Geochemistry, and Ranging (MESSENGER) spacecraft will orbit Mercury for one Earth year after completing two flybys of the planet following two flybys of Venus. The necessary flybys will return significant new data early in the mission, while the orbital phase, guided by the flyby data, enables a focused scientific investigation of this least-studied terrestrial planet.

Knowledge of the planet Mercury is critical to the understanding of how terrestrial planets formed and evolved. Determining the surface composition of Mercury, a body with a ratio of metal to silicate higher than any other planet or satellite, will provide a unique window on the processes by which planetesimals in the primitive solar nebula accreted to form planets.

At the time of this publication, MESSENGER project is on schedule and on budget for a March 2004 launch. MESSENGER will be the first spacecraft to visit Mercury in more than 30 years and the first spacecraft to be placed in orbit about that planet. Observations to be made during the MESSENGER advance substantially our knowledge of the formation and evolution of Mercury and of the terrestrial planets in general. Comparative studies of planetary geology, planetary composition and structure, magnetic field generation, and planetary exospheres and magnetospheres will all benefit from the new information that MESSENGER will reveal.

Contact: David Smith, dsmith@ tharsis.gsfc.nasa.gov

2001 Refereed Publications

The Laboratory's publications for the year 2001 are listed in the various discipline sections. The total number of our refereed publications that actually appeared in print in 2001 was 112 (i.e., this does not include papers that were "accepted" and/or "in press"). This figure includes refereed journal articles, book chapters, and/or books authored by our civil servants, post doc's, visiting scientists, contractors, and people from other agencies co-located in our physical space who conduct joint research with us. The 39 publications in Geodynamics & Space Geodesy are listed below.

Bills B.G., Nerem R.S., "Mars Topography: Lessons Learned from Spatial and Spectral Domain Comparisons of Mars Orbiter Laser Altimeter and US Geological Survey Data", J GEOPHYS RES-PLANET 106: (E12) 32915-32925 DEC 25 2001.

Cheng, A. F., O. Barnouin-Jha, M. T. Zuber, J. Veverka, D. E. Smith, G. A. Neumann, M. Robinson, P. Thomas, J. B. Garvin, S. Murchie, C. Chapman, L. Prockter., "Laser Altimetry of small-scale features on 433 Eros from NEAR-Shoemaker"., Science v292, 488-491, 2001

Chao, B. F., W. O'Connor, D. Zheng, and A. Y. Au, Reply to comment by C. Wunsch on 'Wind stress forcing of the North Sea pole tide', Geophys. J. International, 146, 266, 2001.

Cohen S.C., Freymueller JT, "Crustal Uplift in the South Central Alaska Subduction Zone: New Analysis and Interpretation of Tide Gauge Observations", J GEOPHYS RES-SOL EA 106: (B6) 11259-11270 JUN 10 2001.

Egbert G.D., Ray R.D., "Estimates of M-2 Tidal Energy Dissipation from TOPEX/Poseidon Altimeter Data", J GEOPHYS RES-OCEANS 106: (C10) 22475-22502 OCT 15 2001.

Hernandez-Pajaeres, M., J. Miguel Juan, Jaume Sanz, and O. L. Colombo A new strategy for real-time integrated water vapor determination in WADGPS networks, Geophys. Res. Lett., 28(17), 3267-3270, 2001.

Hollis, J.M., Boboltz, D.A., Pedelty, J.A., White, S.M., and Forster, J.R. "R Aquarii: Evidence for Differential Rotation of the SiO Maser Shell," 2001, ApJ (Letters), 559, L37.

Iorio L. and E. C. Pavlis "Tidal satellite perturbations and the Lense-Thirring effect", Journal of the Geodetic Society of Japan, Vol. 47, 1, pp. 1-7, 2001.

Jaeger, J., B. Hallet, T. Pavlis, J. Sauber and others, 'Orogenic and glacial research in pristine southern Alaska", EOS Trans. Am. Geophys. Un. 82, 213, 216, 2001.

Johnson, Thomas J., C. R. Wilson, and B. F. Chao, "Nontidal oceanic contributions to gravitational field changes: Predictions of the Parallel Ocean Climate Model", J. Geophys. Res., 106(B6), 11315-11334, 2001.

Harding D.J., Lefsky M.A., Parker G.G., et al., "Laser Altimeter Canopy Height Profiles - Methods and Validation for Closed-canopy, Broadleaf Forests", REMOTE SENS ENVIRON 76: (3) 283-297 JUN 2001.

Kellogg, E.M, Pedelty, J.A., and Lyon, R.G. "The X-ray System R Aquarii: A Two-sided Jet and Central Source," 2001, ApJ (Letters), 563, L151.

Kuang, Weija and B. F. Chao, "Topographic core-mantle coupling in geodynamo modeling", Geophys. Res. Lett., 28(9), 1871-1874, May 1, 2001.

Lemoine FG, Smith DE, Rowlands DD, et al., "An Improved Solution of the Gravity Field of

Mars (GMM-2B) from Mars Global Surveyor", J GEOPHYS RES-PLANET 106: (E10) 23359-23376 OCT 25 2001.

Liu, H.S. “Obliquity modulation of the incoming solar radiation”, Recent Res. Develop. In Atmos. Sci., 1, 15-37,2001,, 08/01.

Liu, H.S. “Orbital noise in the Earth system and climate fluctuations”, Noise in Physical Systems and 1/f Fluctuations (book and journal), pp 801-804, 2001.

Lowe, Parker, M. Purucker and Constable, “Estimating the Crustal Power Spectrum from Vector Magsat Data”, J. Geophys. Res. 106, 8589-8598, 2001.

Lowman, P. D., “Evidence from Apollo: How science teachers can show students that humans have landed on the Moon”, The Science Teacher, 68, 22-25, 2001, 05/01

Lowman, P.D. “A new Sputnik surprise?”, Space Times, American Astronautical Society, Iss. 6, v. 40, p. 15-20, 2001 11/01.

Luthcke, S.B., C.C. Carabajal, D.D. Rowlands and D.E. Pavlis,Improvements in spaceborne laser altimeter data geolocation, Surveys in Geophysics, Vol. 22, pp. 549-559, 2001.

McGovern, P.J., S.C. Solomon, J.W. Head, D.E. Smith, M.T. Zuber, and G.A. Neumann, “Extension and Uplift at Alba Patera, Mars: MOLA Observations and Loading Models”, J. GEOPHYS. RES. 106, 23,769-23,809, 2001.

Merayo, J.M.G, others and T. Sabaka, “The orthogonalization of magnetic systems”, J. Sensors & Actuators 89, 185-196, 2001.

Neumann, G. A., D. D. Rowlands, F. G. Lemoine, D. E. Smith, and M.T. Zuber, “The crossover analysis of MOLA altimetric data”, J. Geophys. Res., 106(E10), 23753-23768, 2001.

Parker G.G., Lefsky M.A., Harding D.J., "Light Transmittance in Forest Canopies Determined Using Airborne Laser Altimetry and In-canopy Quantum Measurements", REMOTE SENS ENVIRON 76: (3) 298-309 JUN 2001.

Pavlis, N.K., C. M. Cox, E. C. Pavlis and F.G. Lemoine Intercomparison and evaluation of some contemporary global geopotential models, Bollettino di Geofisica Teorica ed Applicata, 40, No. 3-4, pp. 245-254, Sep.-Dec. 1999, (actually published in late 2001).

Ray R.D., "Inversion of Oceanic Tidal Currents from Measured Elevations", J MARINE SYST 28: (1-2) 1-18 FEB 2001.

Ray R.D., Cartwright DE, "Estimates of Internal Tide Energy Fluxes from Topex/Poseidon Altimetry: Central North Pacific", GEOPHYS RES LETT 28: (7) 1259-1262 APR 1 2001 .

Ray R.D., Eanes RJ, Lemoine FG, "Constraints on Energy Dissipation in the Earth's Body Tide from Satellite Tracking and Altimetry", GEOPHYS J INT 144: (2) 471-480 FEB 2001.

Ray R.D., "Comparisons of Global Analyses and Station Observations of the S-2 Barometric Tide", J ATMOS SOL-TERR PHY 63: (10) 1085-1097 JUL 2001.

Ray R.D., Eanes RJ, Egbert GD, et al., "Error Spectrum for the Global M-2 Ocean Tide", GEOPHYS RES LETT 28: (1) 21-24 JAN 1 2001.

Ray R.D., "Resonant Third-degree Diurnal Tides in the Seas off Western Europe", J PHYS OCEANOGR 31: (12) 3581-3586 DEC 2001.

Sakimoto, S.E.H. and T.K.P. Gregg, "Channeled flow: analytic solutions, laboratory experiments and applications to lava flows", J. Geophys. Res. (Solid Earth) 106, 8629-8648, 2001.

Smith D.E., Zuber MT, Frey H.V., et al., "Mars Orbiter Laser Altimeter: Experiment Summary After the First Year of Global Mapping of Mars", J GEOPHYS RES-PLANET 106: (E10) 23689-23722 OCT 25 2001.

Smith, D.E., M.T. Zuber and G.A. Neumann, "Seasonal Variation of Snow Depth on Mars", Science, 294, 2141-2146, 2001.

Smith, D.E., M.T. Zuber, H.V. Frey, J.B. Garvin, J.W. Head, D.O. Muhleman, G.H. Pettengill, R.J. Phillips, S.C. Solomon, H.J. Zwally, W.B. Banerdt, T.C. Duxbury, M.P. Golombek, F.G. Lemoine, G.A. Neumann, D.D. Rowlands, O. Aharonson, P.G. Ford, A.B. Ivanov, P.J. McGovern, J.B.Abshire, R.S. Afzal, and X. Sun, "Mars Orbiter Laser Altimeter (MOLA): Experiment Summary After the First Year of Global Mapping of Mars", J. GEOPHYS. RES 106, 23,689-23,722, 2001.

Solomon, S., others, D. E. Smith, others, "The MESSENGER mission to Mercury: scientific objectives and implementation", Planetary and Space Science, 49(14-15), 1445-1465, 2001.

Tracadas PW, Zuber MT, Smith DE, et al., "Density Structure of the Upper Thermosphere of Mars from Measurements of Air Drag on the Mars Global Surveyor Spacecraft", J GEOPHYS RES-PLANET 106: (E10) 23349-23357 OCT 25 2001.

Tyler G. L., D. P. Hinson, W. L. Sjogren, D. E. Smith, R. A. Simpson, S. W. Asmar, P. Priest, and J. D. Twicken,Radio science observations with Mars Global Surveyor: Orbit insertion through one Mars year in mapping orbit, J. Geophys, Res., 106(E10), 23327-23348, 2001.

Withers, P. and G.A. Neumann, "Enigmatic Ridges on the Plains of Mars", NATURE, 410, 652, 2001.

2001 Conference Proceedings

Carabajal, C.C. and D.J. Harding, Evaluation of Geoscience Laser Altimeter System (GLAS) Waveforms for Vegetated Landscapes Using Laser Altimeter Scanning Data, International Archives of Photogrammetry and RemoteSensing, Vol. XXXIV-3/W4, Annapolis, MD, pp. 125-128, 22-24 Oct., 2001.

Colombo, O. L., A. G. Evans, M. Ando, K. Tadokoro, K. Sato, T. Yamada, Speeding up the estimation of floated ambiguities for sub-decimeter kinematic positioning at sea, Proceedings ION GPS-2001, Salt Lake City, Utah, September 2001.

Colombo, O. L., M. Hernandez-Pajares, J. M. Juan, J. Sanz, Long-Baseline (>400 km) on the fly ambiguity resolution using ionosperic corrections with high geomagnetic activity, Proceedings GNSS-2001 Meeting, Seville, Spain, April 2001.

Lemoine, F. G., D. D. Rowlands, S. B. Luthcke, N. Zelensky, D. S. Chinn and D. Pavlis, "Precise orbit determination for GEOSAT Follow-On using satellite laser ranging data and intermission altimeter crossovers", NASA/CP-2001-209986, Proceedings of the 2001 Flight Mechanics Symposium, NASA GSFC, edited by J. Lynch, 377-392, 2001.

Luthcke, S. B., D. D. Rowlands, and C. Carabajal, Spaceborne laser altimeter instrument calibra-

tion from integrated residual analysis - a brief overview, International archives of Photogrammetry and Remote Sensing, Vol. XXXIV-3/W4, Annapolis, Maryland, pp. 81-83, 22-24 Oct., 2001.

Ma, C., Extension of the ICRF, Proceedings of the 15th Working Meeting on European VLBI for Geodesy and Astrometry, Barcelona, Spain, September 7-8, 2001.

Ma, C., The effect of reference frames on EOP estimates from VLBI, Proceedings of Journees 2001 Systemes de Reference Spatio-Temporels, Brussels, Belgium, September 24-26, 2001.

2001 Presentations & Seminars

Major Meeting Presentations

32nd Lunar and Planetary Science Conference Presenations

Bills, B.G. and R. D. Ray, "Tidal and librational energetics of Europa [#1713]", 32nd Lunar and Planetary Science Conference, 3/15/01

Bradley, B.A. and S.E.H., "Sakimoto Interactions of the Medusae Fossae Formation (MFF), fluvial channels, and the dichotomy boundary southeast of Nicholson Crater, Mars [#1335]", 32nd Lunar and Planetary Science Conference, 3/15/01

Carter, B.L., H. Frey, S.E.H. Sakimoto and J. Roark, "Constraints on Gusev Basin infill from the Mars Orbiter Laser Altimeter (MOLA) topography [#2042]", 32nd Lunar and Planetary Science Conference, 3/15/01

Frey, H., K.M. Shockey, E.L. Frey, J.H. Roark and S.E.H. Sakimoto, "A very large population of likely buried impact basins in the northern lowlands of Mars revealed by MOLA data [#1680]", 32nd Lunar and Planetary Science Conference, 3/15/01

Gregg, T.K.P., D.A. Crown and S.E.H. Sakimoto, "Evolution and erosion of Tyrrhena and Hadriaca Paterae, Mars: new insights from MOC and MOLA [#1628]", 32nd Lunar and Planetary Science Conference, 3/15/01

Grosfils, E.B. and S.E.H. Sakimoto, "Topographic constraints on magma reservoir volume and depth for small near-polar volcanoes in the northern plains of Mars [#1111]," 32nd Lunar and Planetary Science Conference, 3/15/01

Grosfils, E.B., S.E.H. Sakimoto, C.V. Mendelson and J.E. Bleacher, "The KECK "Mars 2000" Project: using Mar Orbiter Laser Altimeter data to assess geological processes and regional stratigraphy near Orcus Patera and Marte Valles on Mars [#1110]," 32nd Lunar and Planetary Science Conference, 3/15/01

Moller, S.C., K.E. Poulter, E.B. Grosfils, S.E.H. Sakimoto, C.V. Mendelson and J.E. Bleacher, "Morphology of the Marte Valles channel system, Mars [#1382]", 32nd Lunar and Planetary Science Conference, 3/15/01

Purucker, M., B. Langlais and M. Mandea, "Interpretation of a magnetic map of the Valles Marineris region, Mars [#1865]," 32nd Lunar and Planetary Science Conference, 3/15/01

Riedel, S.J., S.E.H. Sakimoto, B.A. Bradley and A. DeWit, "Lava tube flow models at Alba Patera, Mars: topographic constraints on eruption rates [#1954]," 32nd Lunar and Planetary

Science Conference, 3/15/01

Roark, J. H. and H. V. Frey, "GRIDVIEW: Recent improvements in research and education software for exploring Mars [#1618]", 32nd Lunar and Planetary Science Conference, 3/15/01

Sakimoto, S.E.H., J.B. Garvin, B.A. Bradley, M. Wong and J.J. Frawley, "Small martian north polar volcanoes: topographic implications for eruption styles [#1808]," 32nd Lunar and Planetary Science Conference, 3/15/01

Silver, M.H., A.S. Gendaszek, E.B. Grosfils, S.E.H. Sakimoto, C.V. Mendelson and J.E. Bleacher, "Wrinkle ridges formation north of Orcus Patera region of Mars [#1043]", 32nd Lunar and Planetary Science Conference, 3/15/01

Therkelsen, J.P., S.S. Santiago, E.B. Grosfils, S.E.H. Sakimoto, C.V. Mendelson and J.E. Bleacher, "Eruption constraints for a young channelized lava flow, Marte Valles, Mars [#1112]", 32nd Lunar and Planeary Science Conference, 3/15/01

Van der Kolk, D.A., K.L.T. Gribbett, E.B. Grosfils, S.E.H. Sakimoto, C.V. Mendelson and J.E. Bleacher, "Orcus Patera, Mars: impact crater or volcanic caldera [#1085]", 32nd Lunar and Planetary Science Conference, 3/15/01

Wong, M., S.E.H. Sakimoto and J.B. Garvin, "Topography of small volcanoes in Tempe terra and Ceraunius Fossae: implications for eruptive style [#1563]," 32nd Lunar and Planetary Science Conference, 3/15/01

Yoburn, JB., R. Yazzie, E.B. Grosfils, S.E.H. Sakimoto, C.V. Mendelson and J.E. Bleacher, "Age relationships and chronology for the Orcus Patera region of Mars [#1077]", 32nd Lunar and Planetary Science Conference, 3/15/01

Nazarova, Katherine A., and James R. Heirtzler, “Tectonics From Satellite Geomagnetic Measurements”, 7th Zonenshain International Conference on Plate Tectonics, Moscow, Oct. 31, 2001.

Spring 2001 American Geophysical Union Meeting Presentations

Bradley, B.A. and S. E. H. Sakimoto, "Layers and jointing within the Medusae Fossae Formation, Mars (P41A-02)", Spring 2001 AGU Meeting, Boston, MA, 5/30/01

Frey, H., K.M. Shockey, J.H. Roark, E.L. Frey and S.E.H. Sakimoto, "Buried impact basins in the northern lowland of Mars: implications for crustal evolution and the crustal dichotomy (P31A-04)", Spring 2001 AGU Meeting, Boston, MA, 5/30/01

Gregg, T.K. and S. E. H. Sakimoto, "Martian lava: emplacement parameters using MOLA data and numerical models (V42A-05)", Spring 2001 AGU Meeting, Boston, MA, 5/30/01

Glaze, L. and S. E. H. Sakimoto, "Use of slopes of small martian edifices (V42A-10)", Spring 2001 AGU Meeting, Boston, MA, 5/30/01

Ma, S., and W. Kuang, “The effect of high frequency field and heterogeneous conductivity on magnetic core-mantle coupling”, (S42A-06).

Miller, J.L., D. Ravat, P. T. Taylor, H. Frey, others, "Interpretation of the martian southern highland magnetic anomalies using the Euler and analytic signal methods (GP22A-05)", Spring 2001 AGU Meeting, Boston, MA, 5/30/01

Purucker, M., B. Langlais and M. Mandea, "Terrestrial and martian magnetizations of lithospheric origin: comparative planetology (P22A-04)", Spring 2001 AGU Meeting, Boston, MA, 5/30/01

Purucker, M.E., B. Langlais, G. Hulot, M. Mandea, and N. Olsen, "Global lithospheric magnetization model validated and refined using new satellite observations (GP32A-05)", Spring 2001 AGU Meeting, Boston, MA, 5/30/01

Rubincam, D.P., "Polar wander on Triton and Pluto (T51A-13)", Spring 2001 AGU Meeting, Boston, MA 5/30/01

Sakimoto, S.E.H., others, "The Mars 2000 Keck undergraduate research project: assessing the regional geology of the Cerberus Plains region (ED21B-04)", Spring 2001 AGU Meeting, Boston, MA 5/30/01

Sanchez, B. V., Atmospheric gravitational torque variations based on various gravity fields. (A42A-01).

Solomon, S.C., others, H.V. Frey, others, "What happened when on Mars? (P31A-06, invited) Spring 2001 AGU Meeting, Boston, MA, 5/30/01

Smith, D. E., M. T. Zuber, and G. A. Neumann, Observations of the CO2 and dust cycles on Mars seen by MOLA. (P32A-02, Invited)

Taylor, P.T., R.R. von Frese and H. Kim Oersted, "Magsat and airborne observations of the Kursk magnetic anomaly (GP32A-03)," Spring 2001 AGU Meeting, Boston, MA, 5/30/01

Taylor, P.T., J. J. Frawley, D. Ravat, S. Zatman and H.V. Frey, "Satellite magnetic anomalies from MGS over the South Tharsis Region of Mars (GP22A-06)," Spring 2001 AGU Meeting, Boston, MA, 5/30/01

Zatman, S., others, P.T. Taylor and J. J. Frawley, "Geodynamic constraints on the age of martian magnetic anomaly construction (GP32A-01)," Spring 2001 AGU Meeting, Boston, MA, 5/30/01

Fall 2001 Geological Society of America Meeting Presentations

Bradley, B.A. and S. E. H. Sakimoto, "Layers and jointing within the Medusae Fossae Formation, Mars (P41A-02)", Fall 2001, GSA Meeting Boston, MA 11/05/01

Frey, H., K.M. Shockey, J.H. Roark, E.L. Frey and S.E.H. Sakimoto, "Ancient lowlands on Mars: Buried impact basins and the age of the crustal dichotomy," Fall 2001, GSA Meeting Boston, MA 11/05/01

Sakimoto, S.E.H., S.J. Reidel and D. Burr, "Geologically recent volcanism and flooding in Elysium Planitia and Cerberus Rupes: plains style volcanism and related water release?", Fall 2001, GSA Meeting Boston, MA, 11/05/01

Fall 2001 American Geophysical Union Meeting Presentations

Altamimi Z., D. Angermann, D. Argus, G. Blewitt, C. Boucher, B. Chao, H. Drewes, R. Eanes, M. Feissel, R. Ferland, T. Herring, B. Holt, J. Johannson, K. Larson, C. Ma, J. Manning, C. Meertens, A. Nothnagel, E. C. Pavlis, G. Petit, J. Ray, J. Ries, H.-G. Scherneck, P. Sillard, and M. Watkins "The Terrestrial Reference Frame and the Dynamic Earth", EOS, Transactions, AGU, 82(85), pp. 273, 278-279, 2001.

Beckley, B.D., C. J. Koblinsky, Y. Wang, and N. P. Zelensky, High resolution SSH Anomaly Fields from Coincident TOPEX, ERS-2 and GFO Altimeter observations, EOS, Trans. AGU, 82(47), G22A-0204, F256, 2001.

Bills, B.G. Bonneville, "Lahonton and Minchin: new estimates of crust and upper mantle viscosity and density structure from large lake loads (T42-F-07)," Fall 2001 AGU Meeting, San Francisco, CA, 12/08/01

Blair, B., and M. A. Hofton, Topographic change detection using Full-waveform imaging Lidar, EOS, Trans. AGU, 82(47), G22C-0225, F260, 2001.

Burr, D., A.S. McEwen and S. E. H. Sakimoto, "Recent aqueous floods from the Cerberus Rupes, Mars (P22A-0537)", Fall 2001, AGU Meeting, San Francisco, CA, 12/08/01

Cohen, S.C. and D.J. Darby, "Tectonic plate coupling and elastic thickness using a viscoelastic model of crustal deformation in southern North Island, New Zealand (T42F-11)", Fall 2001, AGU Meeting San Francisco, CA, 12/08/01

Cox, C.M., A. Y. Au, B. F. Chao, Investigation of recent Interannual variations in the geopotential, EOS, Trans. AGU, 82(47), G51C-0263, F294, 2001.

Derby, C. A., G. A. Neumann and S. E. H. Sakimoto, "The topography of Mars: understanding the surface of Mars through the Mars Orbiter Laser Altimeter (ED51A-0225)", Fall 2001, AGU Meeting San Francisco, CA, 12/08/01

Freymueller, J., C. Zwec, H. Fletcher, S. Hreinsdttir, S.C. Cohen, and M. Wyss, "The great Alaska "earthquake" of 1998-2001 (G22D-11)", Fall 2001 AGU Meeting, San Francisco, CA, 12/08/01

Fujita, M., B. F. Chao, B. Sanchez, T. Johnson, Oceanic torques on the solid Earth and their effects on rotation,EOS, Trans. AGU, 82(47), G42A-08, F289, 2001.

Gregg, T. K. P, S. E. H. Sakimoto, D. A Crown, B. R. Meyers and H. Gittings, "The western Hesperian Planum region of Mars: MGS-based revelations (P31B-11)", INVITED, Fall 200,1 AGU Meeting San Francisco, CA, 12/08/01

Harding, D.J. and C. C. Carabajal, "SRTM and laser altimeter views of western Washington State topography (G22B-0222)", Fall 2001, AGU Meeting San Francisco, CA, 12/08/01

Hofton, M. A., L. E. Rocchio, J. B. Blair, R. Dubayah, Validation of large-footprint lidar subcanopy topography measurements beneath a dense tropical forest, EOS, Trans. AGU, 82(47), G22C-0227, F260, 2001.

Ivanov, A.B., G. A. Neumann, D. O. Muhlemann,Joint analysis of the MOLA radiometry data and TES Lambert albedo, EOS, Trans. AGU, 82(47), P42A-0556, F723, 2001.

Kolenkiewicz, R, D.E. Smith, M.H. Torrence, and P. J. Dunn, "Geodynamic Motion at European SLR Sites (G22C-0241)", Fall 2001, AGU Meeting San Francisco, CA, 12/08/01

Kuang, W., Numerical modeling of laboratory dynamos, EOS, Trans. AGU 82(47), GP31A-0179, 2001.

Lemoine, F.G., G. A. Neumann, D. S. Chinn, D. E. Smith, M. T. Zuber, D. D. Rowlands, D. P. Rubincam, and D. E. Pavlis, Soltuions of Mars Geophysical parameters from Mars Global Surveyor tracking data, EOS, Trans. AGU, 82(47), P42A-0545, F721, 2001.

Lillibridge, J., N. Zelensky, F. Lemoine, D. Rowlands, D. Chinn, and B. Beckley, Operational and precise orbit determination for GEOSAT Follow-On Altimetry, EOS, Trans. AGU, 82(47), G22A-0202, F256, 2001.

Luthcke, S.B., D. D. Rowlands, F. G. Lemoine, D. E. Pavlis, O. L. Colombo, R. D. Ray, B. Thompson, R. S. Nerem, and T. A. Williams, CHAMP Tracking and Accelerometer Data Analysis Results EOS, Trans. AGU, 82(47), G41C-05, F287, 2001.

Ma, C., D. S. MacMillan, and L. Petrov, The Terretrial reference frame derived from VLBI, EOS, Trans.AGU, 82(47), G32A-11, 2001.

MacMillan, D.S., L. Petrov, C. Ma, Earth rotation results using Mark 4 VLBI EOS, Trans, AGU, 82(47), G51C-0253, F293, 2001.

McGeary, S., B. G. Bills and G. Jimenez, "High resolution seismic reflection imaging of lacustrine stratigraphy of the Salar de Uyuni", Bolivia (PP22A-0510) Fall 2001 AGU Meeting, San Francisco, CA, 12/08/01

Pavlis, E. C. New Satellite Laser Ranging TRF and EOP Series for Mass Transport Studies in the Earth System, ", Eos Trans. AGU, 82(47), Fall Meet. Suppl., Abstract G51C-0254, F293, 2001.

Ray, R.D., and G. Egbert, Polar motion constraints on models of the fornightly tide, EOS, Trans. AGU, 82(47), G42A-11, (INVITED), F289, 2001.

Rowlands, D., R. D. Ray, D. S. Chinn, and F. G. Lemoine, Gravity estimation from a simulated GRACE mission: Short vs. Long arcs, EOS, Trans. AGU, 82(47), G51A-0237, F290, 2001.

Sakimoto, S. E. H., T. K. Gregg and S. J. Reidel, "Channel, lava tube, and edifice flow models: developments and recent applications for Mars (P22D-07)", Fall 2001, AGU Meeting, San Francisco, CA, 12/08/01

Sakimoto, S. E. H., D. Mitchell, S. J. Reidel and B. Bradley, "The new martian plains volcanism: how MGS is rewriting our understanding of plains and small edifice emplacement (P31B-09)", INVITED Fall 2001, AGU Meeting, San Francisco, CA, 12/08/01

Sauber, J., G. A. Carver and C. C. Carabajal, "Topography and surface change at the shallow subduction zone near Kodiak Island, Alaska (G22B-0221)", Fall 2001, AGU Meeting, San Francisco, CA, 12/08/01

Schmerr, N. C., J. B. Garvin, G. A. Neumann and S. E. H. Sakimoto, "Seasonal changes in the thickness of martian polar crater deposits from the Mars Orbiter Laser Altimeter (P31A-0544)", Fall 2001, AGU Meeting, San Francisco, CA, 12/08/01

Smith, D.E., F. G. Lemoine, M. H. Torrence, P. J. Dunn, Observed temporal variations in the low degree gravity field of Mars, EOS, Trans. AGU 82(47), P32E-11, F717, 2001.

Sun, X. J. B. Abshire, G. A. Neumann, and M. T. Zuber, Radiometry measurements of Mars at 1064nm using the Mars Orbiter Laser Altimeter, EOS, Trans. AGU, 82(47), P42A-0557, F723, 2001.

Thompson, B., S. Nerem, D. Rowlands, S. Luthcke, F. Lemoine, D. Pavlis and B. Chao, A preliminary analysis of temporal gravity field variations using CHAMP satellite data, EOS Trans. AGU 82(47), G51A-0238, 2001.

Zelensky, N. P., B. D. Beckley, D. D. Rowlands, F. G. Lemoine, S. B. Luthcke, D. S. Chinn, and T. A. Williams, Towards 1-cm Orbits, EOS, Trans. AGU, 82(47), G22A-0203, F256, 2001.

Zuber, M.T., D. E. Smith, and G. A. Neumann, Seasonal variations in the topography of Mars from the Mars Orbiter Laser Altimeter, EOS, Trans. AGU 82(47), P32E-10, F716, 2001.

2001 European Geophysical Society Meeting Presentations

Bosworth, J. D. Carter, and W. Wildes, Future Evolution of NASA's SLR and VLBI Networks, Session G8.02, EGS XXVI General Assembly, Nice, France, March 2001.

Chao, B. F., A. Au, and T. Johnson, Gravitational signal of mass redistribution due to interannual meteorological oscilations in the atmosphere and ocean, Session G3.01, EGS XXVI General Assembly Nice, France, March 2001.

Cox, C. M., S. M. Klosko, and B. F. Chao, Decadal scale mass balance implications of existing observed geodetic parameters, Session G3.01, EGS XXVI General Assembly Nice, France, March 2001.

Cox. C. M., A. Au, and B. F. Chao, Intercomparison of satellite derived gravity time series with-inferred gravity time series from TOPEX/Poseidon sea surface, Session G3.01, EGS XXVI General Assembly Nice, France, March 2001.

Lemoine, F. G., D. D. Rowlands, S. B. Luthcke. N. P. Zelensky, D. S. Chinn, D. E. Pavlis, and G. Marr, Precise orbit determination for Geosat-Follow-On using satellite laser ranging data and intermission altimeter crossovers, Session G8.02, EGS XXVI General Assembly, Nice, France, March 2001.

Ma, C., D. Macmillan, and L. Petrov, Integration of reference frames through VLBI, Session G6, EGS XXVI General Assembly, Nice, France, March 2001.

Macmillan, D., T. Van damm, A. Au, P. Milly, J. Wahr, Hydrological loading in VLBI measured site displacements (Invited), Session G3.02 EGS XXVI General Assembly Nice, France, March 2001.

Pavlis, E. C. Satellite Laser Ranging constraints on global mass transport in the Earth system, presented at the European Geophysical Society (EGS) General Assembly, Nice, France, March, 2001.

Pavlis, E. C. Combination and evaluation of satellite laser ranging contributions towards a single ILRS product, presented at the European Geophysical Society (EGS) General Assembly, Nice, France, March, 2001.

Pavlis, E. C. Earth orientation from satellite laser ranging (SLR): quality, content and resolution, presented at the European Geophysical Society (EGS) General Assembly, Nice, France, March, 2001.

Pavlis, E. C., and V. B. Mendes Validation of improved mapping functions for atmospheric corrections in laser ranging, presented at the European Geophysical Society (EGS) General Assembly, Nice, France, March 2001.

Petrov, L., Determination of ocean loading deformations using VLBI, Session G3.02, EGS XXVI General Assembly Nice, France, March 2001.

Zuber, M., and D. Smith, Seasonal elevation changes in the icecaps of Mars, Session PS2.02, EGS XXVI General Assembly, Nice, France, March 2001.

Zuber, M. and D. Smith, Topography and gravity of Mars and locations of past surface water, Session PS2.03, EGS XXVI General Assembly, Nice, France, March 2001.

2001 International Association of Geodesy Scientific Assembly Presentations

Chao, B. F., A. Y. Au, and T. Johnson, Non-seasonal gravitational effects of Interannual meteorological oscillations in the atmosphere and the ocean.

Cox, C. M., B. Chao, A. Au, S. M. Klosko, Investigation of Interannual variations in the geopotential, and the implications for the determination of decadal scale signals and their use in constraining geophysical models.

Kenyon, S., C. Jekeli, E. C. Pavlis, N. K. Pavlis, and C. K. Shum Future Enhancements and Developments for the Next Generation of WGS, presented at the 2001 IAG Scientific Assembly: Vistas of Geodesy, of the International Association of Geodesy, Budapest, Hungary, September 2-7, 2001.

Lemoine, F. G., N. P. Zelensky, D. S. Chinn, D. D. Rowlands,S. B. Luthcke, D. E. Pavlis, T. A. Williams, and G. C Marr,Orbit determination for the GFO-1 Altimeter mission.

Pavlis, E. C. Dynamical Determination of Origin and Scale in the Earth System from Satellite Laser Ranging, presented at the 2001 IAG Scientific Assembly: Vistas of Geodesy, of the International Association of Geodesy, Budapest, Hungary, September 2-7, 2001.

Pavlis, E. C. Earth Orientation Variations from Satellite Laser Ranging (SLR): Quality, Content and Resolution, presented at the 2001 IAG Scientific Assembly: Vistas of Geodesy, of the International Association of Geodesy, Budapest, Hungary, September 2-7, 2001.

Pavlis, E. C. and S. Kenyon A Geopotential Solution Incorporating Data from Recent Satellite Missions, presented at the 2001 IAG Scientific Assembly: Vistas of Geodesy, of the International Association of Geodesy, Budapest, Hungary, September 2-7, 2001.

Pavlis, N. K., E. C. Pavlis and S. Kenyon, Combination Geopotential Solution Development Anticipating Data from GRACE and GOCE, presented at the 2001 IAG Scientific Assembly: Vistas of Geodesy, of the International Association of Geodesy, Budapest, Hungary, September 2-7, 2001.

Mertikas, S., E. C. Pavlis, Th. Papadopoulos, and X. Frantzis, Preparatory steps for the establishment of a European radar altimeter calibration and sea-level monitoring site for JASON, ENVISAT and EURO-GLOSS, presented at the 2001 IAG Scientific Assembly: Vistas of Geodesy, of the International Association of Geodesy, Budapest, Hungary, September 2-7, 2001.

Ray, R. D., and G. Egbert, Fortnightly polar motion.

Other Presentations (Seminars, Colloquia and Workshops)

Carabajal, C. C., "Evaluation of Geoscience Laser Altimeter System (GLAS) Waveforms for Vegetated Landscapes Using Airborne Laser Altimeter Scanning Data," presented at ICESat Science Team Meeting, Greenbelt, MD, November 15-16, 2001.

Chao, B. F., "Global Geophysical Fluids Center of IERS: A Progress Report," Asia Pacific Space

Geodynamics (APSG) 2001 meeting, Shanghai, China, May 14-18, 2001.

Cohen, S.C. and D.J. Darby, "Tectonic plate coupling and elastic thickness derived from the inversion of geodetic data using a steady-state viscoelastic model: application to southern North Island, New Zealand", Int. Assoc. Geodesy Symp. on Recent Crustal Movements, Helsinki, Finland, 8/27/01

Cohen, S.C. and J. T. Freymueller, "The complex temporal and spatial pattern of crustal deformation in the southcentral Alaska subduction zone from GPS, leveling, and tide gauge observations", Int. Assoc. Geodesy Symp. on Recent Crustal Movements, Helsinki, Finland, 8/27/01

Frey, H., "Moon, Mars, Earth", Delaware Space Academy Newark, DL, 7/09/01

Frey, H., "Exploration of Mars", National Space Club Scholars Summer Program, GSFC, 7/17/01

Frey, H., "Exploring Mars", Visiting teachers summer program, GSFC, 7/18/01

Frey, H., "Ancient Lowlands on Mars", Geophysics Workshop, University of Maryland, 7/26/01

Frey, H., "Buried ancient lowlands on Mars: laser altimetry, buried craters and a primordial crustal dichotomy", GSFC Scientific Colloquium, GSFC, 11/02/01

Harding, D.J., "Future directions in laser altimeter measurements of the Earth's surface", NASA Earth Science Enterprise Technology Planning Workshop, Greenbelt, MD, 1/23/01

Harding, D.J. and J.Degnan, "Laser altimeter overview and SLA-03 pathfinder role for imaging lidar", Code Y Program Managers, GSFC, Greenbelt, MD, 4/10/01

Harding, D.J., "Airborne scanning laser altimetry: high resolution topographic and canopy structure mapping", National Park Service, Fish & Wildlife Service Remote Sensing Short course, Shepherdstown, WV, 5/24/01"

Harding, D.J., "Status of Cal/Val Site Specific Plan: Puget Lowland", ICESat Science Team Meeting, GSFC, Greenbelt MD, 5/31/01

Harding, D., "Imaging lidar: Techniques and capabilities", GESS Investigators Meeting, 10/09/01

Lowman, P.D., "The New Mars" GSFC Retirees Club, 1/09/01

Lowman, P.D., "Lunar samples: how do we know they are from the Moon?" Lunar and Meteorite Sample Certification Training, 3/02/01

Lowman, P.D., "Rocketry and science: what have we learned from space flight?", GSFC Visitor Center TV panel Discussion, 3/13/01

Lowman, P.D., "New views of the Moon", Physics Dept., Morgan State University, Baltimore, MD, 3/20/01
Lowman, P.D., "A digital tectonic activity map Frostburg State Teachers vist to GSFC", 4/10/01

Lowman, P.D., "Tectonics from Space", Anne Arundel HS teachers, GSFC, Greenbelt, MD, 6/16/01

Lowman, P.D., "Remote sensing in geology", Visiting Teachers from Salish, Kootenai tribes, Washington State, Greenbelt, MD, 6/22/01

Lowman, P.D., "How to become an astronaut", National Space Club Scholars Summer Program, GSFC, 7/01/01

Lowman, P.D., "Return to the Moon", Baltimore Science Center, 7/17/01

Lowman, P.D., "Tectonics and Space Maryland Space Grant Consortium Course: Earth Observations from Space", Columbia, MD, 71/19/01

Lowman, P.D., "Back to the Moon", NASA Space Academy, GSFC, 7/20/01

Luthcke, S.B., J. Bufton, D.D. Rowlands. D.J. Harding, J. Sauber, C.C. Carabajal,"Status of Precision Geolocation System and Integrated Residual Analysis for ICESat Calibration and Validation," ICESat Science Team Meeting, La Jolla, CA, Feb. 14-15, 2001.

Luthcke, S.B. Precision Geolocation System for Laser Altimetry (PGSLA) Status and Plans for Launch + 90 days, presented at ICESat Science Team Meeting, Greenbelt, MD, May 31, 2001.

Luthcke, S.B., D.D. Rowlands, C.C. Carabajal, "Spaceborne Laser Altimeter Instrument Parameter Calibration from Integrated Residual Analysis - A Brief Overview," ISPRS Workshop on Land Surface Mapping and Characterization using Laser Altimetry, Annapolis, MD, Oct. 22, 2001.

Luthcke, S.B., J. Bufton, D.D. Rowlands. D.J. Harding, J. Sauber, C.C. Carabajal,"Status of Precision Geolocation System and Integrated Residual Analysis for ICESat Calibration and Validation," ICESat Science Team Meeting, Greenbelt, MD, Nov. 15, 2001.

Ma, C. Considerations for ITRF solutions, Second International VLBI Service Analysis Workshop, NASA GSFC, Greenbelt, Maryland, February 12-14, 2001.

Ma, C. and Z. Altamimi, VLBI and the ITRF2000, Asia Pacific Space Geodynamics (APSG) 2001 meeting, Shanghai, China, May 14-18, 2001.

MacMillan, D.S, "EOP Modeling: Current Status and New Approaches,"Second International VLBI Service Analysis Workshop, NASA GSFC, MD, Feb. 12-14, 2001.

Petrov., L., "Unresolved problems of VLBI data analysis," Second International VLBI Service Analysis Workshop, NASA GSFC, Greenbelt, MD, Feb. 12-14, 2001.

Purucker, M., "Martian and terrestrial magnetic fields: comparative planetology", Danish Space Research Institute, Copenhagen, 10/23/01

Purucker, M., "Martian magnetic field: from Mars Global Surveyor to Netlander, Netlander Symposium", Nantes, France, 4/1/01

Sakimoto, S.E.H., "Changing views of Mars water and volcanism from the Mars global Surveyor mission", KECK Undergraduate Research Symposium, GSFC., 4/06/01

Sakimoto, S.E.H., Invited planetary talks (6 hours) “Space Science XVI: Space Explorations teacher workshop", Tufts University, Boston, MA, 6/21/01

Sakimoto, S.E.H., "Recent mission results in Planetary Geology", Anne Arundel HS teachers, GSFC, Greenbelt, MD, 6/25/01

Sakimoto, S.E.H., "Planetary Volcanology: Topographic and Modeling Constraints for Earth and

Mars", Geophysics Workshop, University of Maryland,7/26/01

Sakimoto, S.E.H., "Computational models of channelized lava flows on Earth and Mars" Un., MD Center for Scientific Computation and Mathematical Modeling, College Park, 11/20/01

Sauber, J., "Ice mass fluctuations and GPS observations", ICESat Science Team Meeting", 3/12/01

Sauber, J., "Solid Earth science", College faculty from non-PhD institutions, GSFC, Greenbelt, MD, 5/25/01

Sauber, J., "Plate tectonics: Earth's unique style", Anne Arundel County Public Schools Earth & Space Science Teacher Academy, GSFC, 7/20/01

Sauber, J., "Mechanics of Shallow Subduction under the Influence of Glacial Fluctuations", Geophysics Workshop, University of Maryland, 7/26/01

Sauber, J., "Mechanics of shallow subduction", Dept., Geology Seminar, Un. MD. College Park, MD, 10/15/01

Taylor, P.T., "Evolution of the Moon", Lunar and Meteorite Sample Certification Training, 3/02/01

Taylor, P.T., "New views of the Moon", Physics Dept., Morgan State University, Baltimore, MD, 3/20/01

Taylor, P.T., "Polycrystalline diamonds (carbonados) and theorigin of the large magnetic field anomaly over Central Africa", Morgan State University, 4/25/01

Taylor, P.T., "The Role of Remanent Magnetization in the Interpretation of Crustal Magnetic Anomalies at Satellite Altitude", Geophysics Workshop, University of Maryland, 7/26/01

Rubincam, D.P., "Pluto and Triton: interactions between volatiles and dynamics" Innovative Approaches to Outer Planetary Exploration 2001-2020, Houston, TX., 3/21/01

Rubincam, D.P., "Orbital-Rotational-Climatic Interactions on Earth, Mars, Triton and Pluto", Geophysics Workshop, University of Maryland, 7/26/01

Taylor, P.T., "Satellite altitude magnetic data and the search for mineral resources Deep Structure of the Earth and Concentration of Metals in the Lithosphere", workshop, Reston, VA, 9/20/01

Taylor, P.T. and J. Frawley, "The role of remanent magnetization in the geologic interpretation of crustal magnetic anomalies measured at satellite altitude: a tale of two planets Intern.", Wkshp on Geo-Electro Magnetism, Lerici, Italy, 9/28/01

921 / 926 Science Seminar Series

Bills, B. G. "Fourier, Legendre, and Milankovich, searching for the connection between orbital, rotational and climatic variations", Code 921/926 Science Seminar Series, GSFC., 4/10/01

Boy, J. P. (Code 926), "Mass (atmospheric, ocean tidal) loading effects on surface gravity and deformation", Code 921/926, Science Seminar Series, GSFC., 10/17/01

Bradley, B. A., "The Medusae Fossae Formation, Mars: new views from the Mars Global

Surveyor data", Code 921/926 Science Seminar Series, GSFC., 6/27/01

Bulmer, M., "(CEPS/NASM), An empirical approach to studying debris flows – implications for planetary modeling studies", Code 921/926 Science Seminar Series, GSFC., 8/23/01

Cohen, S. C., "Seismogeodetics of southern North Island, New Zealand", Code 921/926 Science Seminar Series, GSFC., 8/08/01

Cox, C. (Code 926), "And now for something completely different: a brief overview of the technology of medieval European armour and weapons", Code 921/926 Science Seminar Series, GSFC., 11/6/01

Freund, Friedemann, (San Jose State) "Electric charge carriers in crustal rocks and what they may tell us about the solid Earth", Code 921/926 Science Seminar Series, GSFC., 10/31/01

Frey, H., "A fundamental constraint for the fundamental problem of martian geology", Code 921/926 Science Seminar Series, GSFC., 3/7/01

Grammatica, N. (DSRI), "Probing the conductivity of the deep Earth using satellite data", Code 921/926 Science Seminar Series, GSFC., 6/07/01

Harding, D. J., "Tilted terracestell the tale: the Seattle Fault Zone, Washington State", Code 921/926 Science Seminar Series, GSFC., 12/04/01

Hernandez-Pajares, M. (Un. Politec. de Catalunya, Spain),"Precise real-time ionospheric mapping with GPS: benefits to navigation, remote sensing and atmospheric science", Code 921/926 Science Seminar Series, GSFC.,9/07/01

Neumann, G. (Code 926), "How much more topography do you want? A comparative description of MOLA data and results from previous planetary laser altimetry missions", Code 921/926 Science Seminar Series, GSFC., 4/11/01

Reidel, S. J., "Assessing topographic constraints on lave tube flow rates for Alba Patera, Mars ", Code 921/926 Science Seminar Series, GSFC., 6/27/01

Richards, M. (UC Berkeley), "Why Earth has plate tectonics and why Venus does not", Code 921/926 Science Seminar Series, GSFC., 5/03/01

Rubincam, D.P., "Orbital-Rotational-Climatic Interactions on Earth, Mars, Triton and Pluto", Code 921/926 Science Seminar series, GSFC., 7/11/01

Rudnick, R. (Un. MD), "Osmium isotopic investigations of continental growth and instability", Code 921/926 Science Seminar Series, GSFC., 2/28/01

Sacks, I. S. "(DTM), Earthquake prediciton – illusive, but is it possible? (view from seismology)", Code 921/926 Science Seminar Series, GSFC., 5/10/01

Sakimoto, S.E.H., "Mars volcanism from the bottom up: modeling fundamental volcanic parameters from new topographic constraints", Code 921/926 Science Seminar series, GSFC., 4/18/01

Sauber, J., "The mechanics of shallow subduction zones under the influence of glacial fluctuations", Code 921/926, Science Seminar Series, GSFC., 10/18/01